PAP-773

DURANGO PUMPING PLANT MODEL STUDIES
FISCAL YEAR 1996

TONY L. WAHL

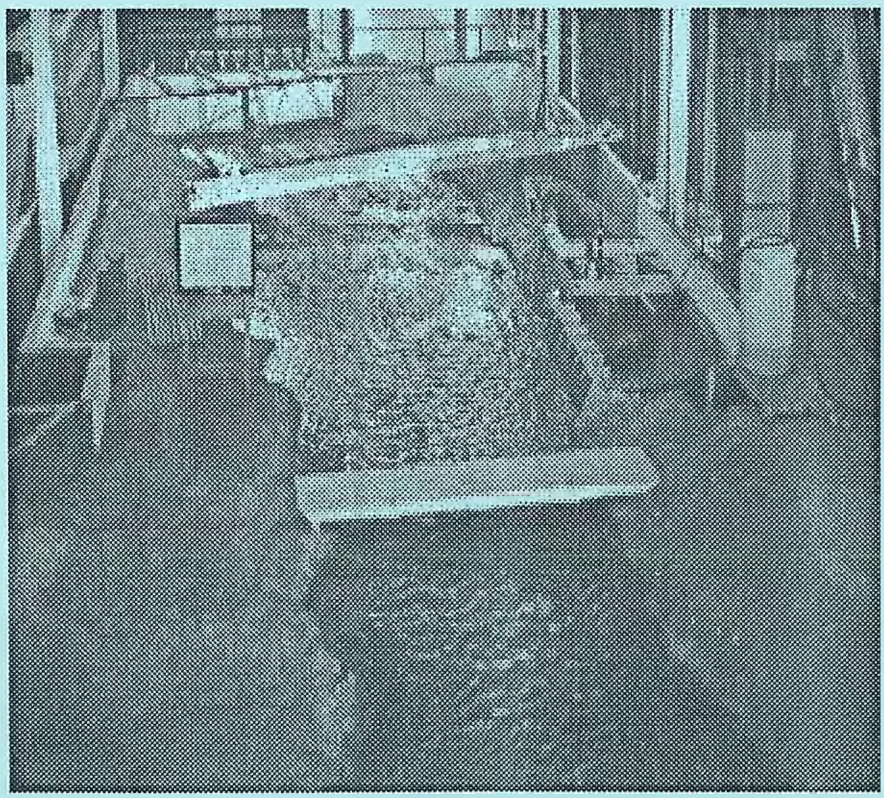

Durango Pumping Plant Model Studies - FY96

TABLE OF CONTENTS

Durango Pumping Plant Model Studies - FY96

by Tony L. Wahl

SUMMARY AND CONCLUSIONS

Physical hydraulic model studies to support the design of Durango Pumping Plant were conducted in FY96 (October 1995-September 1996) by Reclamation's Water Resources Research Laboratory (WRRL) in Denver. The pumping plant design was revised during FY95 to accommodate an increased maximum pumping rate (raised from 550 to 670 ft^3/s) and a modified pumping arrangement, using four large spiral case-type pumps to deliver the majority of the flow. Model studies of the previous design were performed between April 1992 and March 1994, and are documented in WRRL Report PAP-655. At the time of this writing (September 1996) the model was still available for viewing and additional testing and will continue to be available for an indefinite period of time. This peer-reviewed report describes the testing performed and the results and conclusions derived from those tests. The major issues considered in the study were:

- Intake structure flow capacity
- Velocity fields approaching the fish screens
- Sump and pump intake flow conditions
- Velocity fields in the river approaching the intake structure

Principal conclusions of the study are as follows:

- The intake structure has sufficient capacity to meet the withdrawal needs of the project. The intake structure can withdraw the full flow to which the project might be entitled for all but a very narrow range of river flows. For river flows of 700 to 900 ft^3/s, the intake capacity is slightly less than the maximum allowable withdrawal based on minimum aquatic bypass flow requirements.
- The fish screen structures will meet the approach velocity requirements for the design (0.5 ft/s average velocity perpendicular to the screen face with a sweeping component at least 2 times the perpendicular component) for all flow conditions up to the maximum pumping rate. At high river levels (above about 1500 ft^3/s) the intake weir gates must be used to equalize the flow distribution between the two screen structures.
- A single turning vane should be installed in the forebay to the left-hand fish screen structure. This vane is needed to maintain adequate sweeping velocity on the upstream end of the left-hand screen panel in the left-hand V-screen bay. (Left and right orientations are given in terms of an observer looking downstream).
- The sump geometry should be modified as described later in this report to eliminate flow separations and dead zones in the sump, and to eliminate vortex flow conditions observed in the original design. In addition, these modifications reduce the size of the sump and the excavation required during construction.
- Although the maximum pumping plant discharge has increased in this design, the velocity field in the river approaching the intake structure appears to be less intense than in the previous design, due primarily to the increased intake length. The two-dimensional near-surface velocity fields 10 ft and 25 ft away from the face of the intake were mapped for a variety of flow conditions. These data help to quantify the performance of this design and can serve as a standard against which other design alternatives may be measured.

BACKGROUND AND SCOPE OF HYDRAULIC MODEL STUDIES

Durango Pumping Plant will be the primary diversion site for the Animas-La Plata Project. The plant and its associated structures will divert water from the Animas River on the south outskirts of Durango, Colorado, and pump it approximately 525 vertical feet up to Ridges Basin Reservoir, about 2 miles away. The plant uses a combination of vertical turbine pumps and spiral case pumps to deliver a maximum flow of 670 ft^3/s. The vertical turbine pumps will be used in early phases of the project, during times of low river flow, and to supply small increments of flow in combination with the large spiral case units. The spiral case units draw water directly from the main plant sump, while the vertical turbine units draw water from a separate wet sump supplied from the main sump. The four spiral case units have a combined discharge capacity ranging from about 480 ft^3/s to 670 ft^3/s, depending on the water surface elevation at Ridges Basin Reservoir.

A 1:12 scale model of the river reach upstream and downstream of the pumping plant was constructed in the hydraulics laboratory, and was operated using Froude-based scaling. The model spanned a river reach of about 1000 ft, and could be operated up to a maximum prototype discharge of about 5000 ft^3/s. The model made use of existing topography from the previous model studies. The model includes the intake structure, fish screening facilities, main sump (downstream of the fish screens) and the intakes to the five penstocks delivering water to the four spiral case pumps and the wet sump that supplies the vertical turbine pumps. Figure 1 shows a plan view of the pumping plant site.

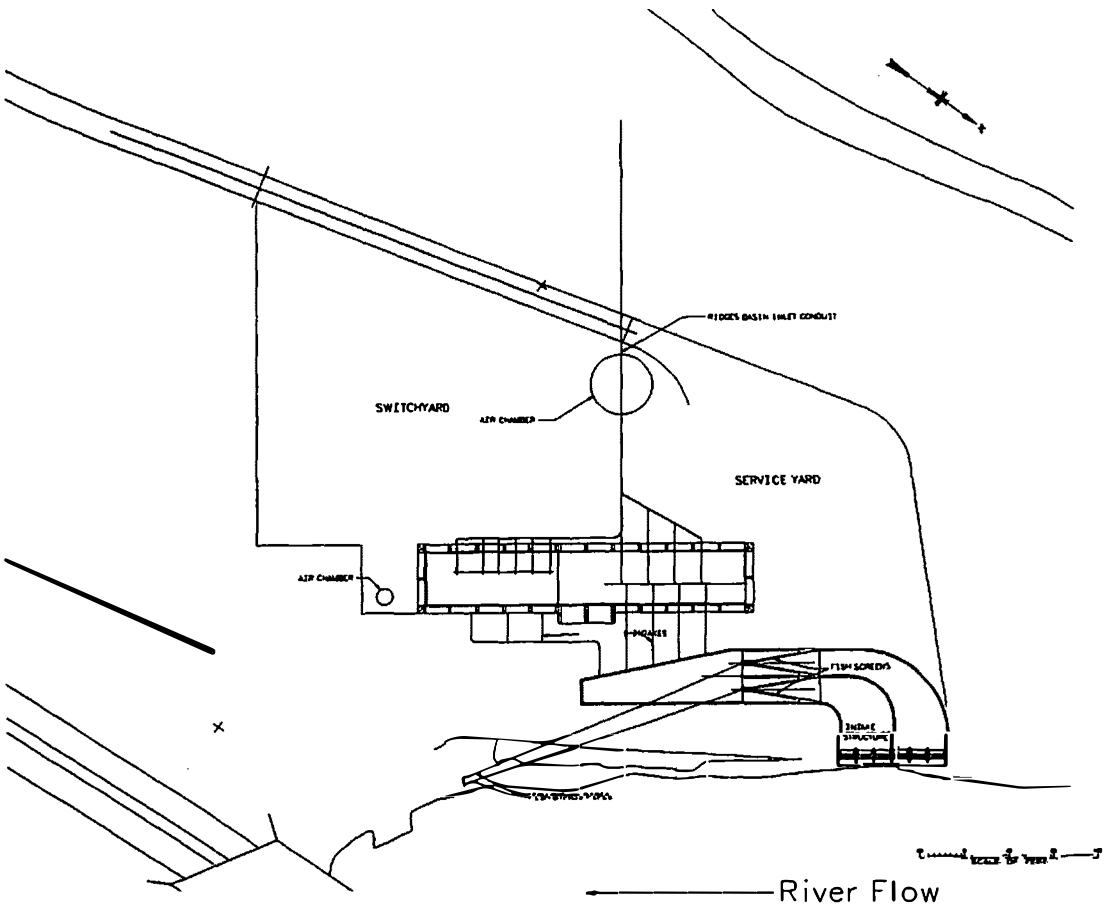

Figure 1. — Plan view of the Durango Pumping Plant site, showing the proposed layout of the intake structure, fish screening facilities, sump, and pumping plant structure.

The model study investigations were focused on four aspects of the pumping plant design:

- Intake structure capacity
- Intake structure velocity fields
- Fish screens
- Sumps and pump intakes

Intake Structure Capacity

The intake structure is located at the right bank of the river and is 96 ft long with a 2-inch clear spacing trashrack on the front face of the intake. (Throughout this report, left and right orientations are described in terms of an observer looking downstream). The intake is composed of 6 independent bays on 16-ft centers, separated by 1.5-ft thick piers. There will not be a diversion dam constructed in the river; flow entering the intake is solely gravity-driven. An inflatable weir gate in each bay can independently control the flow through each intake bay. These gates can be used to equalize the flow through each bay, and will also help to limit the migration of bed sediments into the intake. Figure 2 shows an elevation view of the intake structure. The primary changes in the intake structure design from the previous model studies are the addition of the fifth and sixth intake bays, a flattening of the trashrack slope from 70° to 65°, and the recessing of the gate base slab down to elevation 6436.0.

The model study was used to determine the capacity of the intake structure and identify the range of river flows over which the intake capacity could limit the withdrawal rate of the pumping plant, beyond the limitations already imposed by minimum aquatic bypass flow requirements. At times, the need to meet downstream water delivery obligations may further limit the maximum pumping rate.

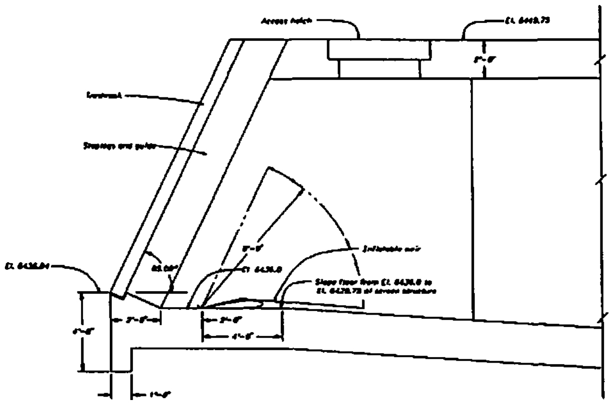

Figure 2. — Elevation view of the intake structure and inflatable weir gate.

Intake Structure Velocity Fields

The velocity field in the river upstream and in front of the intake structure during pumping operations is an important consideration from the standpoint of recreational use of the river, primarily rafting, and kayaking activities. Two dimensional velocity fields were measured for a range of river flow and pumping conditions along two lines 10 ft and 25 ft away from the face of the intake structure. These measurements help quantify the potential for the intake structure velocity field to draw boats up against the face of the intake.

Fish Screens

To minimize the pumping plant's impact on the stocked-trout fishery of the Animas River, the plant will be equipped with a pair of V-style fish screen structures that will separate fish from the flow to be pumped, and return them to the river through a gravity-driven bypass system. Figures 3 and 4 show plan and elevation views of the fish screen structures. The prototype screens will be 3/16-inch clear-spacing wedge-wire panels oriented so that the wires run horizontally down the length of the screen. An automated cleaning system will be supplied, but was not included in the hydraulic model. This screen structure design is a dramatic modification from the fish screen design tested in the first series of model studies. That design used a flatplate screen running the full length of the pumping plant. The new configuration was necessitated by the concentration of the majority of the plant discharge capacity in the four spiral case pumps which are located in one end of the pumping plant.

The 3/16-inch clear spacing of the screens is larger than the 3/32-inch spacing commonly used for screening of salmon fry (less than 60 mm in length) on Reclamation's northern California projects. This screen size was selected for Durango Pumping Plant because we are screening a population of larger fish, comprised mostly of adult trout and stocked juvenile trout greater than 2 inches in length. A clear spacing between wires of 1/4 inch is allowable for this size class of fish. However, due to construction idiosyncrasies in commercially available screens, the open-area ratio of the 3/16-inch screens is greater than that of the 1/4-inch screens. Using a higher open-area ratio should reduce debris problems for the screens.

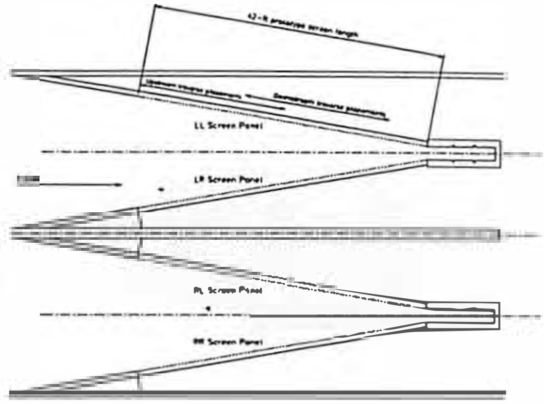

Figure 3. — Plan view of fish screening structures, showing the location of traversing table placements used for the measurement of screen approach velocity fields.

Design criteria for the fish screens require average approach velocities (the local velocity component perpendicular to the screen face) of 0.5 ft/s or less, and sweeping velocities (the component parallel to the screen face) of at least two times the local approach velocity. The State of Colorado has no established criteria for screening of trout, but based on criteria established by the states of Alaska, Idaho, Oregon, and Montana for screening of juvenile salmonids, the previously listed criteria should be suitable for the screening of 2-inch and longer trout, the target species for this screen structure.

Fish screen approach velocity fields were measured for a range of river flows and pumping conditions, with the greatest focus placed on maximum and median pumping rates for given river levels. Tests were also conducted to identify the influence of different pump operating combinations and intake structure gate operations. Approach and sweeping velocities were measured using a 2-D acoustic doppler velocimeter deployed on a traversing table. Measurements could be made at three different elevations on the most upstream 86% of the screen area. Velocities could not be measured on the most downstream 6 ft of each 42-ft long screen panel due to limited access space for the probe in the 1:12 scale model.

Sumps

Flow conditions in the main sump of the pumping plant were evaluated to identify potential problems with vortex formation and other undesirable flow conditions at the penstock entrances. Modifications to the sump

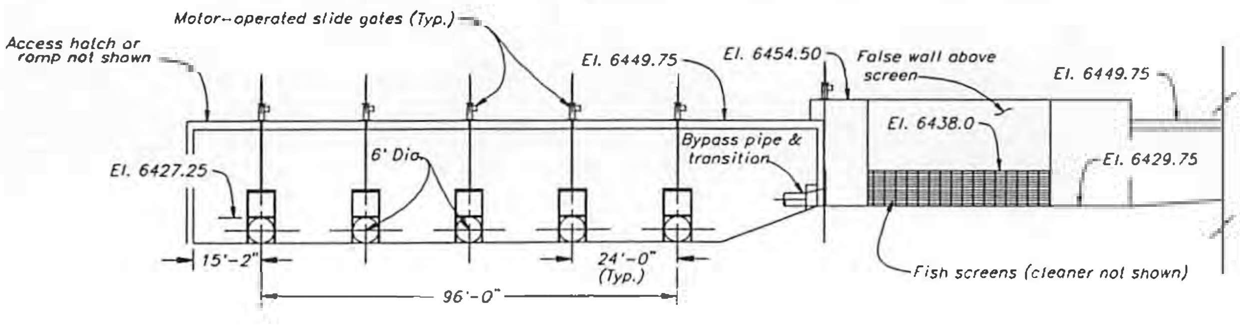

Figure 4. — Elevation view of initial design for fish screen structures and main sump.

geometry were tested in efforts to improve flow conditions and minimize the size of the sump, which will in turn reduce excavation quantities and construction costs. These studies relied exclusively on visual observation of flow conditions using dyes and other indicators.

Model Construction

The model, shown in figure 5, was constructed at an undistorted geometric scale of 1:12, and was operated using Froude-scaling criteria. For a given observed model quantity, X_m, the equivalent prototype quantity is given by $X_p = X_m \lambda_X$, where λ_X is the scaling ratio for parameter X. Scaling ratios for key parameters are summarized below.

Parameter	Scaling Ratio
Length, Head	$\lambda_L=12$
Velocity	$\lambda_V = (\lambda_L)^{0.5} = 3.464$
Discharge	$\lambda_Q = (\lambda_L)^{2.5} = 498.8$
Time	$\lambda_T = (\lambda_L)^{0.5} = 3.464$

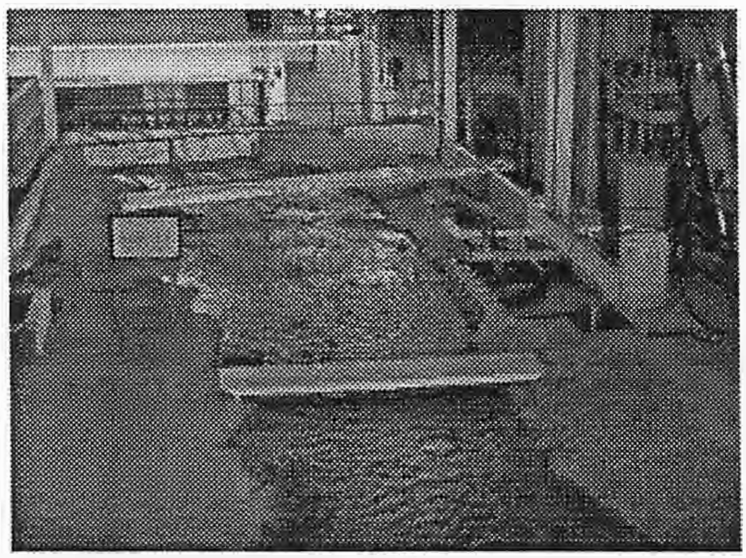

Figure 5. — Downstream view of the 1:12 scale model of Durango Pumping Plant.

The model was constructed in the same box used for the previous model studies, and made use of existing fixed-bed river topography constructed from concrete placed over plywood contours and wire mesh fabric. Use of the existing box and topography fixed the location of the pumping plant structures and required one significant modification in the construction of the model. Due to relocation of the pumping plant and associated structures in this design, portions of the conveyance channel and sumps passed through two columns supporting the roof of the laboratory. These columns would have dramatically interfered with the flow exiting the right-hand fish screen structure and entering the first pump penstock. To avoid this problem, a 25 ft slice was taken out of the channel connecting the intake structure to the fish screen structures, thereby translating the screen structures and main sump 25 ft toward the river, as shown in figure 6. The primary impact of this change is upon the flow conditions approaching the fish screens, especially the left-hand screen structure. However, this modification is considered a conservative approach to the problem, as it reduces the distance available for stilling the flow ahead of the fish screen structures. The radii of the bends connecting the intake and fish screen structures were not modified, and the floor slope through the bend section is higher in the model than the prototype. Thus, the prototype is expected to perform at least as well as the model, and should have better flow conditions on the screens in some respects.

The fish bypass conduits were also rerouted in the model from the prototype design. In the prototype pumping plant the bypasses will discharge back to the Animas River at an undetermined location, but likely several hundred feet downstream of the pumping plant, at a point very near the downstream boundary of the model river reach. There was no way to install the bypasses beneath the existing topography in the model box, so the fish bypass conduits were routed out of the model box, and did not discharge back to the river. This also allowed for measurement and control of the bypass flows.

The main sump design was not yet finalized at the time of these studies, and details of the pump intakes (e.g., bellmouth entrance, square-to-round transitions, bulkhead gates for dewatering) were not well defined. Thus, the model was used primarily for qualitative investigations of sump flow conditions, and the penstock entrances were not modeled in great detail. All penstocks were assumed to be 6-ft inside diameter, and were constructed in the model without including any of the previously listed details. Each penstock was butted flush against the sump wall and attached with bolts. Bolt heads projected into the flow on the inside edge of the sump.

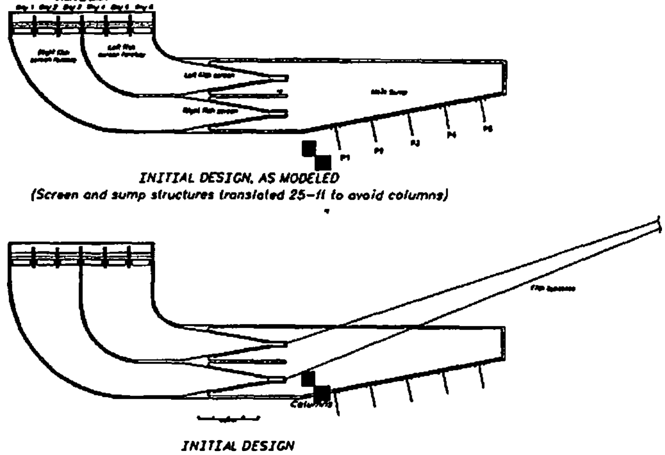

Figure 6. — Plan views comparing initial design and the layout modeled in the laboratory. The structure plan was modified to avoid the laboratory columns.

Model Calibration and Verification

An important measure of how well the model reproduces the prototype behavior is its ability to properly simulate observed water surface elevations for the prototype at given river flows. Prototype water surface elevation measurements at cross-sections within the model reach were available for river flows of 330 ft^3/s, 500 ft^3/s, and 5483 ft^3/s (measurements made in August/September 1992). These measurements were compared to similar data collected from the model, and the model was initially found to produce water surface elevations that were about 1 ft lower than the prototype measurements. The model was then artificially roughened by scattering 1- to 1.5-inch diameter gravel over the fixed model bed and the measurements were repeated. Figure 7 shows the model and prototype comparison for the final configuration used for the model tests. The model water levels match reasonably well at the 5483 ft^3/s flowrate, but are still 0.25 to 0.50 ft below the prototype levels at the two lower river discharges. This was accepted as the final configuration to be used for testing; the lower model water levels are conservative from an intake capacity standpoint for the entire range of flow rates.

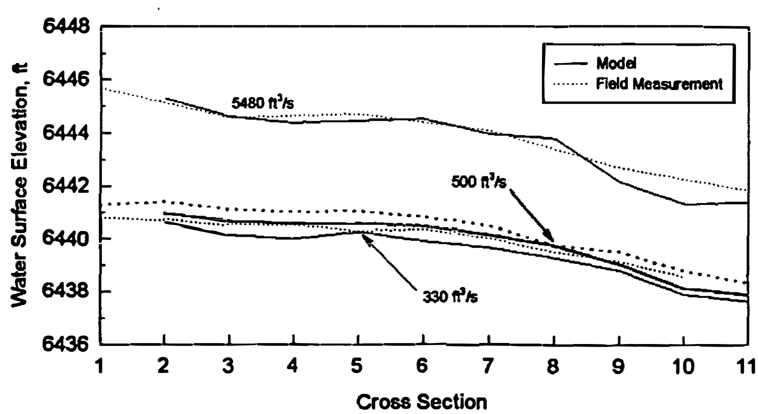

Figure 7. — Comparison of model and prototype water surface elevations at different discharges. Flow is from left to right, with the intake structure located near cross section 5. The proposed location for the fish bypass outfall is near cross section 11. Cross sections are about 75 ft apart throughout the reach.

Discharge Calibration

The model was operated using the main laboratory flow delivery system, with model inflow measured by venturi meters. Flows through each simulated pumping plant penstock and the two fish bypass conduits were measured using custom-built elbow meters calibrated against a V-notch weir.

Velocity Measurements

Measurements of the velocity fields approaching the fish screens and in the river immediately in front of the intake structure were made with a SonTek acoustic doppler velocimeter (ADV probe), shown in place on the fish screen structure in figures 8 and 9. The probe measures the two horizontal components of velocity at user-selected rates ranging from 0.1 Hz to 100 Hz (a three-dimensional probe is also available). The probe uses an ultrasonic signal to measure the velocity of acoustic scatterers in the flow (e.g., suspended sediment, microscale air bubbles, etc.), in a small (approximately 6×6 mm cylinder) sampling volume located about 5 cm (2 inches) away from the probe. The probe also records the signal-to-noise ratio and a correlation score ranging from 0 to 100 for each measurement. The probe manufacturer recommends discarding measurements with a correlation score less than 70. This was accomplished using a Windows-based computer program developed by the author for this project and for other applications of this probe in the hydraulics laboratory.

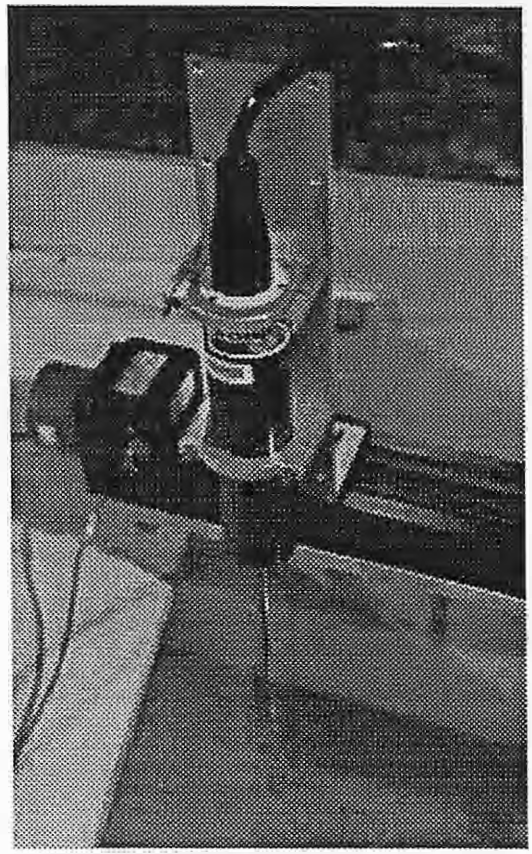

Figure 8. — SonTek acoustic doppler velocimeter installed in the model for measurement of fish screen approach-velocity fields. The probe is mounted on a computer-controlled traversing table.

Most measurements were made at a data collection rate of 4 Hz. The probe was mounted on a traversing table with a 21-inch travel, that was operated at a velocity of 0.050 ft/s. Two passes of the probe were made on each measurement, so that the probe stopped at its original starting position. The computer program mentioned previously computed the probe position corresponding to each measurement and produced output files that could be used for plotting. The program also computed summary statistics for each complete traverse, including mean velocities and turbulence parameters.

The velocity measurements in front of the intake structure were made at prototype distances of 10 ft and 25 ft from the face of the intake structure. Five overlapping traverses were used at the 10 ft distance to span the full length of the 96-ft long intake. Seven traverses were used at the 25 ft distance so that an additional traverse could be made both upstream and downstream of the intake. The objective of these measurements was to determine the surface velocity so that the intake's effects on rafters and kayakers passing the site could be determined. However, the probe must be submerged to operate, so all of these measurements were made with the probe positioned about 1 inch below the water surface. This is equivalent to a prototype submergence of 1 ft.

Velocities approaching the fish screens were measured using eight different placements of the traversing table, four placements for each of the two V-screen structures. The probe was positioned so that the sampling volume would be located about 0.25 inches from the screen face, equivalent to a prototype distance of 3 inches. This is the recommended distance for measuring approach velocities to such screens (Pearce and Lee, 1991). Two traversing table placements were used for each of the four 42-inch long model screen panels. The upstream placement spanned the distance from the upstream edge of the screen to the midpoint of the screen, while the downstream placement spanned the distance from a point 15 inches downstream of the start of the screen to a point 6 inches from the downstream end of the screen. The most downstream 6 inches of each screen panel could not be spanned because of the physical size of the probe and the need to position it about 2.25 inches away from the face of each panel. The prototype fish screen panels are 8.25 ft high and located with their base at elevation 6429.75. Velocity measurements could be made in the model at three elevations, 6431.0, 6434.0, and 6437.0. However, for the majority of the tests, only the 6434.0 elevation was used.

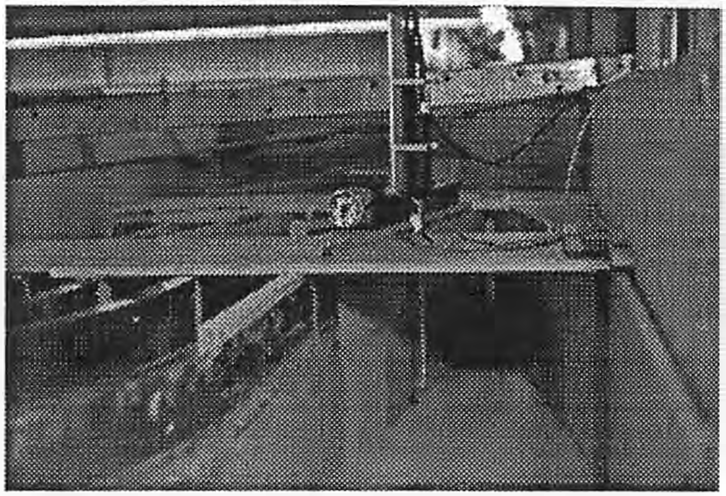

Figure 9. — ADV probe and traversing table located at the upstream traverse placement on the RL screen panel. The probe is located at prototype elevation 6434.0 ft in this view.

Specific details of the velocity measurements will be discussed in later sections. A check on the validity of the velocity measurements could be made by using them to estimate the total discharge through the fish screens, and then comparing that estimate to the total penstock discharges measured with the elbow meters. These estimates were made by assuming that the average velocities measured over the upstream 36 inches of each screen panel were representative of the average velocity over the full screen panel. Figure 10 shows a summary of these comparisons. The tendency is for the discharge based on screen velocity measurements to be slightly less than the elbow-meter discharges for higher flow rates, and higher than the elbow-meter discharges at low flowrates. This may indicate some inaccuracy in the elbow-meter ratings at low flows, where viscous effects begin to dominate. Still, the comparisons are quite good, especially considering that the model approach velocities were only 2 to 4.5cm/s for most tests.

INTAKE CAPACITY

The nominal maximum pumping capacity of Durango Pumping Plant is about 670 ft^3/s. However, the actual pumping rate at any given time depends on a number of factors including:

- Flows in the Animas River
- Downstream, non-Project water demands, whose rights are senior to the Project
- Tribal Project water demands, and delivery locations, as identified in the Settlement Act
- Project demands for New Mexico municipal and industrial water
- Minimum bypass flows to maintain the aquatic ecosystem in the Animas River (*minimum bypass flow requirements*)
- Capacity of Durango Pumping Plant as affected by intake structure withdrawal capacity and pumping capacity
- Ridges Basin Reservoir water level, which affects pumping capacity

These studies can best address the issues related to intake structure capacity as a function of Animas River flowrates and the restrictions imposed by minimum bypass flow requirements. Because there will be no diversion dam at this site, the capacity of the intake will vary dramatically with river stage.

Minimum aquatic bypass flow requirements established for the pumping plant are as follows:

- April through September-- 225 ft^3/s
- October and November – 160 ft^3/s
- December through March – 125 ft^3/s

The pumping plant must allow these minimum quantities of flow to bypass the plant and continue flowing downstream in the Animas River; if total river flows are less than these minimums immediately upstream of the plant, no pumping would be allowed. In addition, the need to meet water delivery demands further downstream on the Animas River may be more restrictive than these requirements at some times. Based on the minimum aquatic bypass flow requirements, the maximum allowable intake structure withdrawal rate can be computed for a given river flow, and this can be compared to the intake structure capacity at that river flow.

The intake structure, fish screens, and fish bypass conduits will operate as a gravity-driven system. The difference in river elevation between the intake structure and the fish bypass outfall location defines the total energy available to drive flow through the system. The total head available is about 2.6 to 2.8 ft for most conditions (depending on the exact fish bypass outfall location). Fish bypass flows of about 33 ft^3/s through each of the two bypass conduits are needed to maintain adequate sweeping velocity on the fish screens and good flow guidance for fish entering the bypass conduits. (This discharge is intended to maintain a 2 ft/s velocity through the 2-ft wide by 8.25-ft high opening at the entrance to the bypass structure.) Because the design of the fish bypass conduits is not yet finalized, the assumption was made for this study that a 1-ft differential head across the bypass conduits would maintain adequate fish bypass flowrates. This leaves about 1.6 to 1.8 ft of head available to drive flow into the intake structure. This head is consumed in friction losses as the flow approaches the intake, losses through the trashrack structure, head loss across the intake weir gate (when raised), and losses in the conveyance channel connecting the intake structure to the fish screen structures. The only loss that can be controlled is the loss across the intake weir gate; all other losses increase as the intake flow increases. When the total head loss through the intake structure becomes too great, the head available to drive flow through the fish bypass conduits will no longer meet the 1 ft requirement. The intake capacity can be defined for any given river discharge and stage as the flowrate at which there is exactly 1 ft of head remaining to drive flow through the fish bypass conduits. When the intake operates at less than this capacity, there will be additional head on the fish bypass conduits, or excess head can be consumed by raising the weir gates.

Unfortunately, it is nearly impossible to manually adjust the operation of the model to produce exactly 1 ft of head across the fish bypass conduits. In the prototype this may be achieved through the use of a closed-loop control system on the intake weir gates, but such a control system was not included in the model. However, by operating the model at a variety of river and pumping conditions and then plotting the available fish bypass heads, one can make some general conclusions regarding the intake capacity.

Figure 11 shows a plot of the maximum allowable intake structure withdrawal rates by season (assuming a total fish bypass flow of 66 ft^3/s), for river discharges of 0 to 1500 ft^3/s. The figure also shows the measured head drop across the fish bypass structure for several operating conditions tested in the hydraulic model. This head drop was determined by recording the water surface elevations in the forebays upstream of the fish screen structures and in the river near the proposed fish bypass outfall location. The figure shows that for a given river flow, the available fish bypass head is reduced as the intake discharge

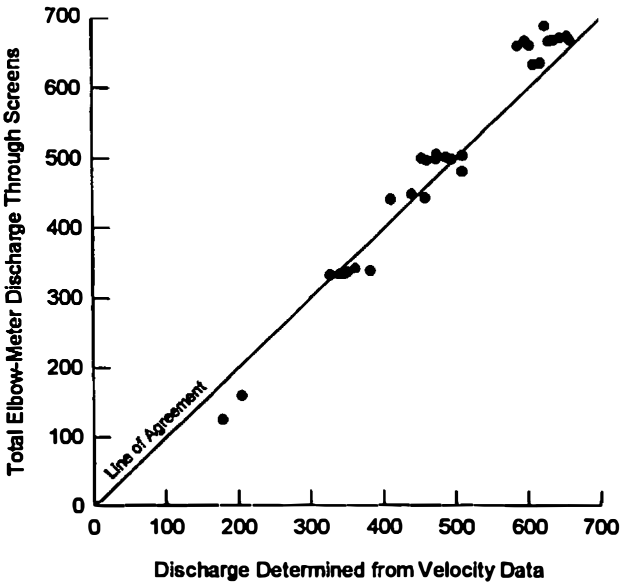

Figure 10. — Comparison of elbow-meter discharge measurements to discharges determined by integrating screen velocity measurements.

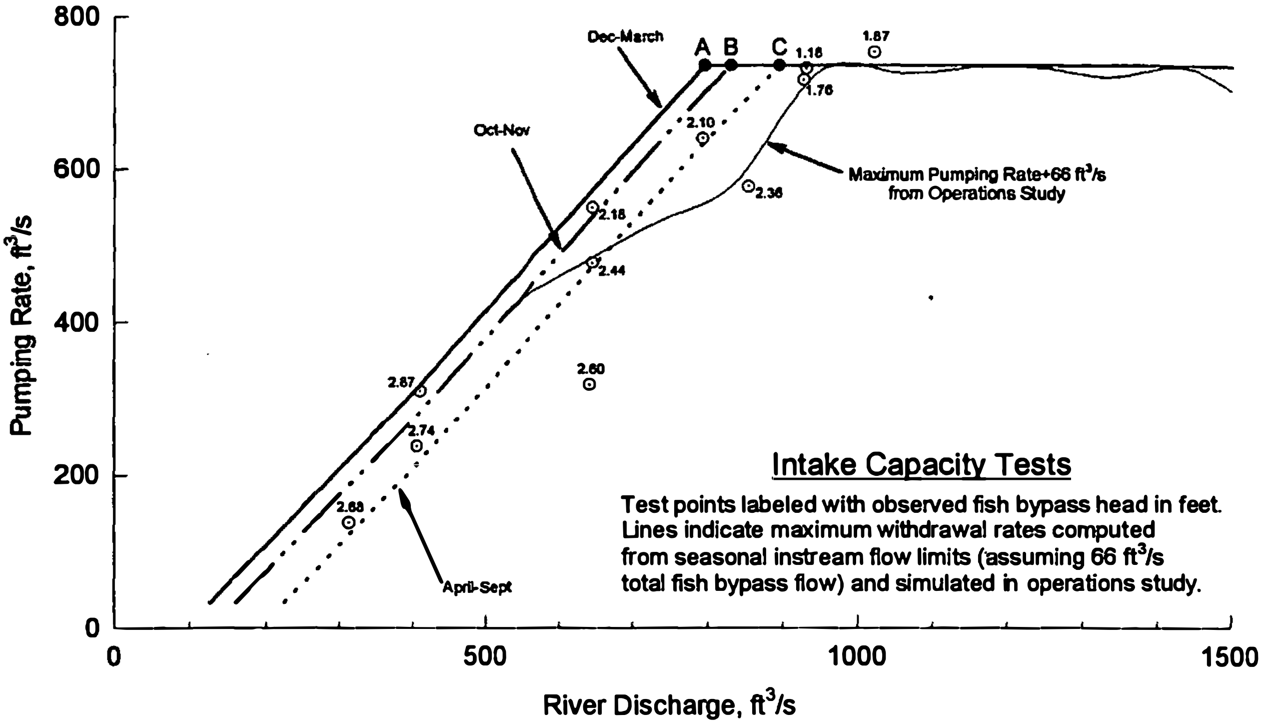

Figure 11. — Summary of allowable discharge limits based on minimum aquatic bypass flow requirements, simulated maximum discharges from operations studies, and data collected during testing of intake structure withdrawal capacity as a function of river discharge.

increases. Also, for a given intake discharge, the fish bypass head is reduced as the river flow decreases. These observations suggest that the most critical operating conditions for each season are at Points A, B, and C, indicated on the figure.

The figure shows that the fish bypass head did not drop below 1 ft for any of the conditions tested. At the nearest test condition to Point C the fish bypass head is only slightly more than 1 ft, so the capacity of the intake in the April-September season has nearly been reached at that operating condition. The intake structure could not physically withdraw enough flow to reach B and C, so the intake capacity must be reached between those points and the surrounding test points shown on the figure (where the available fish bypass head is still greater than 1 ft). Thus, for the October-November and December-March seasons, the intake structure is not able to divert the full quantity of water that the project might be otherwise allowed to divert, based solely on minimum aquatic bypass flow requirements. The impact of this limitation upon operation of the project may be very slight, since as was previously described, there are other limiting factors that may prevent operation at flowrates approaching Points B and C.

Figure 11 illustrates this point by also showing the maximum pumping rates experienced during a simulation of project operations. This operational simulation was run by the Durango Project Office and uses historical hydrologic data to simulate project operations over a 60 year period, including the effects of minimum aquatic bypass flow requirements, downstream demands that must be satisfied on the Animas River, and variations of the water level in Ridges Basin Reservoir. The figure shows that the plant never operated at Points A, B, or C in the simulation.

FISH SCREENS

Fish Screen Design and Performance Concepts

Fish screen design and performance criteria were summarized earlier and will be reviewed here briefly. The screen structures are intended to separate 2-inch and longer fish from the flow to be pumped. This is accomplished with two V-type screen structures located upstream of the main plant sump. Each screen structure consists of two 42-ft long by 8.25-ft high wedge-wire screen panels installed in a V arrangement with a bypass entrance at the throat of the V. The screen panels will be constructed from a stainless steel wedge-wire material with a 3/16-inch clear spacing between 3 mm wires. The wires will be oriented horizontally, and an automated cleaning system will be used to sweep debris down the screen panel toward the bypass entrance. The screen panels were modeled with stainless steel perforated plate panels, with 3/16" diameter openings on 1/4" centers. The model screen panels have a 51% open area ratio, compared to a 57% open area ratio for the prototype screens and their supporting structure. Figure 3 showed plan and elevation views of the screen structures. The panels are labeled LL, LR, RL, and RR for easier identification in the discussion that follows, with the first letter signifying the bay (left vs. right), and the second letter indicating the left or right side of the specific V-screen structure.

Fish will be transported down the approach channel leading to the screen structures, then past the screens and into the bypass conduits. The average approach velocity (the local velocity component perpendicular to the screens, typically measured 3 inches from the screen face) should be less than 0.5 ft/s over the full area of the screens to avoid impingement of fish against the screen panels. The average sweeping component of velocity should be at least 2 times the local approach velocity to maintain continuous transport of fish down the screen. The total travel time past the screen panel should be less than 60 seconds.

Fish Screen Testing

Figure 12 shows the minimum, maximum, and median pumping plant discharges versus river flowrate. These data were produced by the operations simulation described previously. The figure shows that although the maximum pumping rate is about 670 ft^3/s, the median pumping rate is only about 500 ft^3/s, and does not increase once a river flow of about 1000 ft^3/s is reached. The figure also identifies the flow conditions at which fish screen velocity data were collected. The majority of testing was focused on the median and maximum pumping rates.

As described previously, fish screen velocity fields were measured for various flow conditions using a SonTek 2-D acoustic doppler velocimeter (ADV) probe and a traversing table. Table Al in Appendix A summarizes the flow conditions tested and the types of measurements made. Letter prefixes for each test correspond to different alternative designs and operating modes, as follows:

Test Series	Description
A	Initial design
B	Initial design with two turning vanes in left bay
C	Initial design with one turning vane
D	Design C tested at high discharges with baffles installed downstream of the left fish screen structure
E	Design C tested at high discharges with intake gate operated to equalize intake flow distribution

For the majority of flow conditions, measurements were made on all four screen panels at prototype elevation 6434.0 ft. For these tests, the velocity data were plotted versus position along the screen and linear regressions were performed to determine average velocities as a function of distance along the screen. These plots also indicated relative turbulence levels for each condition. For three operating conditions measurements were made at three elevations (6431.0, 6434.0, and 6437.0 ft) to investigate vertical variation of the velocity fields. These data were plotted in a similar manner, and were also used to construct contour plots of average approach and sweeping velocity components and turbulence levels. Full-page plots of the screen velocity data for each test are included in Appendix A. These figures show the individual velocity data collected during each traverse, along with 95% confidence limits for the regression line through the velocity profile. (The actual regression lines are not shown to avoid unnecessarily cluttering the figures).

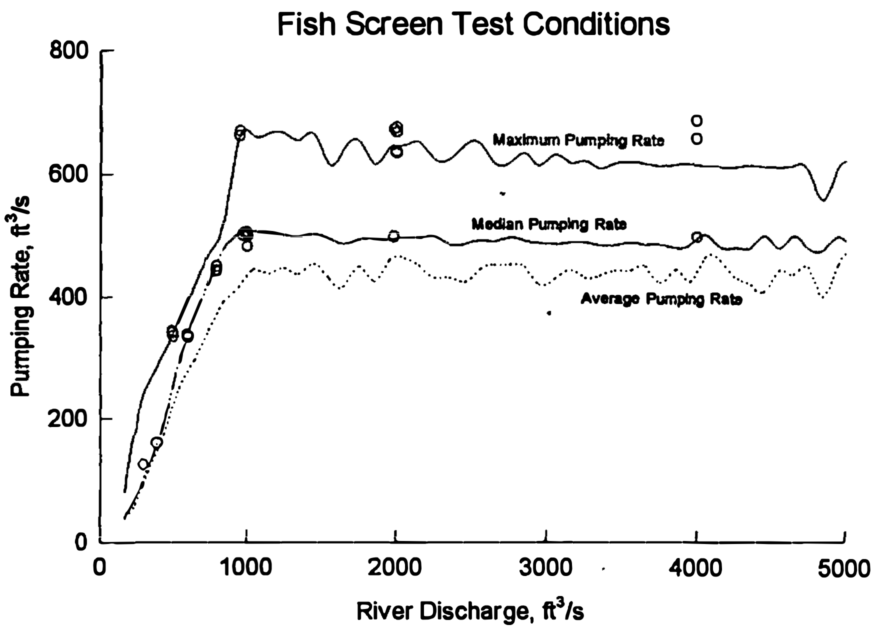

Figure 12. — Symbols indicate test points at which fish screen velocity fields were measured. Lines indicate average, median, and maximum pumping rates versus river discharge, as simulated in a 60-year project operations study.

Effect of Gate Operations

Early testing at low river flows (1000 ft³/s and less) showed that the setting of the intake structure weir gates was an important issue. These weir gates are intended to be raised at high river flows to prevent transport of bed sediments into the pumping plant. At lower river flows the gates can be partially raised, as long as the desired 1-ft head across the fish bypass conduits is maintained (see earlier discussion of INTAKE CAPACITY), or they may be fully lowered to admit the maximum amount of flow. Three different flow conditions for the gates were identified:

(1) Gates fully down, not controlling the flow.

(2) Gates raised so that they begin to control the intake flow. This produces a skimming flow off of the gate leaf, similar in appearance to an undular hydraulic jump, with a great deal of visible surface turbulence.

(3) Gates raised so that they fully control the intake flow. This produces a plunging flow off of the gate leaf, with little visible surface turbulence, but with a reverse roller downstream of the gate; energy dissipation takes place primarily below the water surface.

Measurement of velocity fields on the fish screens showed that the first condition (gates fully lowered) was best from a fish-screen velocity field standpoint (test A02). The other two gate settings (tests A01 and A03) exhibited much higher turbulence levels, especially in the left-hand screen bay (fig. 13). The skimming flow condition (test A01) appeared to be marginally better than the plunging flow (test A03) from a turbulence

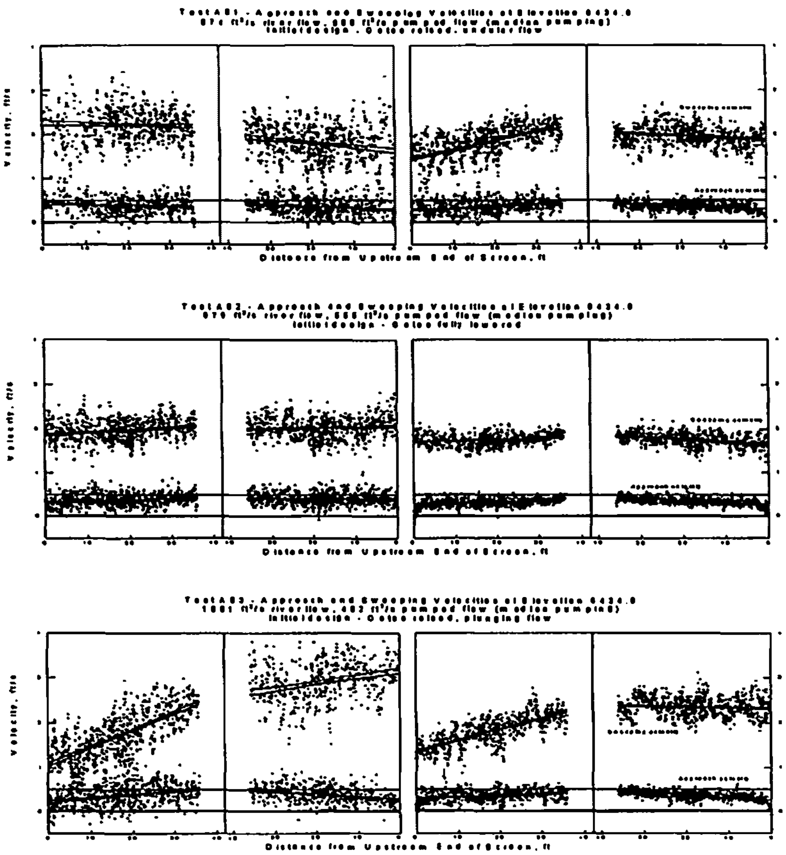

Figure 13. — Comparison of the effects of different intake structure weir gate settings on fish screen velocity fields. Each plot is an elevation view of the four fish screen panels as seen by an observer looking downstream at the screen structures. The lower cluster of data on each plot is the approach velocity, and the upper cluster is the sweeping velocity. 95% confidence limits for the regression line through each data set are shown, as well as a horizontal line indicating the 0.5 ft/s allowable approach velocity. These plots are reproduced at a larger scale in Appendix A.

standpoint. As a result of these tests, all subsequent testing at river flows of 1000 ft^3/s and less was conducted with the intake gates fully lowered.

Effect of Different Pump Operation Scenarios

The layout of the sumps, with the penstocks oriented almost perpendicular to the primary flow direction through the fish screen structure, suggests that the operation of different combinations of pumps could produce differences in the flow through the fish screens, even if the total pumping rate is the same. The location of the first penstock (most upstream) very close to the right hand screen structure suggests that variations in the operation of this pump may have the greatest impact. Variations in the operation of pumps close to the screens or at the far end of the sump could occur in the prototype when attempting to deliver incremental flow amounts. The first four penstocks all serve the large spiral case pumping units with a maximum discharge of about 165 ft^3/s. The last penstock supplies the smaller vertical turbine pumps located in a secondary sump; these units have a combined maximum discharge that is about equal to one spiral case unit. Under some pumping scenarios the vertical turbine units could be shut down and the first spiral case unit started up, thereby transferring discharge from the far end of the sump to the penstock immediately adjacent to the right-hand fish screen.

Several tests were made to determine the influence of different pumping combinations on the fish screen velocity fields. In these tests the operations of the first and last penstocks were reversed, but there was little change in the fish screen velocity fields (e.g., test B06 vs. B07, and test B13 vs. B14).

Screen Velocity Fields - General

The hydraulic performance of the right-hand V-screen structure was good for most operating conditions. Approach velocities meet the 0.5 ft/s criteria and sweeping velocities are well above the required level. At low pumping plant discharges the left-hand V-screen structure also performs well (e.g., test A05, shown in figure 14), but as pumping rates increase above median levels, the flow conditions deteriorate in the short-radius curved channel connecting the intake structure with the fish screen structure. The flow separates from the left-hand wall and secondary currents develop in the flow. The most noticeable effect at the fish screen structure is a reduction of sweeping velocity on the left-hand panel, increased sweeping velocity on the right-hand panel, and increased turbulence levels (e.g., test A08, shown in figure15).

To improve the flow conditions in the left-hand screen structure, two turning vanes were installed in the curved channel leading from the downstream three bays of the intake structure to the left-hand V-screen (fig. 16). These vanes effectively turned the flow and aligned it with the screen, significantly improving sweeping velocities on the LL screen panel. The vanes also reduced the turbulence levels on the left-hand screens, although they were still higher than in the right-hand screen bay. Further testing showed that only the inside turning vane (vane A in figure 16) was required to achieve these benefits, and the single-vane modification was used for all subsequent testing. Figure 13 shows the effect of this modification, comparing tests A07 (no vanes) and C07 (only vane A).

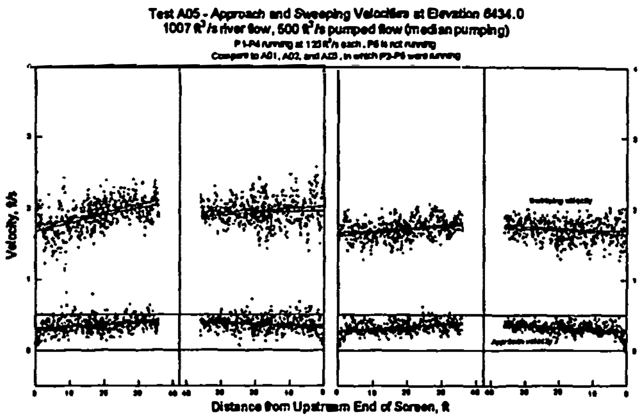

Figure 14. — Fish screen velocity profiles collected during test A05

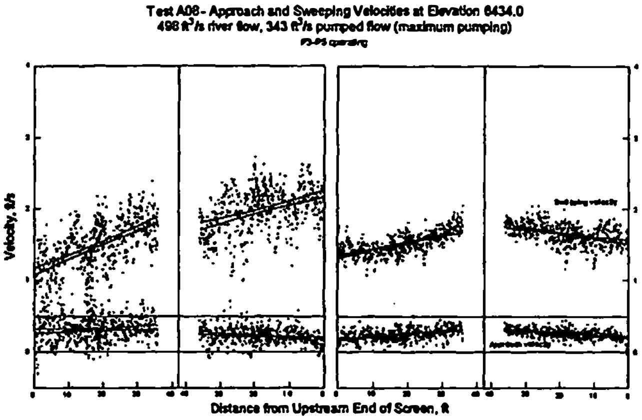

Figure 15. — Test A08, illustrating poor flow conditions in the left fish screen bay due to separation of flow from inside radius of left-hand screen structure forebay.

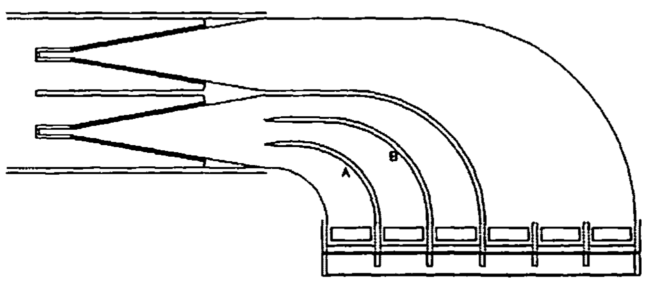

Figure 16. — Plan view of the intake and fish screen structures showing the two turning vanes (A and B) added to the model.

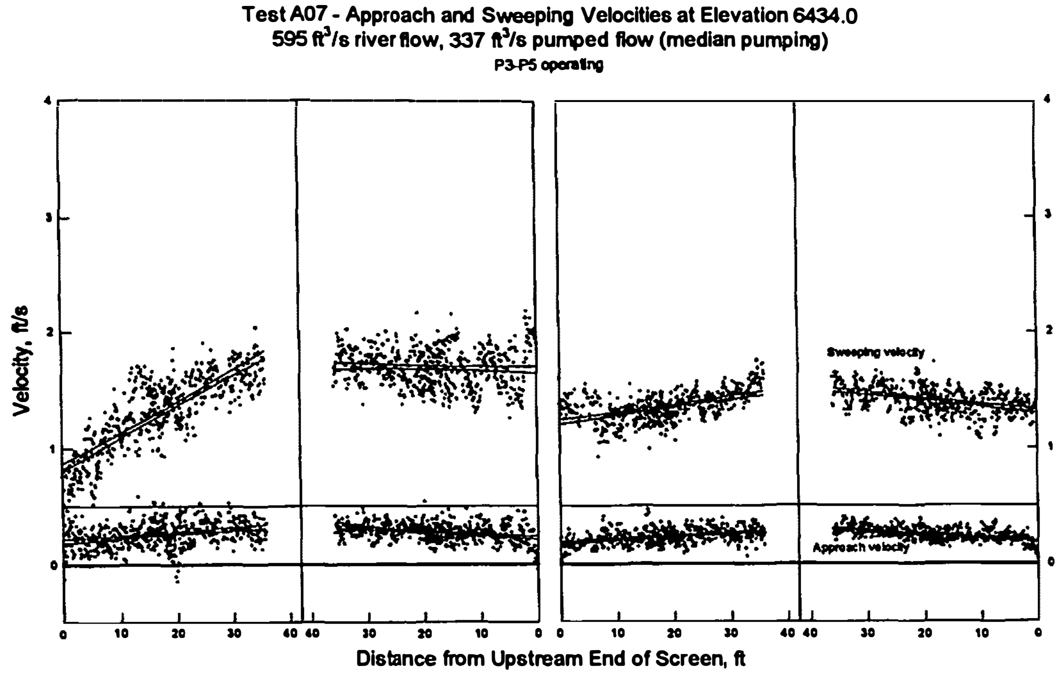

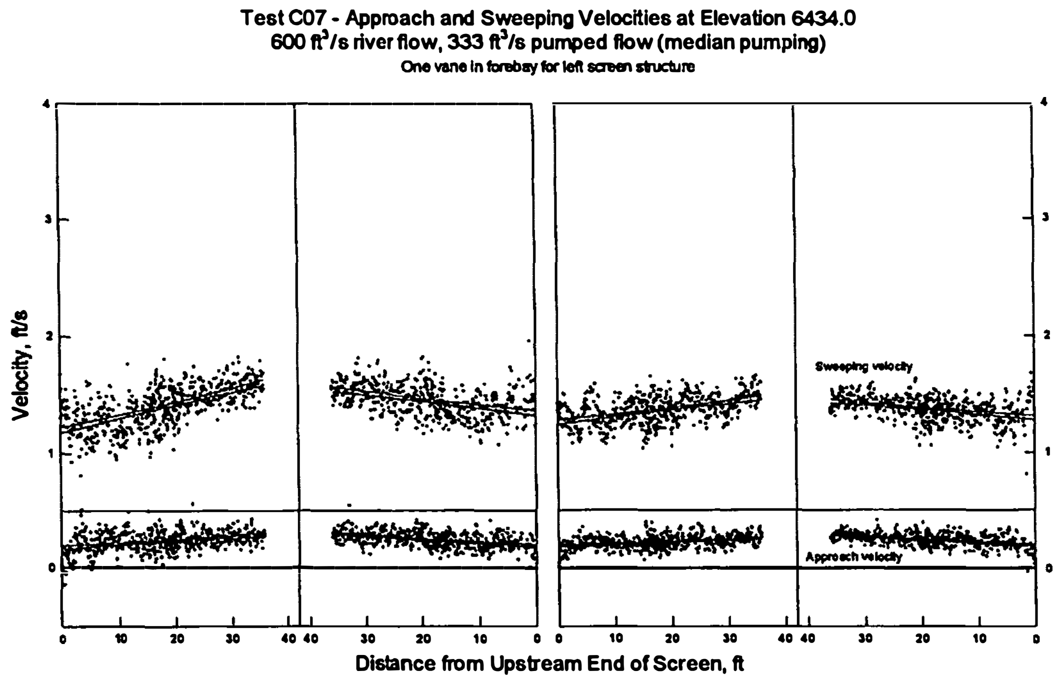

Figure 17. — Comparison of fish screen velocity fields at 600 ft^3/s river discharge and median pumping rate (~335 ft^3/s) for the initial design (top) and with vane A installed. These plots also appear at larger scale in Appendix A.

Tests A04 and B04 (see figures in Appendix A) also illustrate the effect of the turning vanes, and show variations of the screen velocity fields with depth. With two vanes installed in test B04 the turbulence levels in the left hand screen bay are much lower and the sweeping velocity distribution along the screen is much more uniform. Test B04 does exhibit higher turbulence levels in the right hand screen bay, but this is due to a slight variation in pumping plant discharge which produced a lower water surface elevation on the screens;

there were no physical changes to the right hand screen structure or approach channel between the two tests. Test B04 also exhibits clockwise secondary currents that intensify toward the downstream end of the V-screen structures. The secondary currents produce non-uniform vertical profiles of the approach velocity. The secondary current is strongest in the right-hand bay, which is curious because there was no secondary current evident in test A04, which had an identical configuration for the right bay. This behavior was not reproduced in test C05, which was also a similar operating condition. The existence of this secondary current is apparently sensitive to unknown factors that could not be reproduced in subsequent tests.

Balancing Flows at High River Stage

Testing at 2000- and 4000- ft^3/s river flows was initially conducted with the intake gates fully lowered. This testing revealed an uneven distribution of flows between the left-hand and right-hand fish screen bays (e.g., test A12). At a river flow of 2000 ft^3/s, about 59 percent of the pumping plant flow was through the left-hand bay and 41 percent was through the right-hand bay (determined from the fish screen velocity measurements). At 4000 ft^3/s, the split was about 75 percent to 25 percent. These flow splits were initiated at the intake structure, where the main flow of the river began to separate from the right bank as the discharge increased. This put the upstream portion of the intake structure in a slack-water zone. The flow splits were essentially independent of the pumping plant flow rate and different pump sequencing combinations. Figure 18 illustrates the increasing disparity between flows through the two fish screen structures as the river discharge increases.

The uneven distribution of flows between the two bays led to several problems, including approach velocities that far exceeded the 0.5 ft/s criteria in the left-hand screen bay (e.g., test D80 at 4000 ft^3/s river flow), high turbulence levels in the left-hand bay, and low sweeping velocities in the right-hand bay. This uneven flow distribution also had a strong impact on the flow conditions in the main sump. Furthermore, the unequal flow distribution along the length of the intake structure trashracks was undesirable from a recreational standpoint.

Efforts were made to equalize the flow distribution between bays by adding baffles (head loss elements) downstream of the left-hand screen structure. This was moderately successful at the 2000-ft^3/s river flow condition, but could not overcome the severe problems at 4000 ft^3/s. Observations of the flow in the river approaching the intake showed that the uneven flow split was originating in the river; as the discharge was increased the main river flow was separating from the right bank upstream of the intake, making the upstream intake bays ineffective. Normally, realignment of the right bank might be required to correct this problem, but the flow could be redistributed in this intake structure through operation of the intake structure weir gates.

The six intake structure weir gates are operated manually in the model, and can be raised and lowered independently or as a single unit. Raising the gates in a staggered fashion, with the most downstream gate raised the highest, proved to be a very effective means for equalizing the flow distribution, as confirmed by velocity measurements in the fish screen bays. One consequence of using the gates in this manner is increased turbulence on the fish screen panels, especially in the left bay. Figure 19 shows the velocity fields measured during test E42, in which the intake gates were used to equalize the intake flow distribution at a river discharge of 4000 ft^3/s

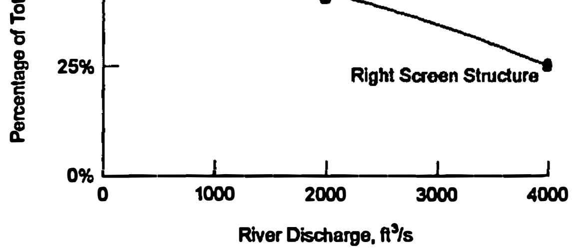

Figure 18. — Flow split as a function of river discharge with intake weir gates fully lowered.

and maximum pumping plant discharge. Although turbulence levels are much greater than with the gates lowered, the approach velocities are much improved. As an example of the degree of staggering required, for this test the elevations of the gate leaves were as follows, from upstream to downstream:

Gate Number (1 is most upstream)	1	2	3	4	5	6
Gate Leaf Elevation, feet	6440.56	6440.88	6441.06	6441.31	6441.50	6441.63

The best criteria to use in the model and in the field for operating the intake gates will be to maintain equal water surface elevations on the upstream sides of the two fish screen structures. Equal water surface elevations at these two points indicate equivalent head losses through each fish screen, and thus equal flowrates through the screens. At 4000 ft^3/s river discharge, with the gates fully lowered, the two prototype water surface elevations differed by 0.145 ft (1.74 inches), and the flow split was approximately 75 percent to 25 percent. Using the intake gates to equalize the flow (test E42), a water level difference of 0.015 ft (prototype) was maintained, which produced a flow split of about 53 percent to 47 percent. It should be noted that there is an upper limit to the river flow at which the gates can be used to equalize the intake structure flow, since at some point the river level becomes so high that the gates cannot be raised enough to control the flow.

Recommended Design

The recommended design uses a single additional turning vane in the curved channel connecting the intake structure to the fish screen structures. The turning vane has a tapered tail (downstream end) to minimize the generation of vortex streets in the flow approaching the fish screens. The intake weir gates should be fully lowered for river flows of about 1500 ft^3/s or less. Test C05 (see figure in Appendix A) shows the very uniform velocity field approaching the fish screens for a river flow of 1000 ft^3/s and pumping rate of 500 ft^3/s, the median pumping rate for that river discharge. For river flows greater than 1500 ft^3/s, the gates should be raised and controlled so that equal water surface elevations are maintained in the forebays upstream of each V-screen structure. Tests E42 (median flow) and E4x (maximum flow) illustrate the fish screen velocity fields that can be expected for this type of flow condition. Although turbulence levels were high, raising the gates corrected the uncontrolled 75/25 percent flow split to about a 47/53 percent flow split for test E4x.

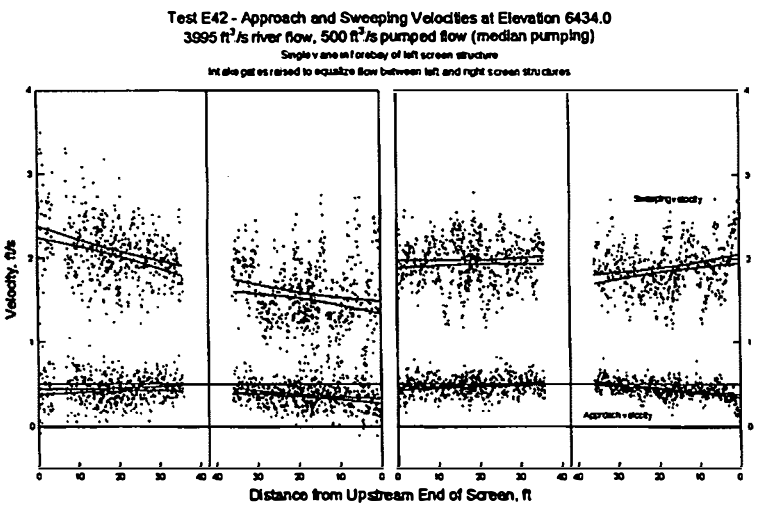

Figure 19. — Fish screen velocity fields measured during test E42, with the intake weir gates raised and staggered to equalize flow between the left and right fish screen structures.

SUMPS

Flow conditions in the sumps were evaluated visually for several different operating conditions. The objective of these observations was to identify poor flow conditions approaching and entering the penstock intakes, correct problems, and make modifications that might provide economic savings during construction or operation of the plant. Dead areas in the sump and vortex structures were the primary focus of most of the work.

Vortex structures in the model can be classified on a numerical scale developed by Alden Research Laboratories (ARL), shown in figure 20. Modeling of vortex flows has been found to very indicative of prototype performance if the model is operated according to Froude-scaling criteria, and the model Reynolds number for the submerged intake is at least 3×10^4. The Reynolds number for this model varied from about 2.4×10^4 to 3.2×10^4, depending on discharge and submergence.

In general, the flow in the sumps is characterized by traveling, transient vortex structures of types 1 or 2, and some large-scale circulation patterns (on the order of the sump dimensions) for specific operating conditions. The initial sump design exhibited several relatively dead zones in the downstream end, back corners, and along the floor immediately downstream of the fish screen structures. Some of these dead zones can be eliminated with the added benefit of reduced excavation volume for sump construction. Figures 4 and 6 show the initial sump design; the penstocks are labeled 1 through 5 from the upstream to downstream end of the sump for ease of reference in the discussion that follows.

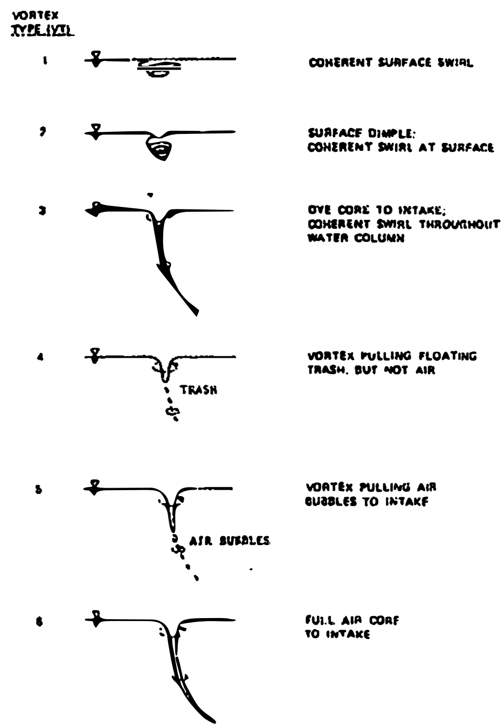

Figure 20. — ARL vortex type classification (from Knauss, 1987).

Phase I - Stage A Operations

Durango Pumping Plant will be constructed and operated in two distinct phases that correspond to three phases/stages of the Animas-La Plata Project, designated Phase I - Stage A, Phase I - Stage B, and Phase II. The pumping plant will have a reduced capacity during Phase I - Stage A, and full capacity during Phase I - Stage B and Phase II. During Phase I - Stage A, only the vertical turbine pumping units will be installed, and plant discharge will be limited to about 80 ft^3/s. The most downstream penstock in the sump will be used to deliver water to the secondary sump supplying the vertical turbine units. All other penstocks will have zero flow. When the model was operated in this manner, clockwise rotation was observed immediately in front of penstock 5, with a persistent type 3 or type 4 vortex. Testing showed that moving the downstream wall of the sump closer to the edge of penstock 5 eliminated this vortex, but not until the downstream wall of the sump nearly coincided with the edge of the penstock entrance.

Phase I - Stage B and Phase II Operations

During Phase I - Stage B and Phase II of the project, the four large spiral case pumps will deliver the majority of the flow to Ridges Basin Reservoir. The vertical turbine units will be used only when river levels and pumping rates are low, or to supply small increments of flow in combination with one or more of the spiral case units. During this phase it will be unusual for the most downstream penstock to experience flow at the same time that all four spiral case units are operating. The dominant flow pattern during these types of operations is shown in figure 21. The flow tends to separate from the left wall of the sump approximately opposite the intake for penstock 3. There is then a counterclockwise rotation in the downstream end of the sump, but this does not become well-organized and never produces anything more than transient surface dimples (vortex type 2). This flow condition suggests that the sump could be narrowed, and this was tested in the model with some success. The separation from the left wall could not be totally eliminated.

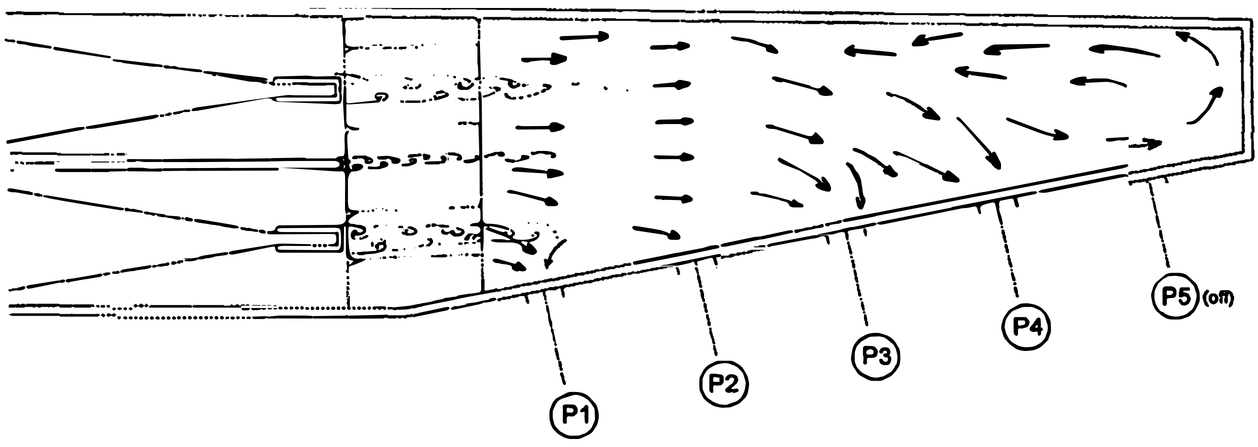

Figure 21. — Dominant flow patterns in the main sump with pumps 1-4 running, and penstock 5 not operating. This should be a typical pumping combination when supplying maximum flowrates during Phase I - Stage B and Phase II of the project. Vortex streets are created by the blunt-tailed divider walls and fish bypass vaults. A reverse-eddy forms in the downstream back corner of the sump.

Need for Balanced Inflow

As described previously, flow distribution between the left and right screen structures was very uneven at high river stages with the intake gates lowered. In addition to the problems this created for the fish screens, it also caused the formation of a large clockwise circulation pattern in the main sump downstream of the screens. The shear zone between the high flow through the left screen structure and the low flow through the right screen structure generated type 3 and type 4 vortex structures in front of penstocks 1 and 2 (the two penstocks nearest to the fish screens). These vortex structures could intensify in the prototype to form air-core vortices that would entrain air into the penstocks.

Operation of the intake gates to equalize flows between the two screen structures returned the sump to a more uniform operating condition and eliminated the strong vortex structures in front of the first two penstocks. Overall, maintaining approximately equal flows through the screen structures is the most important consideration for obtaining good sump flow conditions.

Sump Improvements

Tapered Tails on Fish Screen Structures

Initial operation of the model showed that the blunt tails (downstream ends) of the fish bypass entrance structures and the dividing wall between the two screen structures were generating vortex streets in the sump. Flow alternately separates from opposite corners of such blunt objects, producing alternating vortex structures that travel downstream into the sump. This is a very common hydraulic phenomenon. Although these vortex structures did not appear to be a serious problem, they are easily remedied. Tapered tails were added to these structures with a 6:1 slope away from the flow. These tail pieces were not brought to a point, but rather were squared off when they reached a prototype width of 6 inches. Adding these tails eliminated nearly all surface vortices generated by these structures.

Floor Transition Entering Main Sump

The elevation view of the original sump design shows a steep-sloped floor transition from the fish screen area to the floor of the sumps. This transition is so steep that the flow tends to separate from the floor, especially on the left side of the sump. This produces a large region of no-flow or reverse-flow near the floor in the wake of this transition. On the right side of the sump, the influence of penstock 1 in close proximity to this transition helps to keep the flow attached to the floor. This problem was addressed in the model by installing a warped floor transition. The concept was to extend the transition further downstream on the left side, while maintaining the original floor slope at the right side. This modification successfully eliminated the separation from the floor on the left side. Because of the difficulty of constructing a warped floor section, other similar modifications should be studied further during final design of the pumping plant.

Modified Left Wall and End Wall Alignments

As mentioned previously, there were dead zones in the far downstream end and along the left wall of the sump in the original design. The end of the sump was moved in and the left wall was also angled in, beginning at about the point where initial flow separation was observed. Figure 22 shows a suggested sump configuration based on the observations of flow in the model. Some aspects of this configuration may be undesirable from a construction standpoint, but similar modifications should be incorporated into the final design. There may be a need for some additional model testing once final design work begins.

INTAKE STRUCTURE VELOCITY FIELDS

The velocity field approaching the intake structure was an important concern of the model study because of the possibility that rafts, kayaks, and other boats could be drawn toward the intake structure, placing boaters in a potential danger zone. Although safety features will be included in the design to assist people with egress out of the intake structure area, it is still desirable to limit the potential for people to be drawn into the area. The model was used to help quantify the potential for boats to be drawn toward the intake, and to investigate alternative operational procedures that might reduce the risk of boats being drawn up against the intake.

In general, the attraction flow generated by the intake structure increases as the river flow decreases and the pumping rate increases. General flow patterns and the strength of the attracting velocity field were investigated using model rafts and boats floated toward the intake structure. Boats and rafts that approached the intake structure near the left bank of the river floated safely past the intake. Boats and rafts that started from the right bank of the river were always drawn to the intake and were held against the trashracks by the

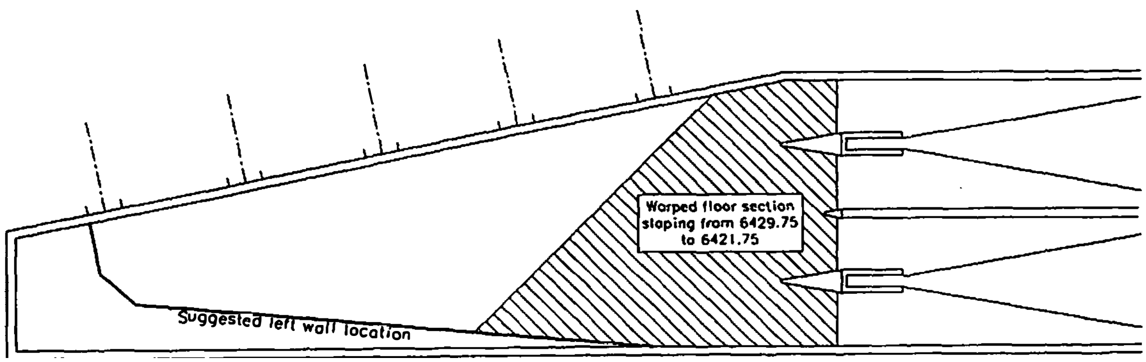

Figure 22. — Suggested configuration of the main pumping plant sump, showing changes to the left and downstream walls, floor transition entering the sump, and streamlining of structures upstream of the sump.

flow. Boats starting from intermediate points between the left and right bank could either float downriver past the intake, or be drawn into the intake. As the river discharge increases and/or as the pumping rate decreases, the location of the intermediate point separating the two outcomes moves further toward the right bank of the river. For river discharges of 2000 ft^3/s or more, boats will not be drawn up against the intake unless they begin their approach to the intake from very near the right bank. Of course, a person actively propelling their craft could resist and avoid the velocity field drawing them toward the intake structure, although the degree to which they could do this would depend on their boating experience, physical condition, and other intangible factors.

These observations are similar to those made in the study of the original intake structure design. Although it is difficult to quantify these observations, the intensity of the flow field in the new design appeared to be lower than that of the old design, primarily due to the increased length of the intake structure, which distributes the total withdrawn flow over a greater length of the river bank. The few point velocity measurements made in the previous model study confirm this observation.

In an attempt to quantify the flow field, the acoustic doppler velocimeter (ADV) probe was used to measure the near-surface velocities along two parallel lines 10 ft away from the intake and 25 ft away from the intake (fig. 23). Velocity profiles were measured along several overlapping traverse lines. These data were then combined into a single data set and curve-fit to determine the average velocity vector as function of distance along each line. These curve-fitted velocity vectors were then plotted to scale on a plan view of the site, and are shown in the figures included in Appendix B.

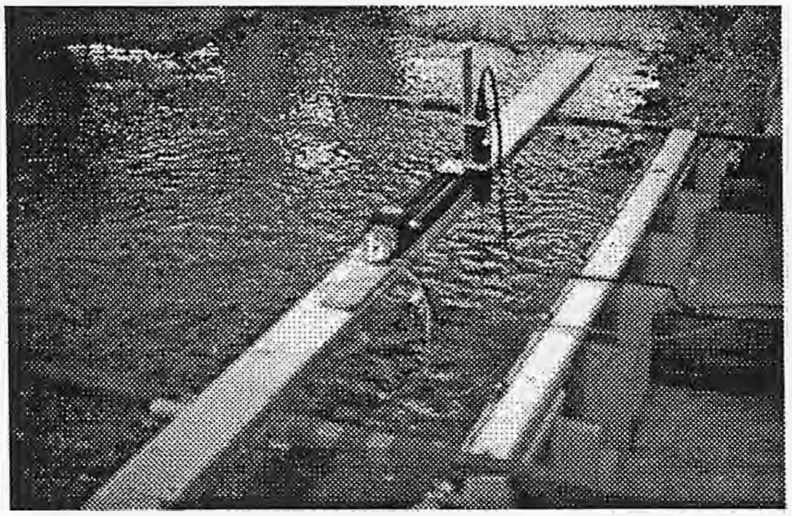

Figure 23. — ADV probe in position for measurement of velocity fields approaching the intake structure.

The operation of the intake structure weir gates influences the uniformity of flow through the bays of the intake structure and the velocity field approaching the structure. At high river discharges there are locally high velocities (i.e., hot spots) on the downstream bays of the intake structure. Raising the intake gates to equalize flows through the intake bays and fish screens has the added benefit of eliminating these hot spots.

1000 ft^3/s, Median and Maximum Pumping

Figure B-1 shows the near-surface velocity vectors at the 1000 ft^3/s river discharge, for both the median pumping rate (500 ft^3/s) and the maximum pumping rate (approx. 670 ft^3/s). The peak velocity at the median pumping rate is about 3 ft/s, directed at a 50° angle into the intake (90° being normal to the intake). At the maximum pumping rate the peak velocities are about 4 ft/s, also at a 50° angle. The intensity of the velocity field on the fourth and fifth bays of the intake, and the downstream extent and strength of the velocity field 25 ft away from the intake are the most striking differences between these two flow conditions.

2000 ft^3/s, Maximum Pumping, With and Without Gates Raised

Figure B-2 shows the near-surface velocities for a river flow of 2000 ft^3/s and the maximum pumping rate, with the intake gates fully lowered, and with the gates raised to equalize the flow as described earlier. The downriver component of velocity is much higher than for the 1000 ft^3/s flow, with the velocity vectors 10 ft from the intake oriented at 30° to the intake face. With the gates fully lowered, the highest velocities are on the downstream end of the intake structure. With the gates raised, velocities are more uniform along the length of the intake, with the peak velocities toward the upstream end of the intake.

5000 ft^3/s, Maximum Pumping, With and Without Gates Raised

Figures B-3 shows the near-surface velocities for a 5000 ft^3/s river flow at the maximum pumping rate. At 25 ft from the intake the velocity field is nearly parallel with the intake structure. Even at 10 ft from the intake, the approach flow is oriented at only a 15° to 20° angle from the intake face; sweeping velocities past the structure are 2.75 to 3.75 times as high as the velocity component toward the structure.

REFERENCES

Knauss, Jost, *Swirling Flow Problems at Intakes*, International Association for Hydraulic Research, Hydraulic Structures Design Manual 1, A.A. Balkema, Rotterdam, 1987.

Pearce, Robert O., and Randall T. Lee, "Some Design Considerations for Approach Velocities at Juvenile Salmonid Screening Facilities," American Fisheries Society Symposium 10.237-248, 1991.

Wahl, Tony L., *Hydraulic Model Studies for Durango Pumping Plant: 1992-1994*, PAP-655, U.S. Bureau of Reclamation, Water Resources Research Laboratory, Denver, Colorado.

ACKNOWLEDGMENTS

Numerous staff in the WRRL and Reclamation contributed to these studies. Mr. Pat Page in the Durango Office provided background information, arranged for field activities to support the model tests, and provided helpful review comments on this report. Mr. Warren Frizell of the WRRL, and Mr. Rick Christensen of the Mechanical Equipment Group in Denver, also reviewed the report and provided helpful suggestions on design alternatives, testing and analysis procedures throughout the study. Construction of the various physical model facilities was performed by Mr. Warren King, Mr. Richard Cuny, Mr. Dane Cheek, and Mr. Doug Huske. Mr. Lee Elgin and Mr. Jerry Fitzwater provided valuable support in assembling instrumentation and collecting data.

APPENDIX A - FISH SCREEN VELOCITY FIELD FIGURES

Table A1. — Fish Screen Test Conditions

Test	Prototype River Q	Model River Q	Pump Discharges					Fish Bypasses		Total Pumped Q	Total Intake Q	Gate setting	Data Collected	Comments
			P1	P2	P3	P4	P5	Left	Right					
A01	974	1.953	0	125	125	125	125	32	33	500	565	Gates up, undular flow	Elev. 6434 only	Median pumping
A02	979	1.963	0	126	127	126	126	32	33	505	570	Gates down	Elev. 6434 only	Median pumping
A03	1001	2.006	0	122	120	120	120	32	32	482	546	Gates up, plunging flow	Elev. 6434 only	Median pumping
A04*	948	1.901	70	153	152	151	136	31	32	662	725	Gates down	All elevations	Max pumping
A05	1007	2.019	125	125	125	125	0	33	33	500	566	Gates down	Elev. 6434 only	Median pumping
A06	797	1.597	148	148	148	0	0	35	35	444	514	Gates down	Elev. 6434 only	Median pumping
A07	595	1.193	0	0	122	120	95	33	33	337	403	Gates down	Elev. 6434 only	Median pumping
A08	498	0.999	0	0	121	122	100	32	32	343	407	Gates down	Elev. 6434 only	Max pumping
A09	399	0.800	125	0	0	0	35	33	33	160	226	Gates down	Elev. 6434 only	Median pumping
A10	303	0.608	125	0	0	0	0	33	33	125	191	Gates down	Elev. 6434 only	Median pumping
A11	1980	3.969	125	125	123	125	0	33	32	498	563	Gates down	Elev. 6434 only	Median pumping
A12	1980	3.969	159	158	159	162	35	33	32	673	738	Gates down	Elev. 6434 only	Max pumping
B04*	948	1.900	148	150	150	152	70	32	32	670	734	Gates down	All elevations	Max pumping
B05	998	2.000	125	126	126	126	0	33	34	503	570	Gates down	Elev. 6434 only	Median pumping
B5b	998	2.000	126	127	127	126	0	16.5	16.5	506	539	Gates down	Elev. 6434 only	Median pumping
B06	798	1.600	150	150	150	0	0	33	33	450	516	Gates down	Elev. 6434 only	Median pumping
B07	599	1.200	0	0	120	120	95	33	33	335	401	Gates down	Elev. 6434 only	Median pumping
B08	499	1.000	0	0	120	120	100	33	33	340	406	Gates down	Elev. 6434 only	Max pumping
B12	1995	4.000	160	160	160	161	35	32	32	676	740	Gates down	Elev. 6434 only	Max pumping
B13	1996	4.002	158	158	160	161	0	33	33	637	703	Gates down	Elev. 6434 only	Near max pumping
B14	1996	4.002	0	159	162	160	153	33	33	634	700	Gates down	Elev. 6434 only	Near max pumping
C05*	1000	2.005	122	125	126	128	0	32	32	501	565	Gates down	All elevations	Median pumping
C07	600	1.203	0	0	118	120	95	32	32	333	397	Gates down	Elev. 6434 only	Median pumping
D01	1996	4.002	132	135	135	136	130	33	33	668	734	Gates down	Elev. 6434 only	Max pumping
D06	798	1.600	147	148	147	0	0	31	32	442	505	Gates down	Elev. 6434 only	Median pumping
D08	500	1.002	0	0	117	117	100	28	28	334	390	Gates down	Elev. 6434 only	Max pumping
D12	1996	4.002	157	160	161	161	30	33	33	669	735	Gates down	Elev. 6434 only	Max pumping
D80	3995	8.009	153	153	157	157	70	33	33	690	756	Gates down	Elev. 6434 only	> Max pumping
D81	3995	8.009	125	125	125	125	0	33	33	500	566	Gates down	Elev. 6434 only	Median pumping
E4x	3995	8.009	132	132	132	138	127	34	33	661	728	Gates raised to equalize flow	Elev. 6434 only	Max pumping
E42	3995	8.009	125	125	125	125	0	33	33	500	566	Gates raised to equalize flow	Elev. 6434 only	Median pumping

Test A01 - Approach and Sweeping Velocities at Elevation 6434.0
974 ft^3/s river flow, 500 ft^3/s pumped flow (median pumping)
Initial design - Gates raised, undular flow

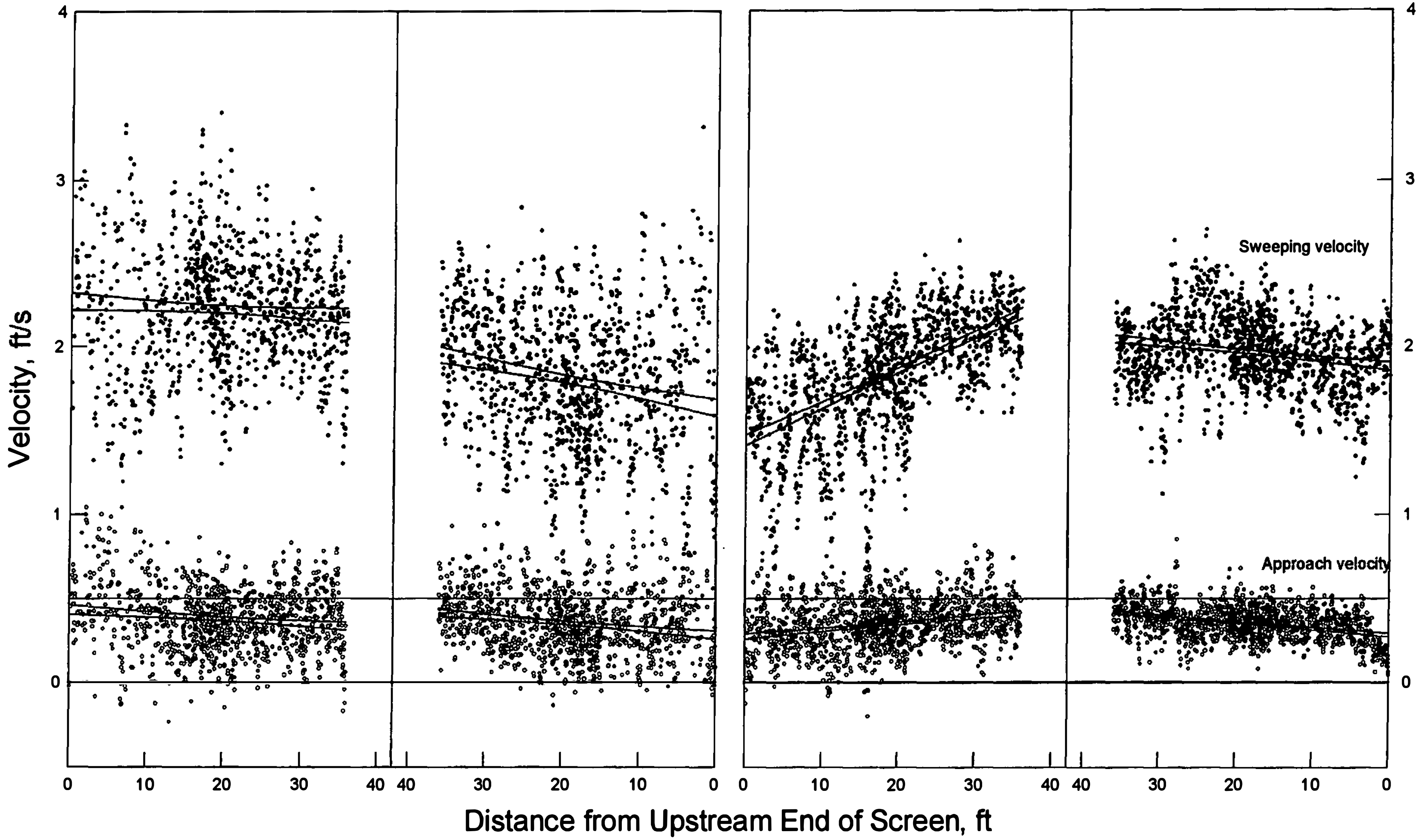

Test A02 - Approach and Sweeping Velocities at Elevation 6434.0
979 ft^3/s river flow, 505 ft^3/s pumped flow (median pumping)
Initial design - Gates fully lowered

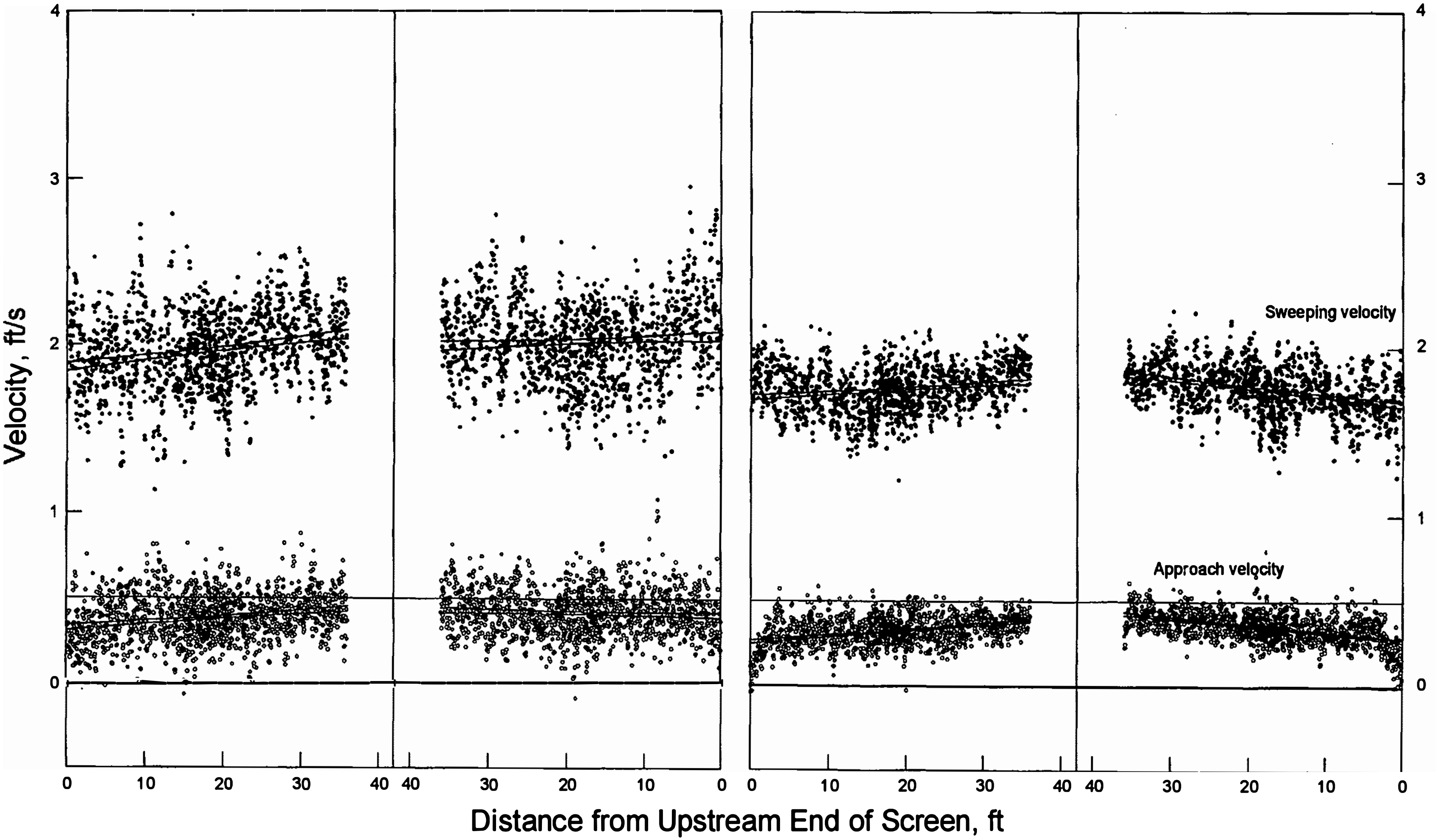

Test A03 - Approach and Sweeping Velocities at Elevation 6434.0
1001 ft^3/s river flow, 482 ft^3/s pumped flow (median pumping)
Initial design - Gates raised, plunging flow

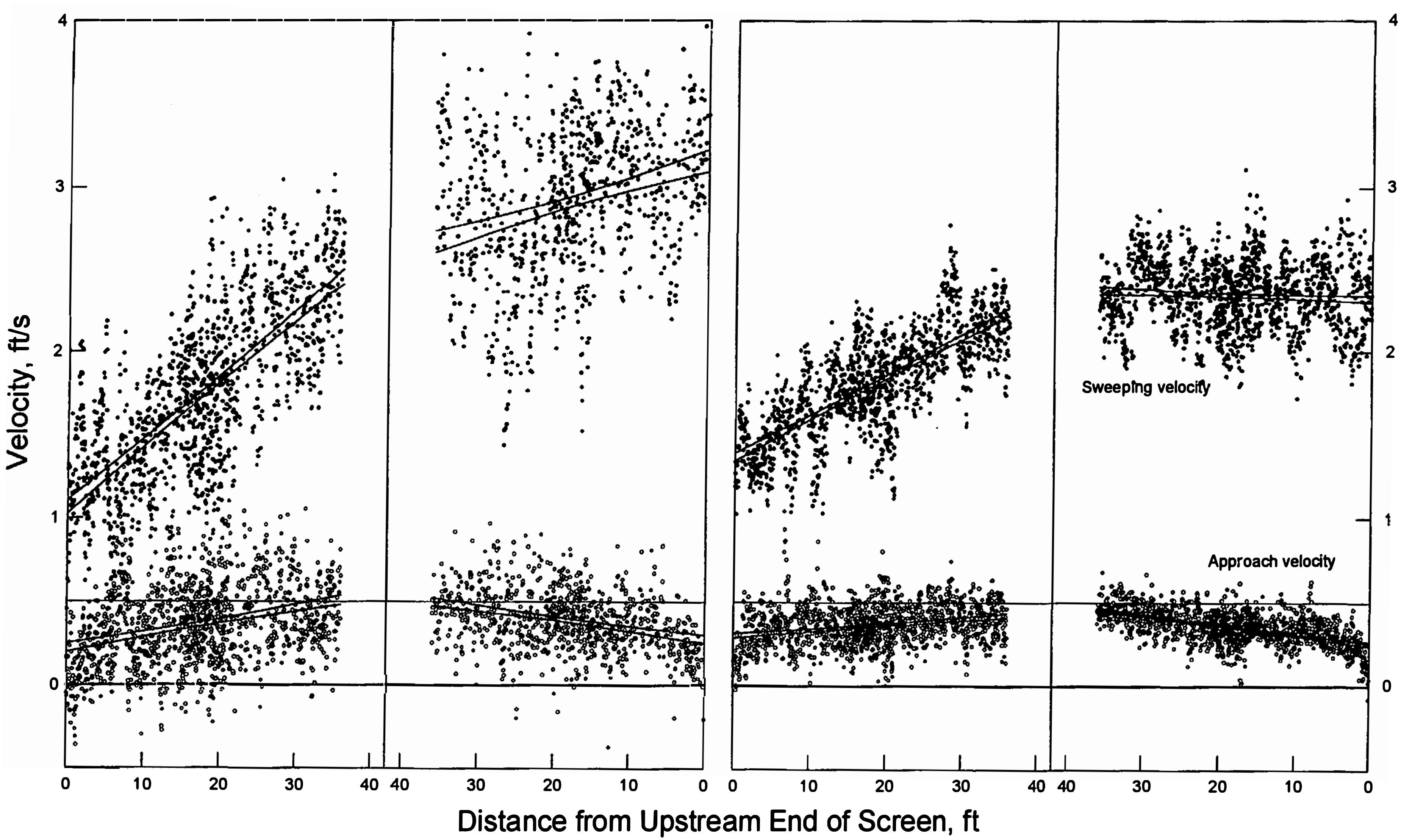

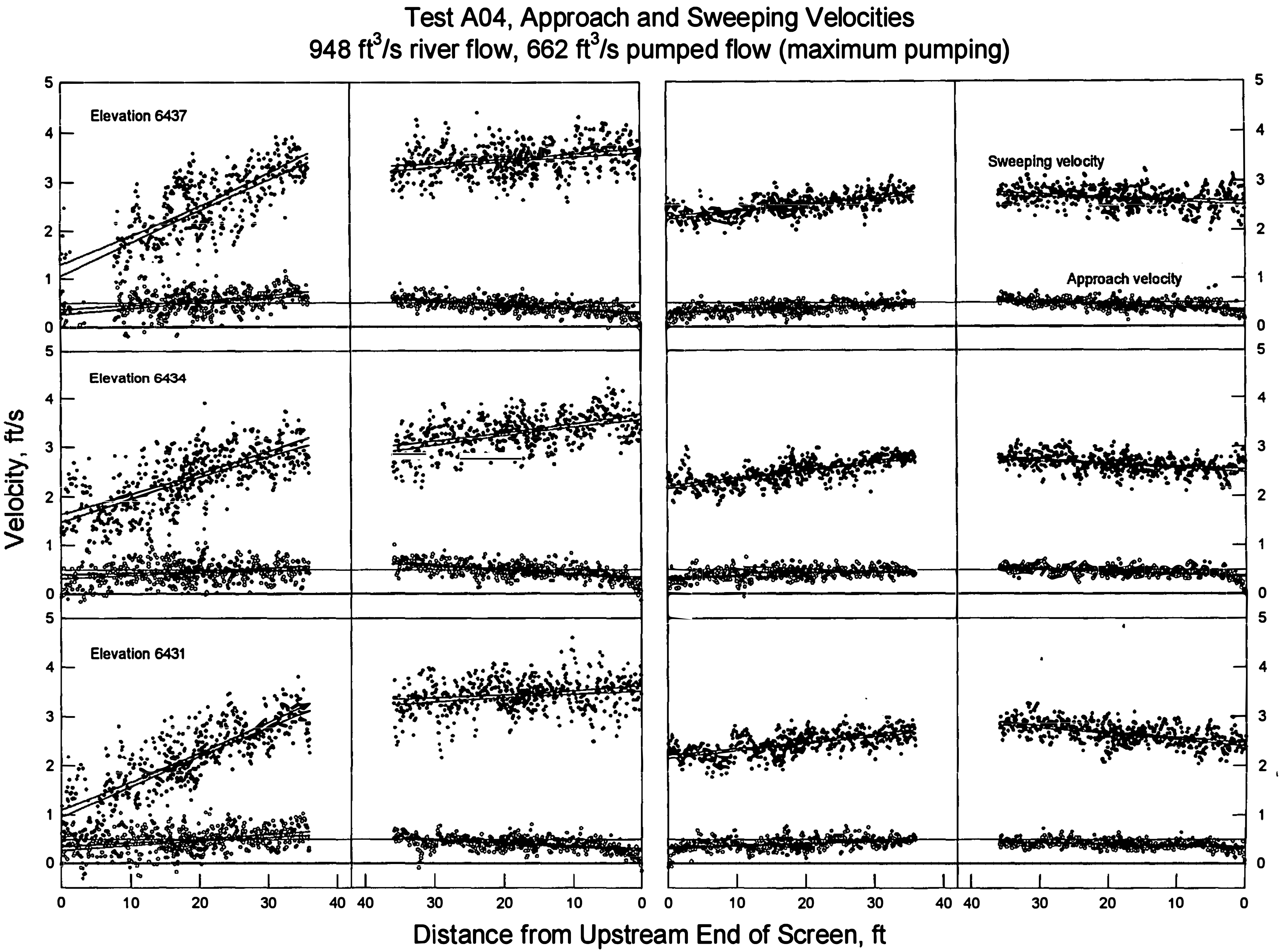

Test A04, Approach and Sweeping Velocities
948 ft³/s river flow, 662 ft³/s pumped flow (maximum pumping)
Elevation 6437
Elevation 6434
Elevation 6431
Sweeping velocity
Approach velocity
Velocity, ft/s
Distance from Upstream End of Screen, ft

Test A05 - Approach and Sweeping Velocities at Elevation 6434.0

1007 ft^3/s river flow, 500 ft^3/s pumped flow (median pumping)

P1-P4 running at 125 ft^3/s each, P5 is not running

Compare to A01, A02, and A03, in which P2-P5 were running

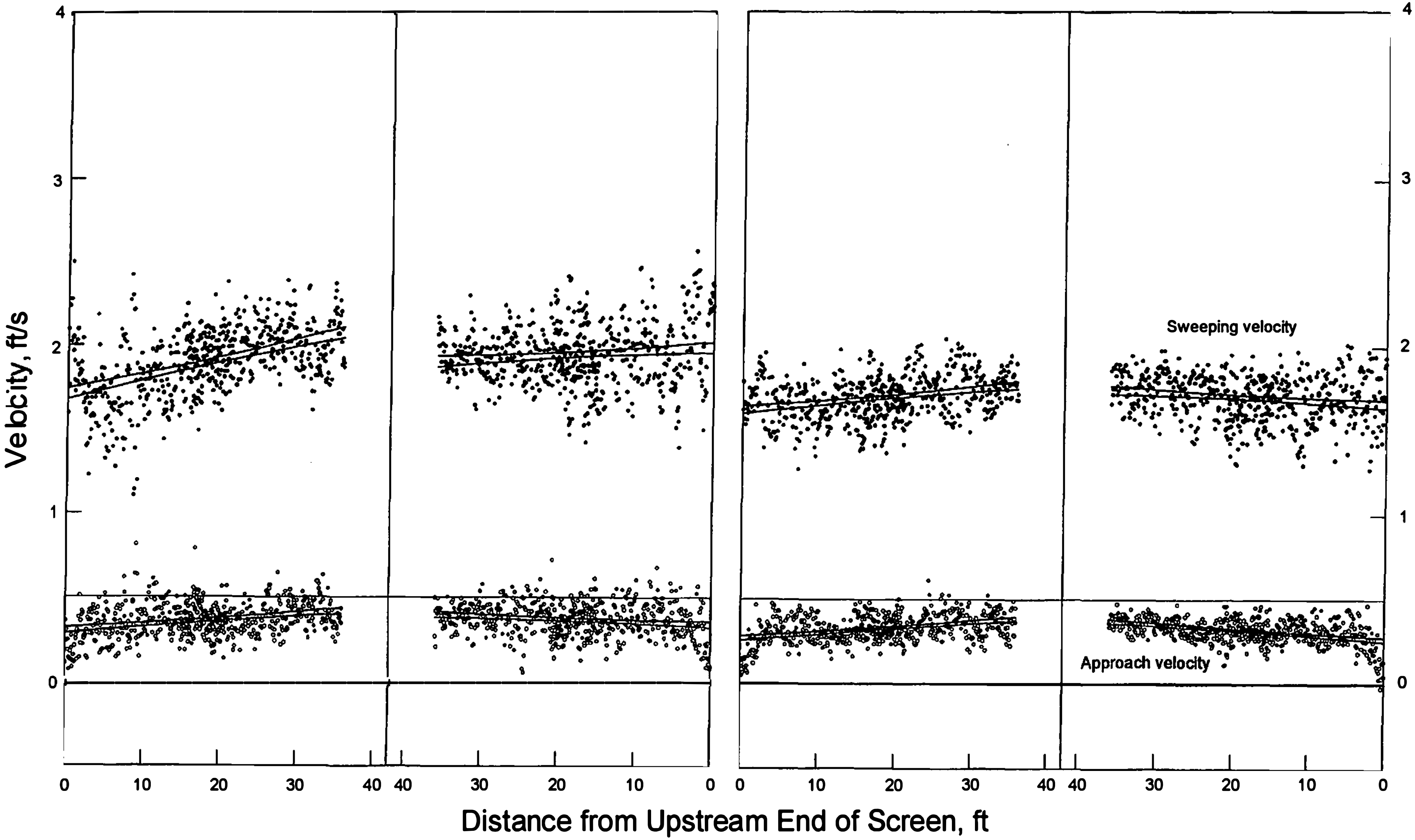

Test A06 - Approach and Sweeping Velocities at Elevation 6434.0
797 ft^3/s river flow, 444 ft^3/s pumped flow (median pumping)
P1-P3 running at 148 ft^3/s each, P4 and P5 are not running

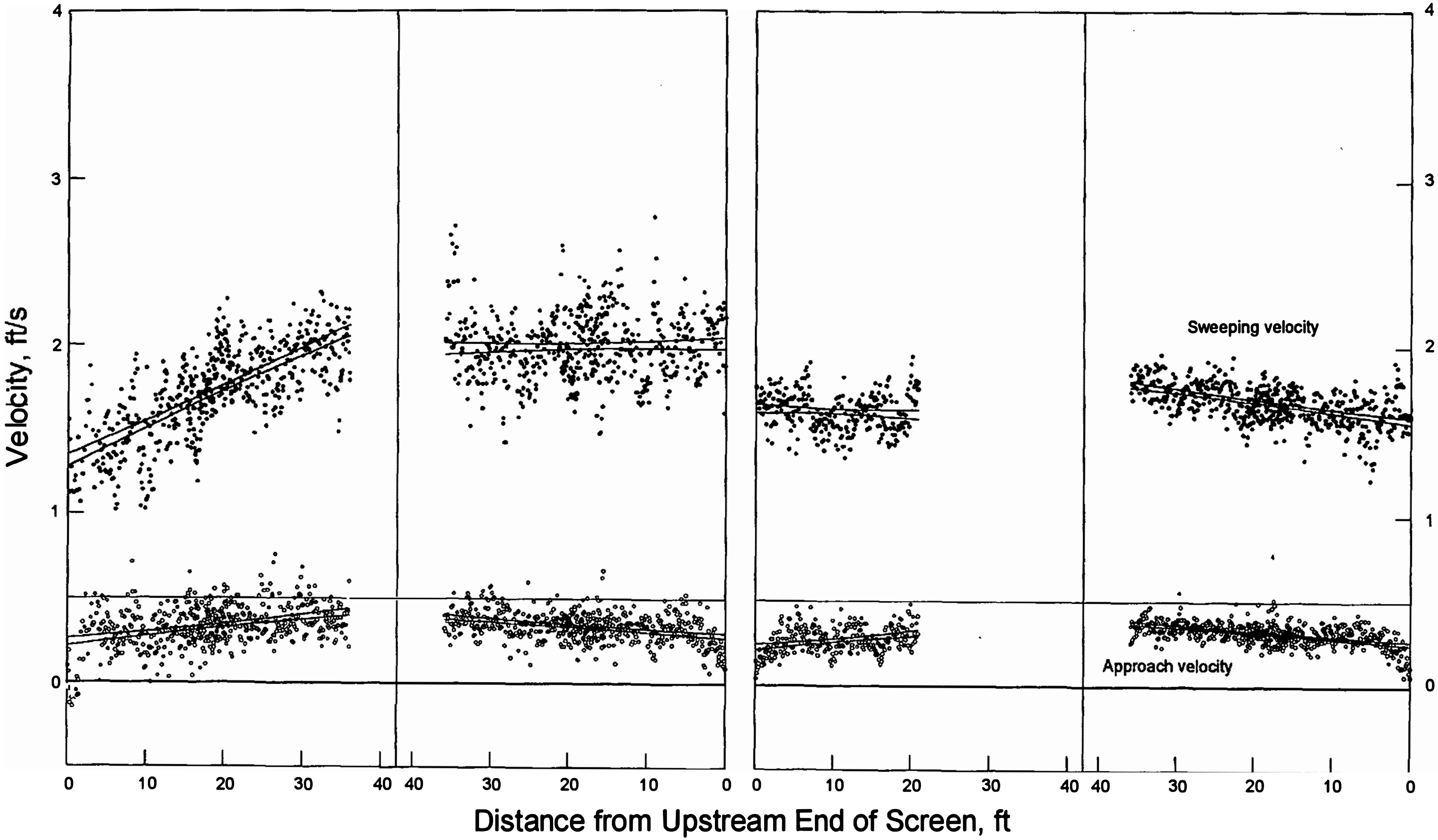

Test A07 - Approach and Sweeping Velocities at Elevation 6434.0
595 ft^3/s river flow, 337 ft^3/s pumped flow (median pumping)

P3-P5 operating

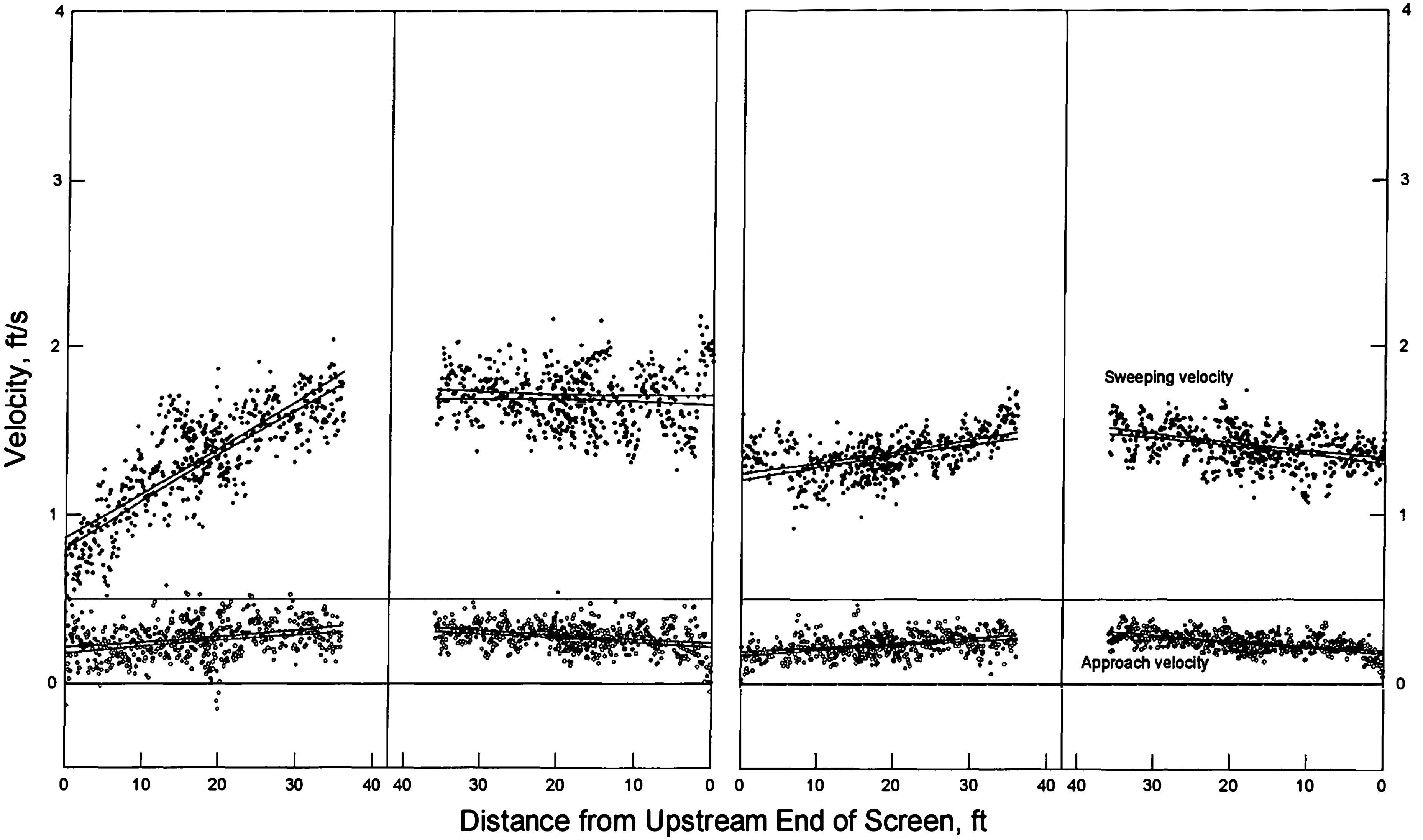

Test A08 - Approach and Sweeping Velocities at Elevation 6434.0
498 ft^3/s river flow, 343 ft^3/s pumped flow (maximum pumping)
P3-P5 operating

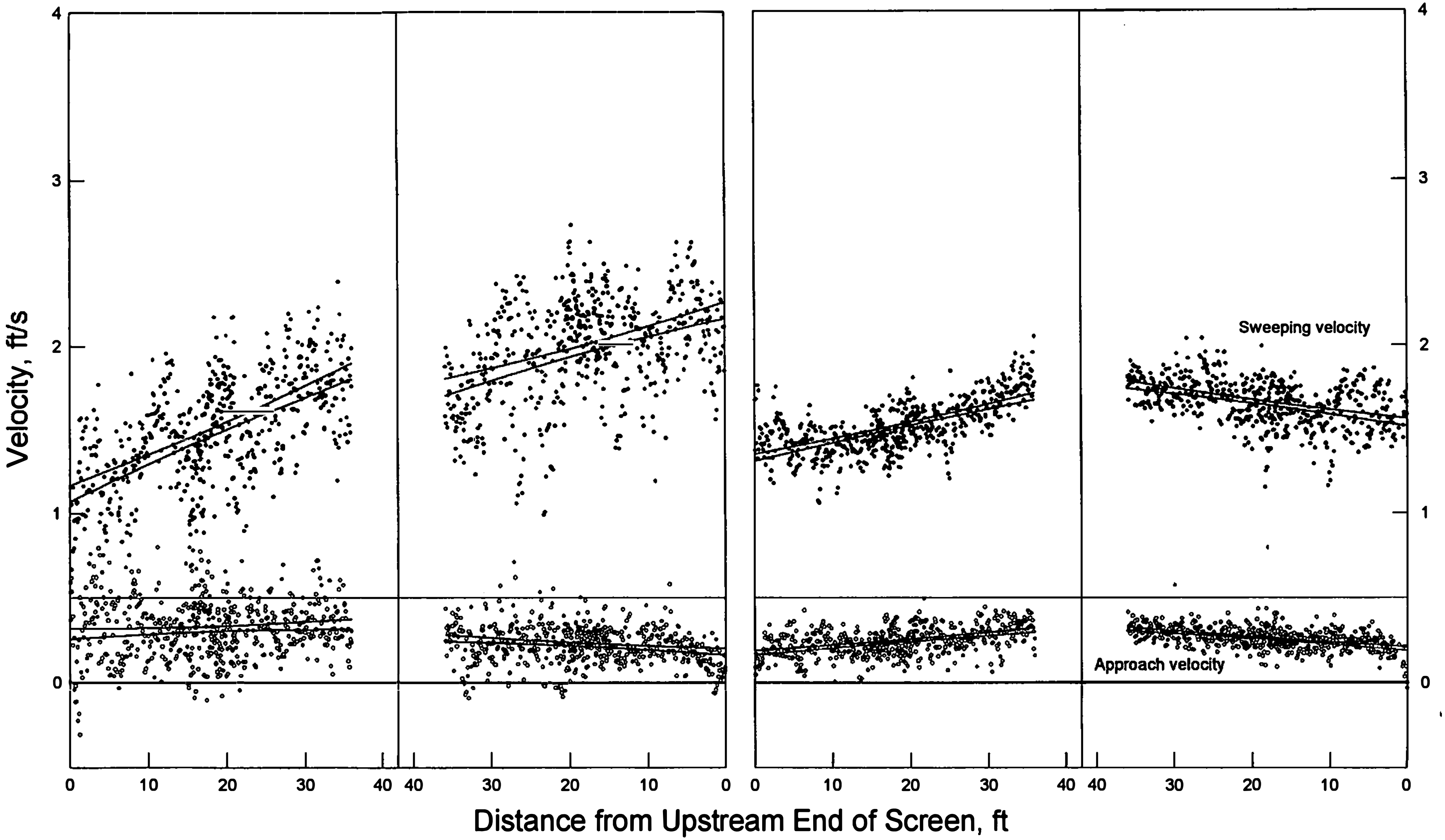

Test A09 - Approach and Sweeping Velocities at Elevation 6434.0
399 ft^3/s river flow, 160 ft^3/s pumped flow (median pumping)

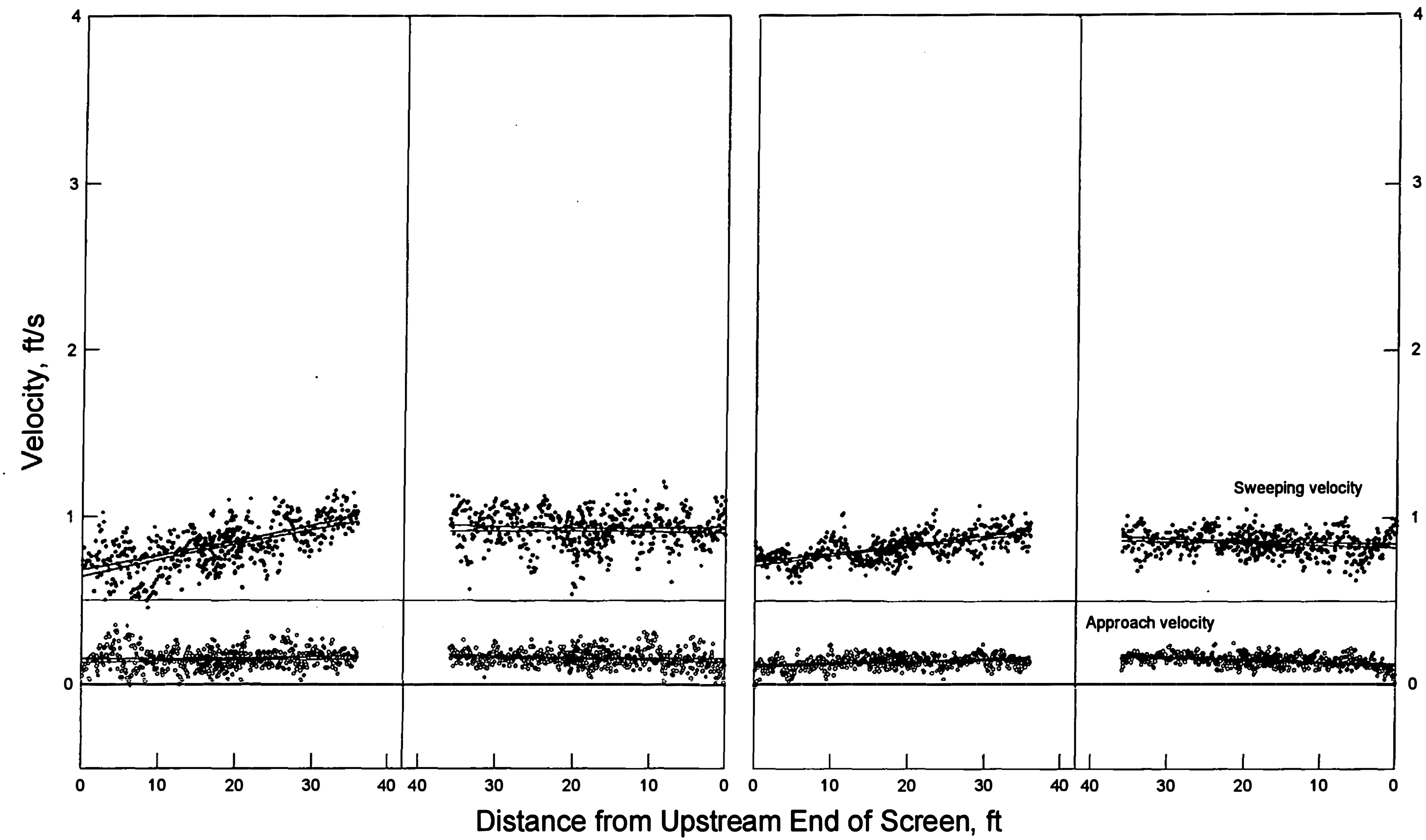

Test A10 - Approach and Sweeping Velocities at Elevation 6434.0
303 ft^3/s river flow, 125 ft^3/s pumped flow (median pumping)

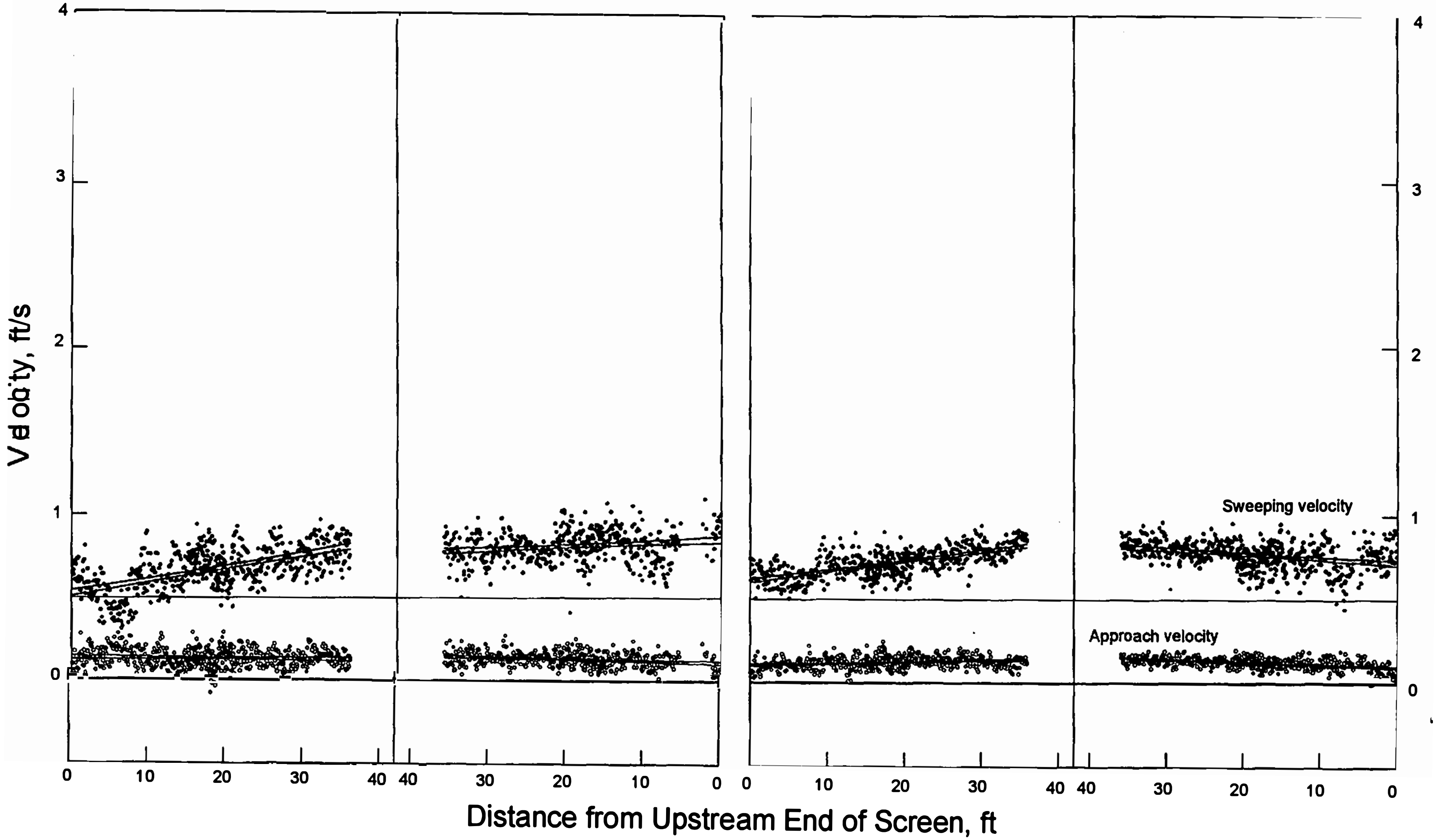

Test A11 - Approach and Sweeping Velocities at Elevation 6434.0
1980 ft^3/s river flow, 498 ft^3/s pumped flow (median pumping)

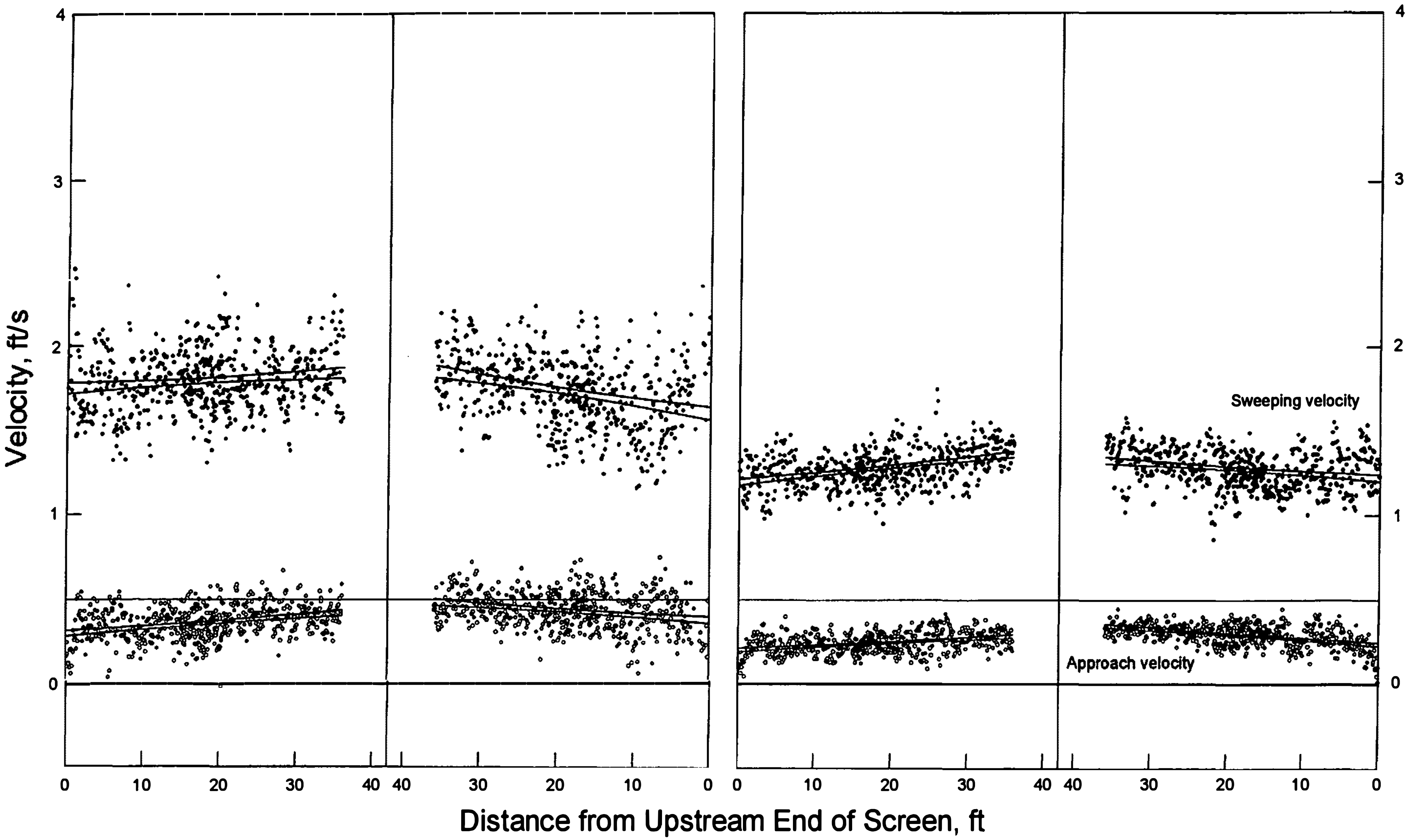

Test A12 - Approach and Sweeping Velocities at Elevation 6434.0
1980 ft^3/s river flow, 673 ft^3/s pumped flow (maximum pumping)

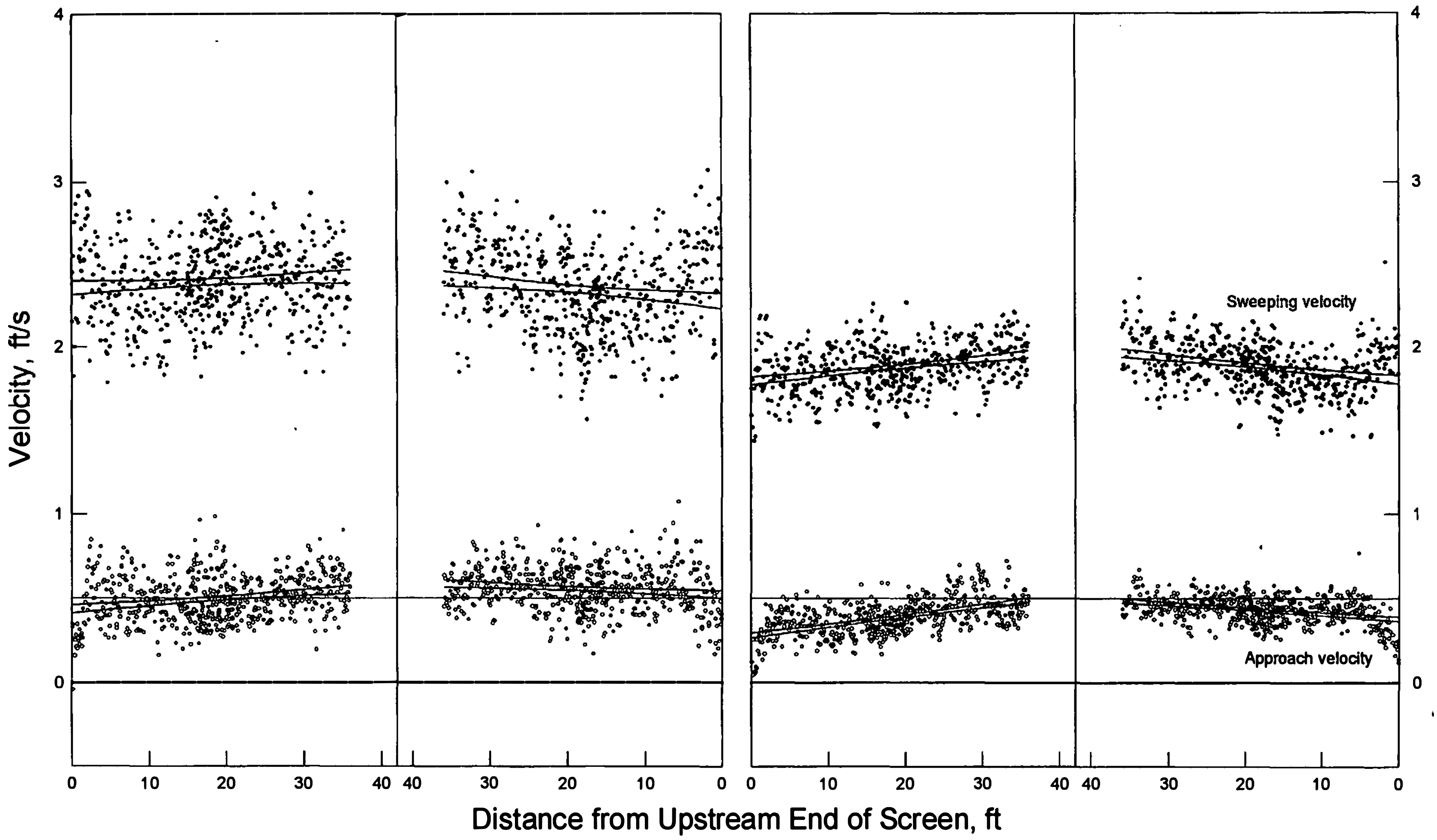

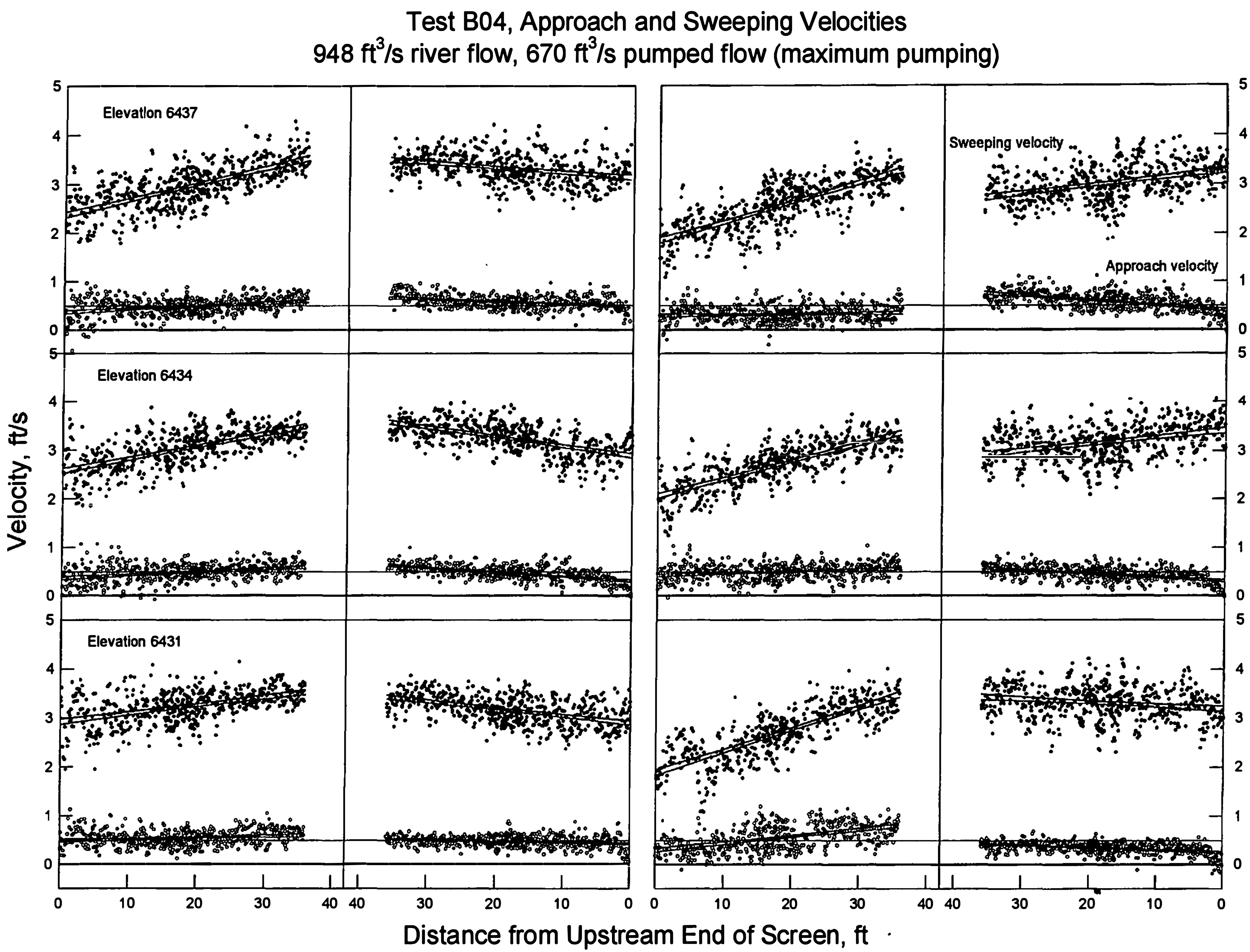
Test B04, Approach and Sweeping Velocities
948 ft³/s river flow, 670 ft³/s pumped flow (maximum pumping)
Elevation 6437
Elevation 6434
Elevation 6431
Sweeping velocity
Approach velocity
Velocity, ft/s
Distance from Upstream End of Screen, ft

Test B05 - Approach and Sweeping Velocities at Elevation 6434.0
998 ft^3/s river flow, 503 ft^3/s pumped flow (median pumping)
33 ft^3/s flow through each fish bypass

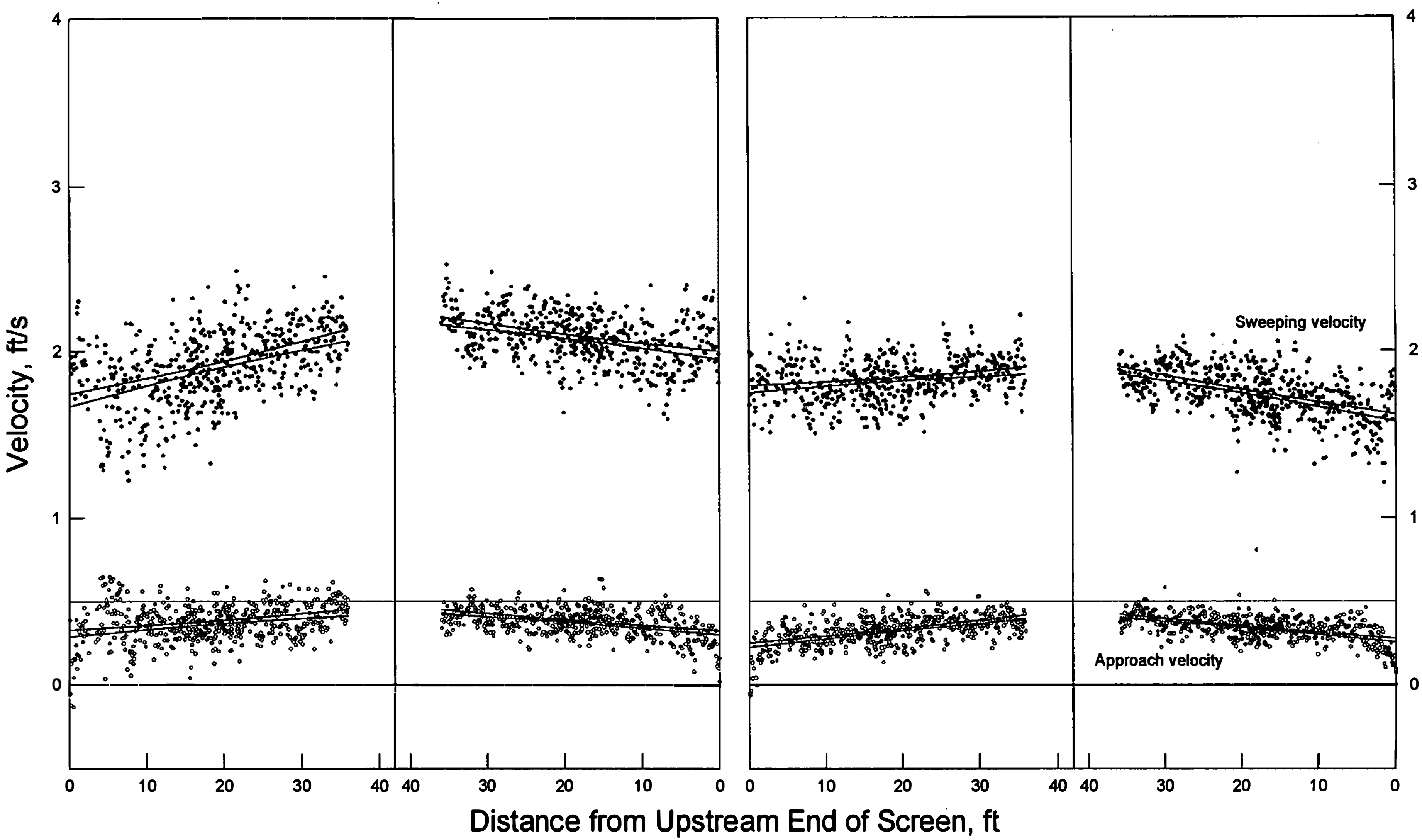

Test B5b - Approach and Sweeping Velocities at Elevation 6434.0
998 ft^3/s river flow, 506 ft^3/s pumped flow (median pumping)
Identical to B05, except 16.5 ft^3/s flow through each bypass

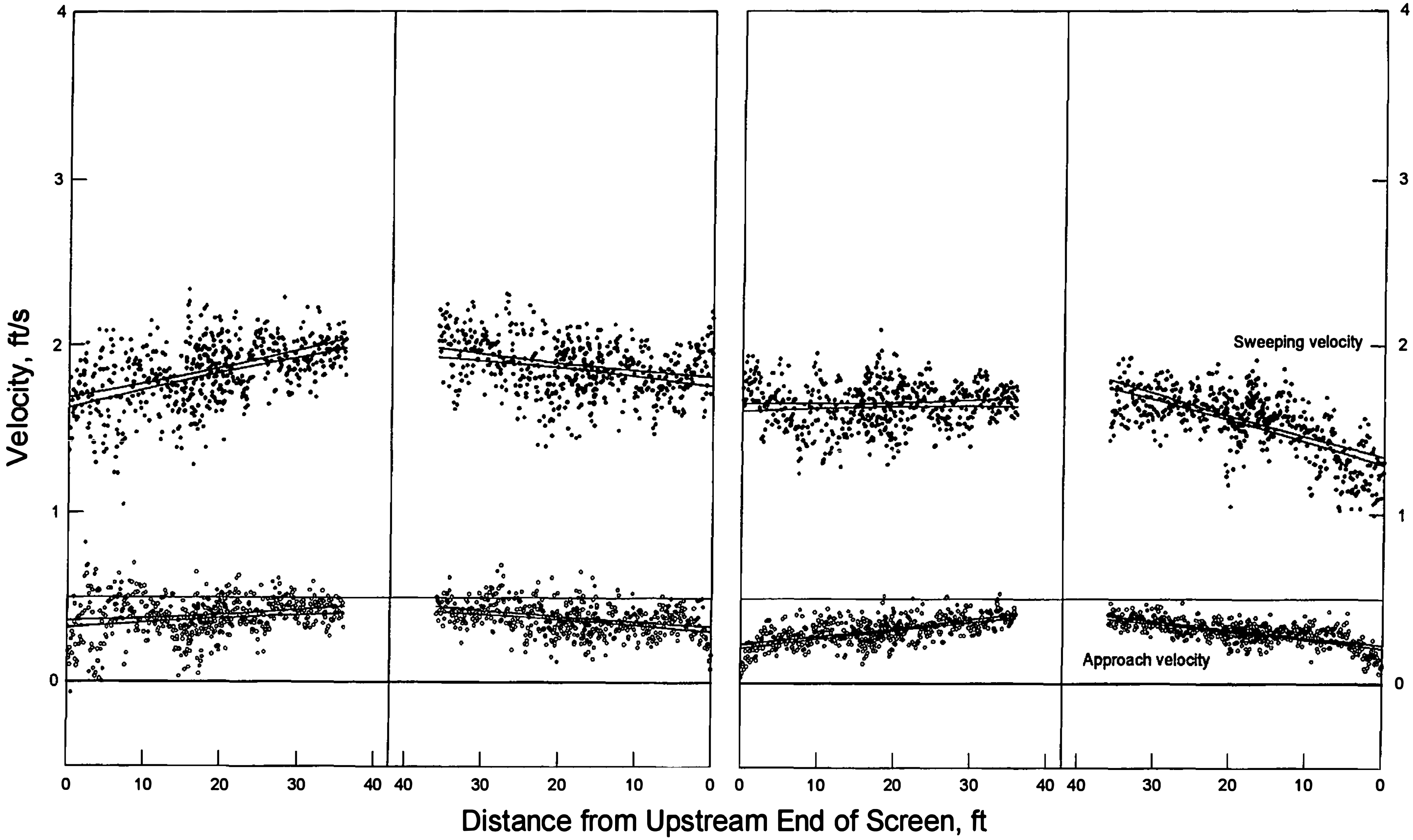

Test B06 - Approach and Sweeping Velocities at Elevation 6434.0
798 ft^3/s river flow, 450 ft^3/s pumped flow (median pumping)

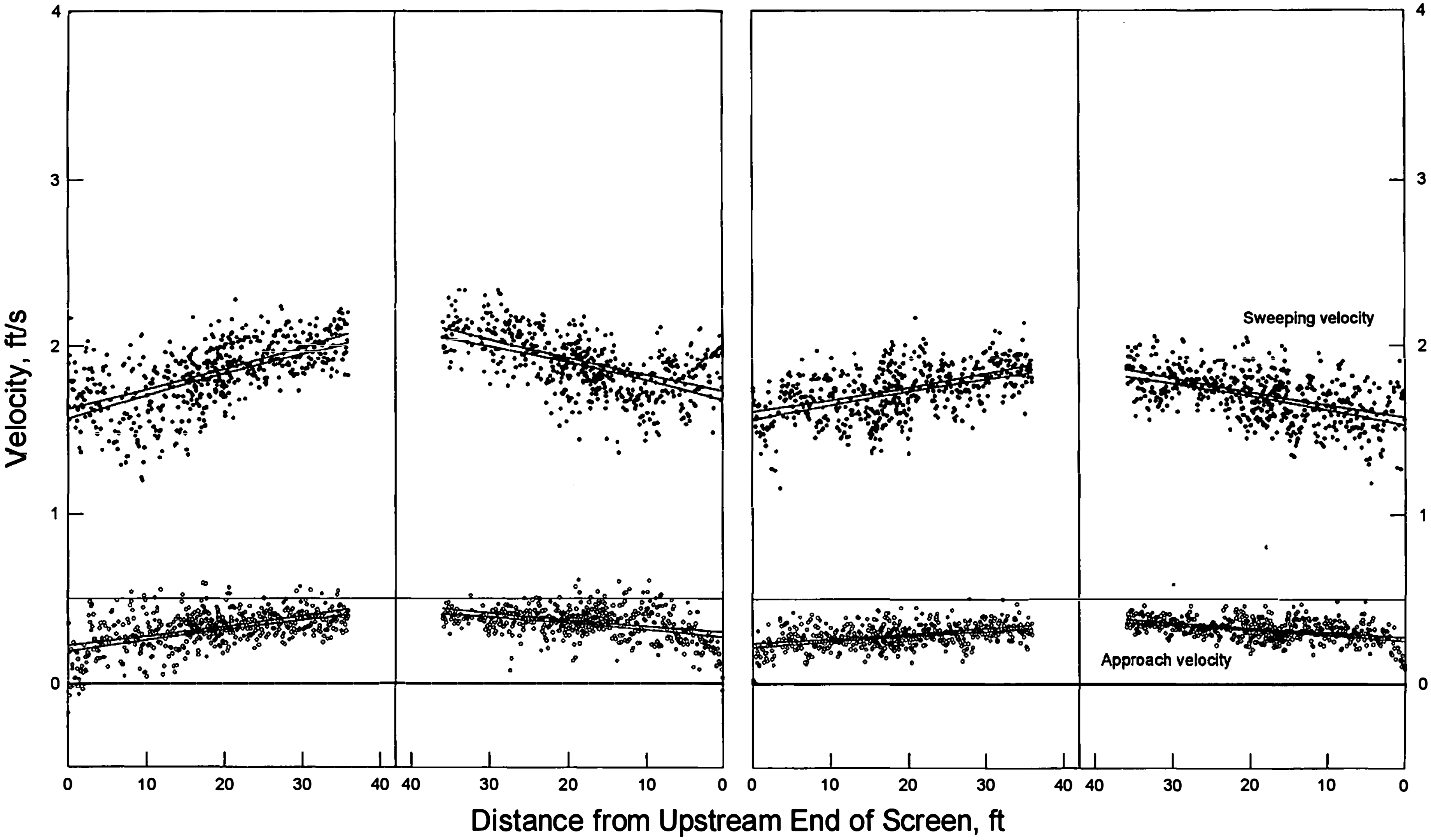

Test B07 - Approach and Sweeping Velocities at Elevation 6434.0
599 ft³/s river flow, 335 ft³/s pumped flow (median pumping)

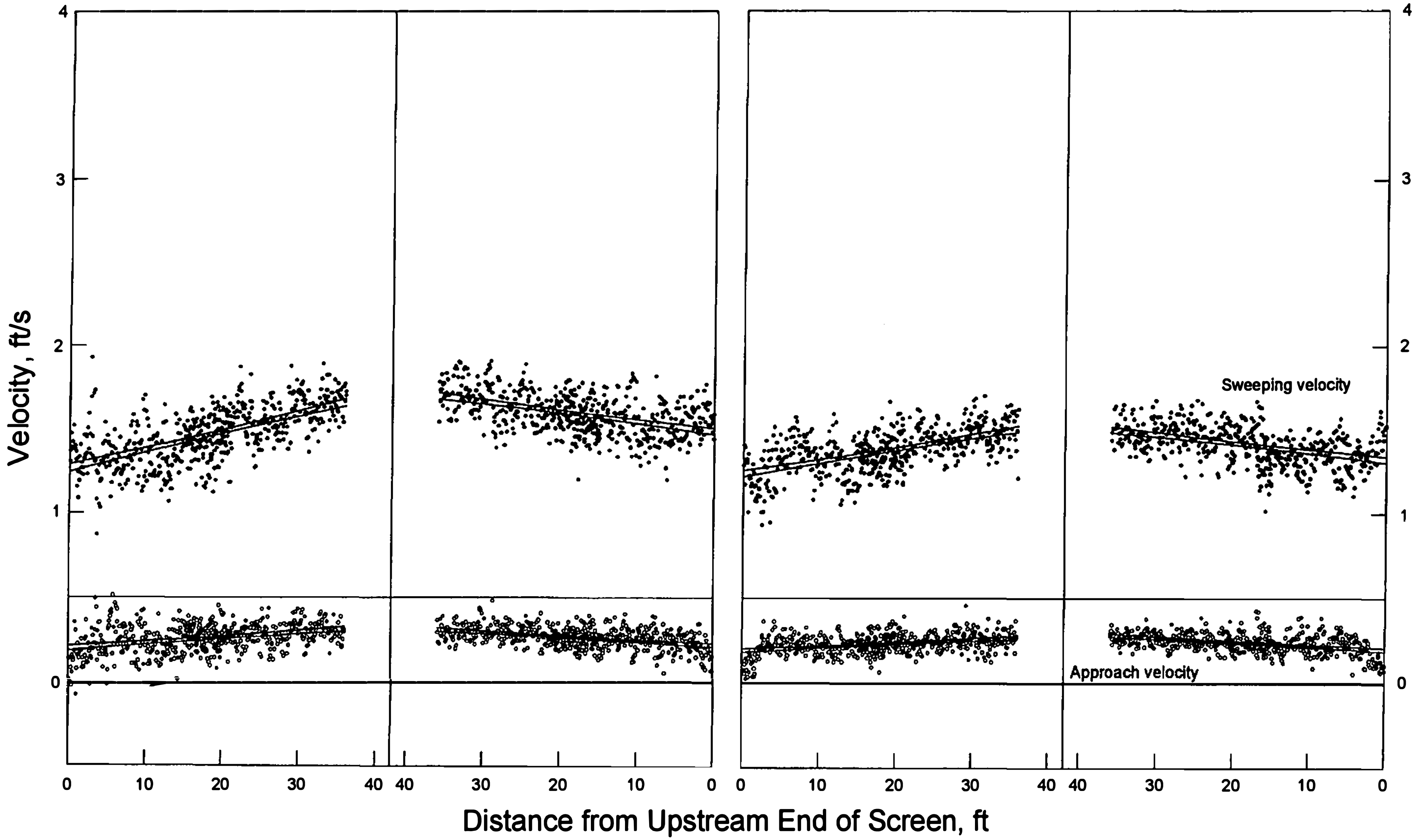

Test B08 - Approach and Sweeping Velocities at Elevation 6434.0
499 ft^3/s river flow, 340 ft^3/s pumped flow (maximum pumping)

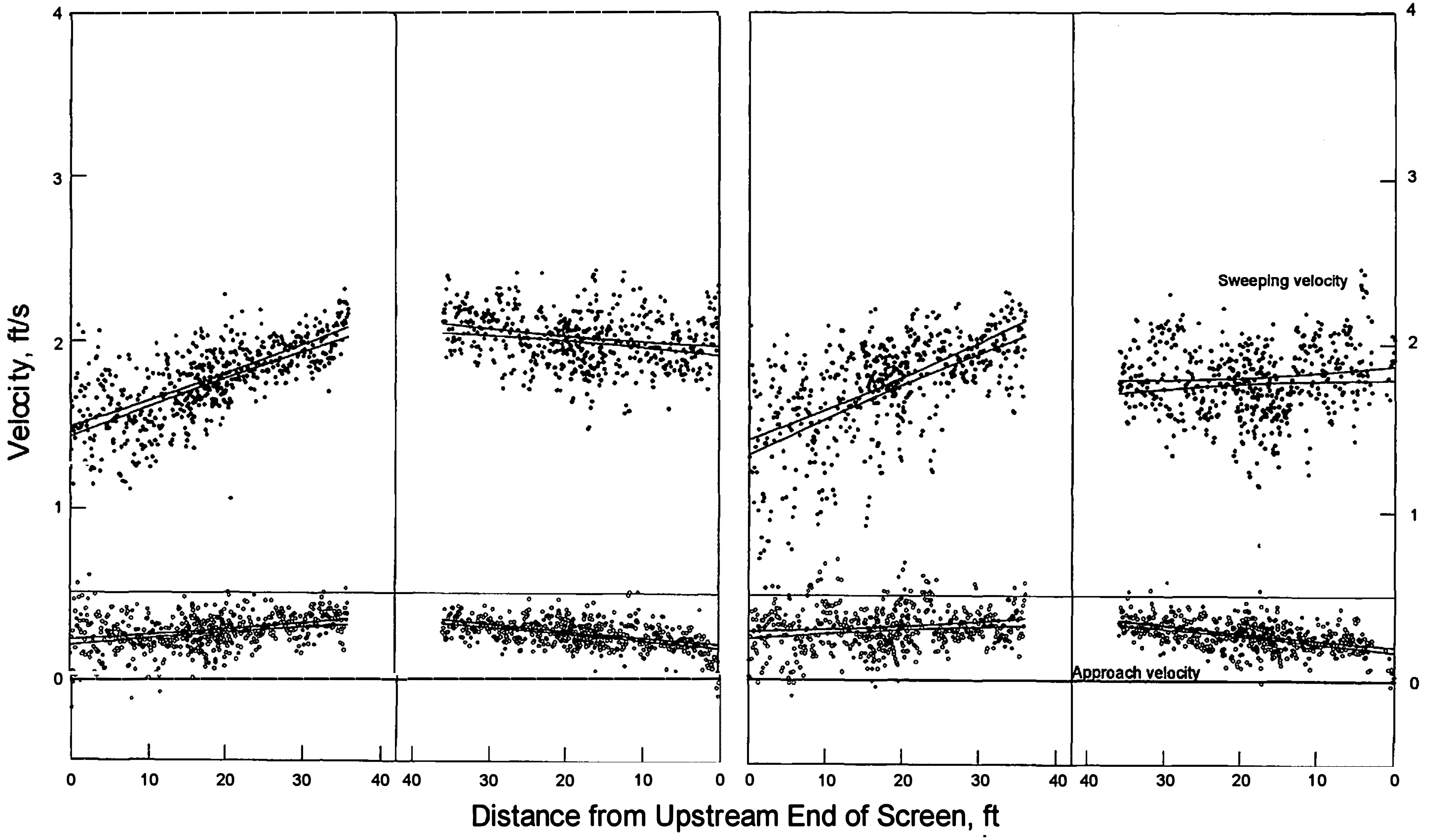

Test B12 - Approach and Sweeping Velocities at Elevation 6434.0
1995 ft^3/s river flow, 676 ft^3/s pumped flow (maximum pumping)

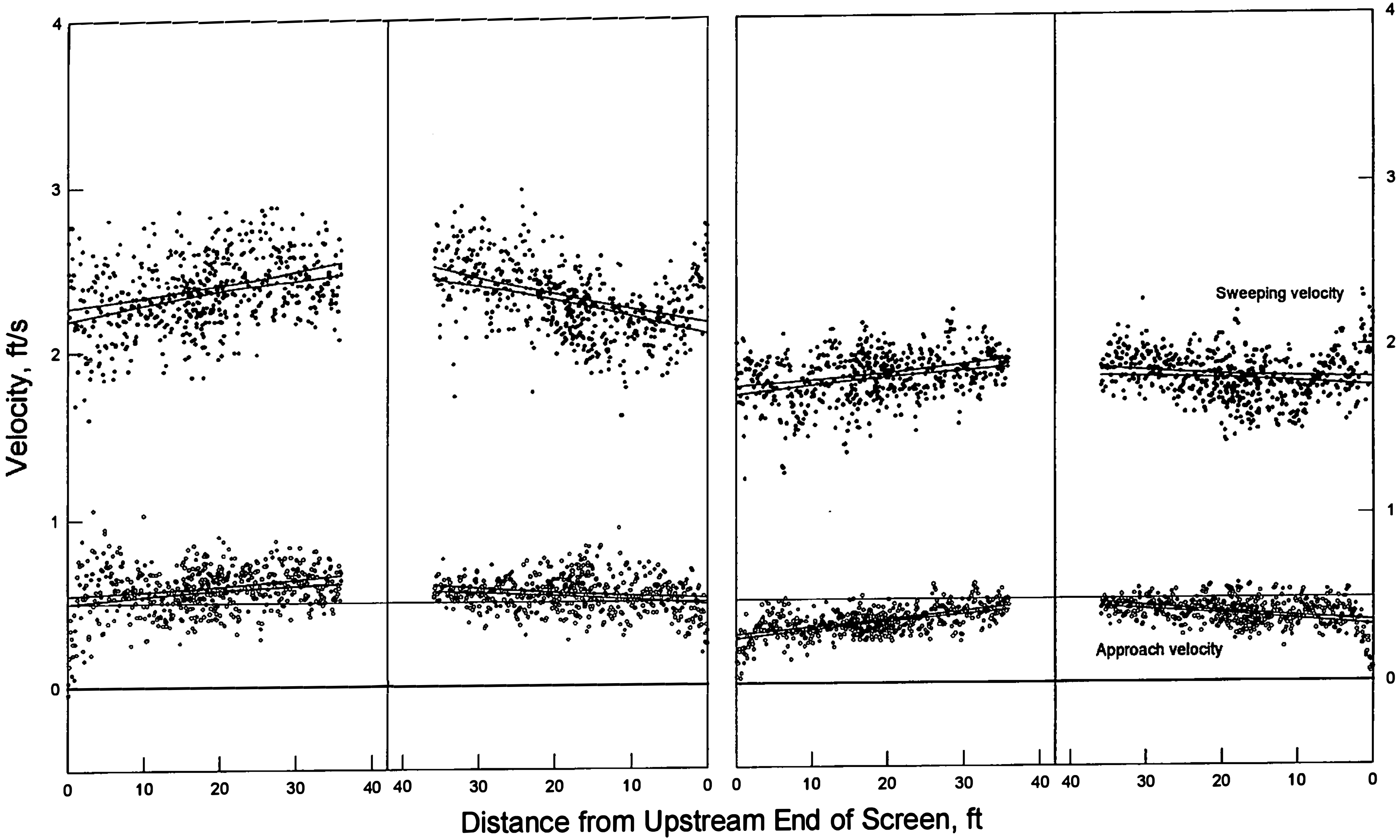

Test B13 - Approach and Sweeping Velocities at Elevation 6434.0
1996 ft^3/s river flow, 637 ft^3/s pumped flow (nearly maximum pumping)
P1-P4 operating

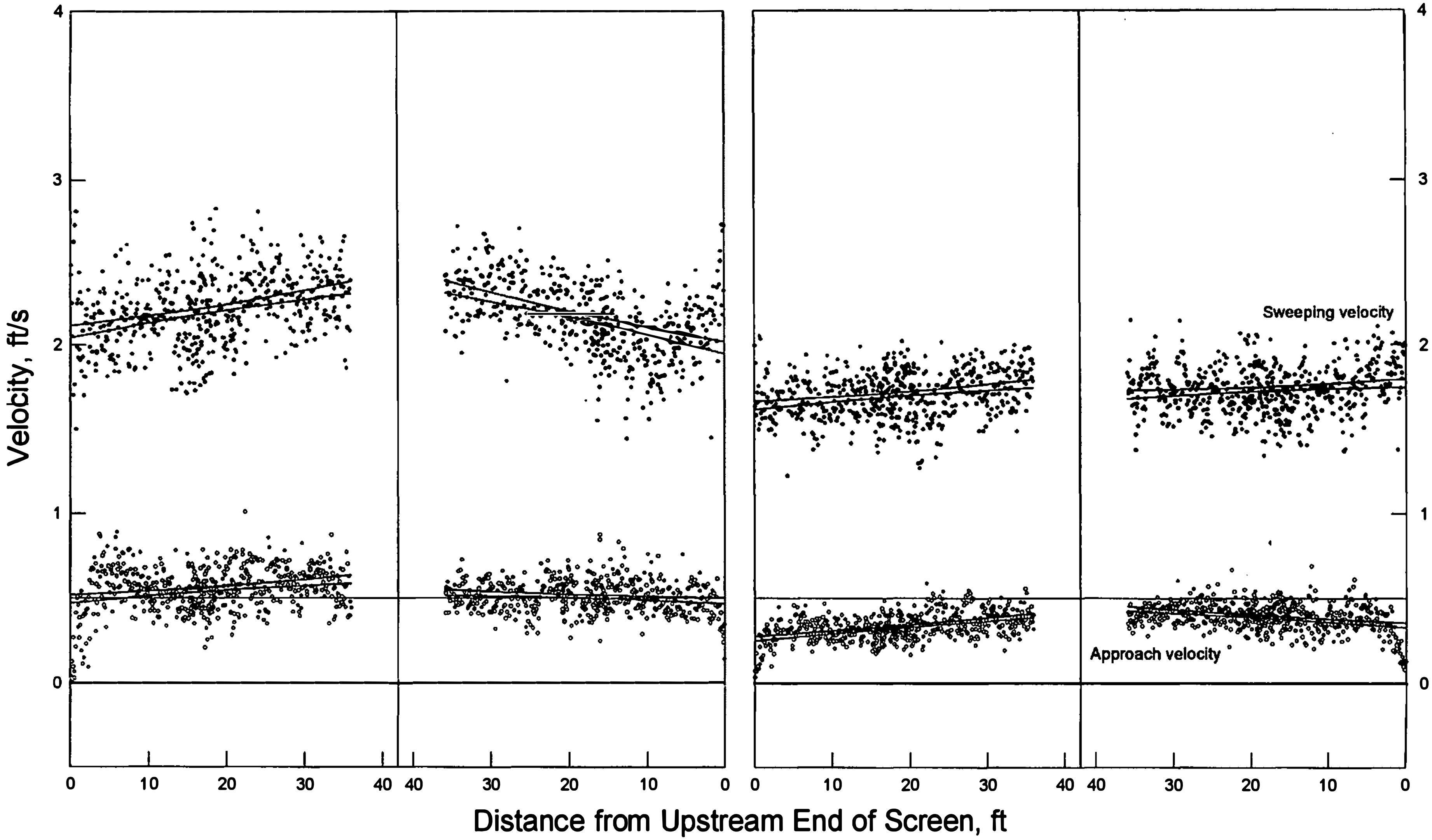

Test B14 - Approach and Sweeping Velocities at Elevation 6434.0
1996 ft^3/s river flow, 634 ft^3/s pumped flow (nearly maximum pumping)
P2-P5 operating

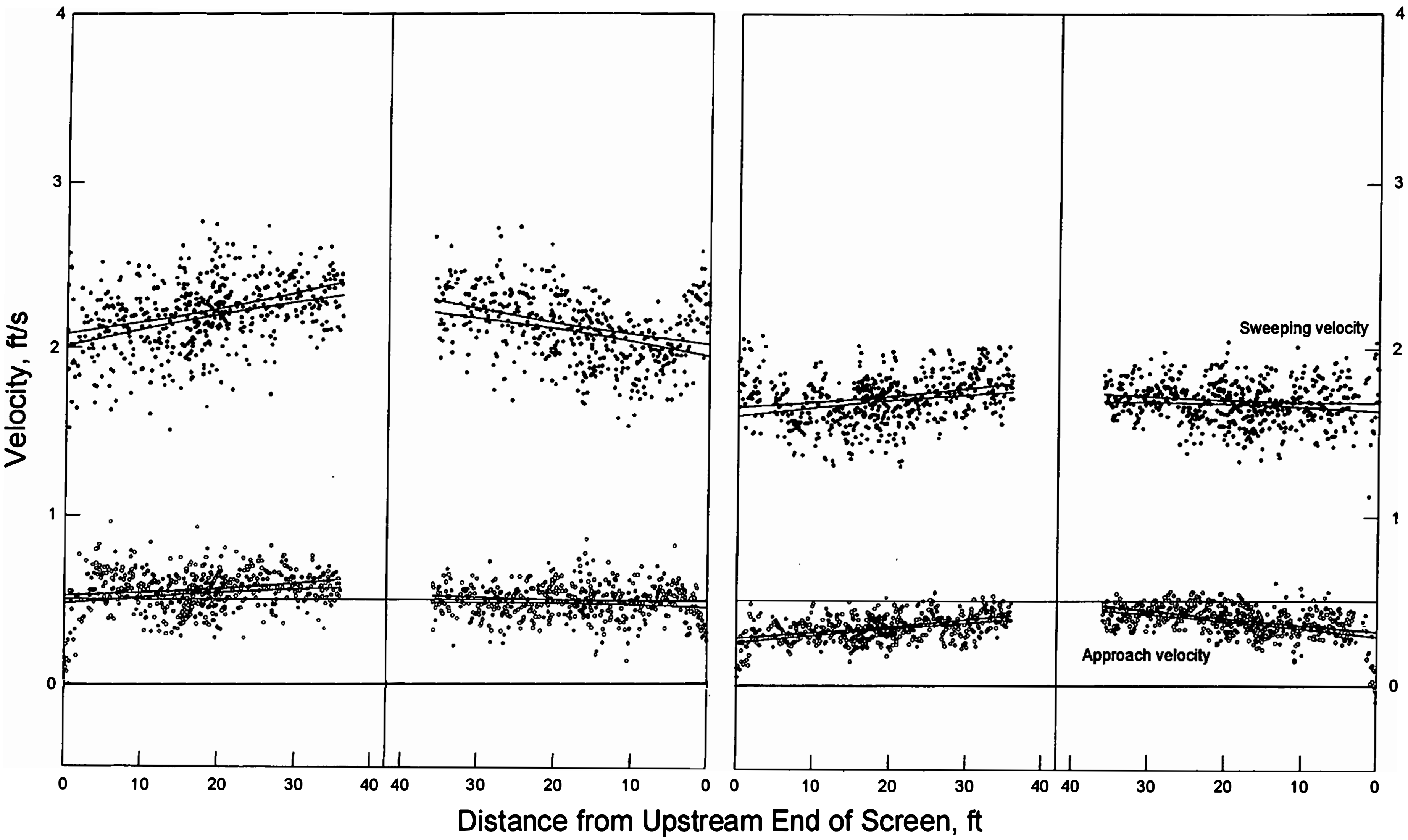

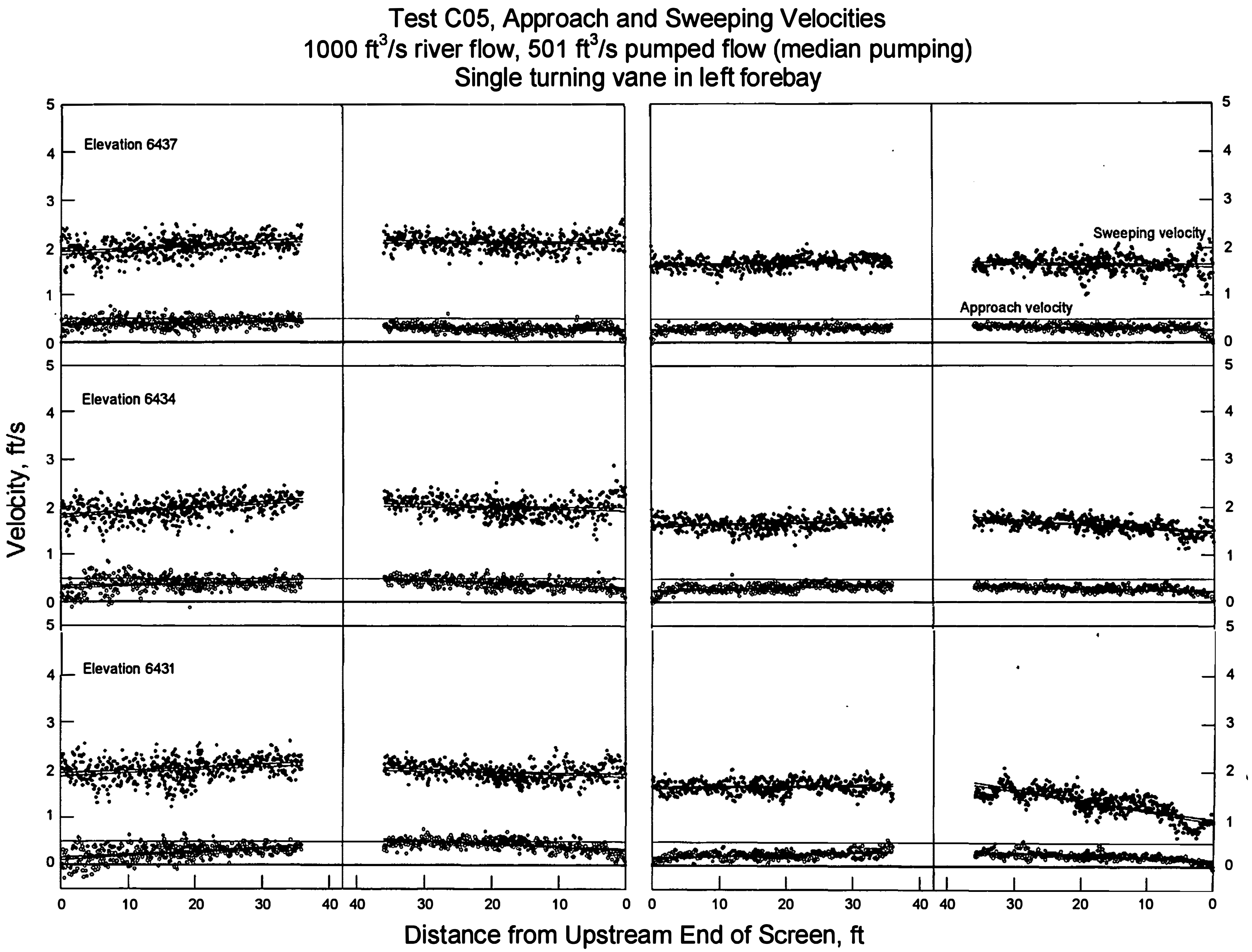
Test C05, Approach and Sweeping Velocities
1000 ft³/s river flow, 501 ft³/s pumped flow (median pumping)
Single turning vane in left forebay
Elevation 6437
Elevation 6434
Elevation 6431
Sweeping velocity
Approach velocity
Velocity, ft/s
Distance from Upstream End of Screen, ft

Test C07 - Approach and Sweeping Velocities at Elevation 6434.0
600 ft^3/s river flow, 333 ft^3/s pumped flow (median pumping)
One vane in forebay for left screen structure

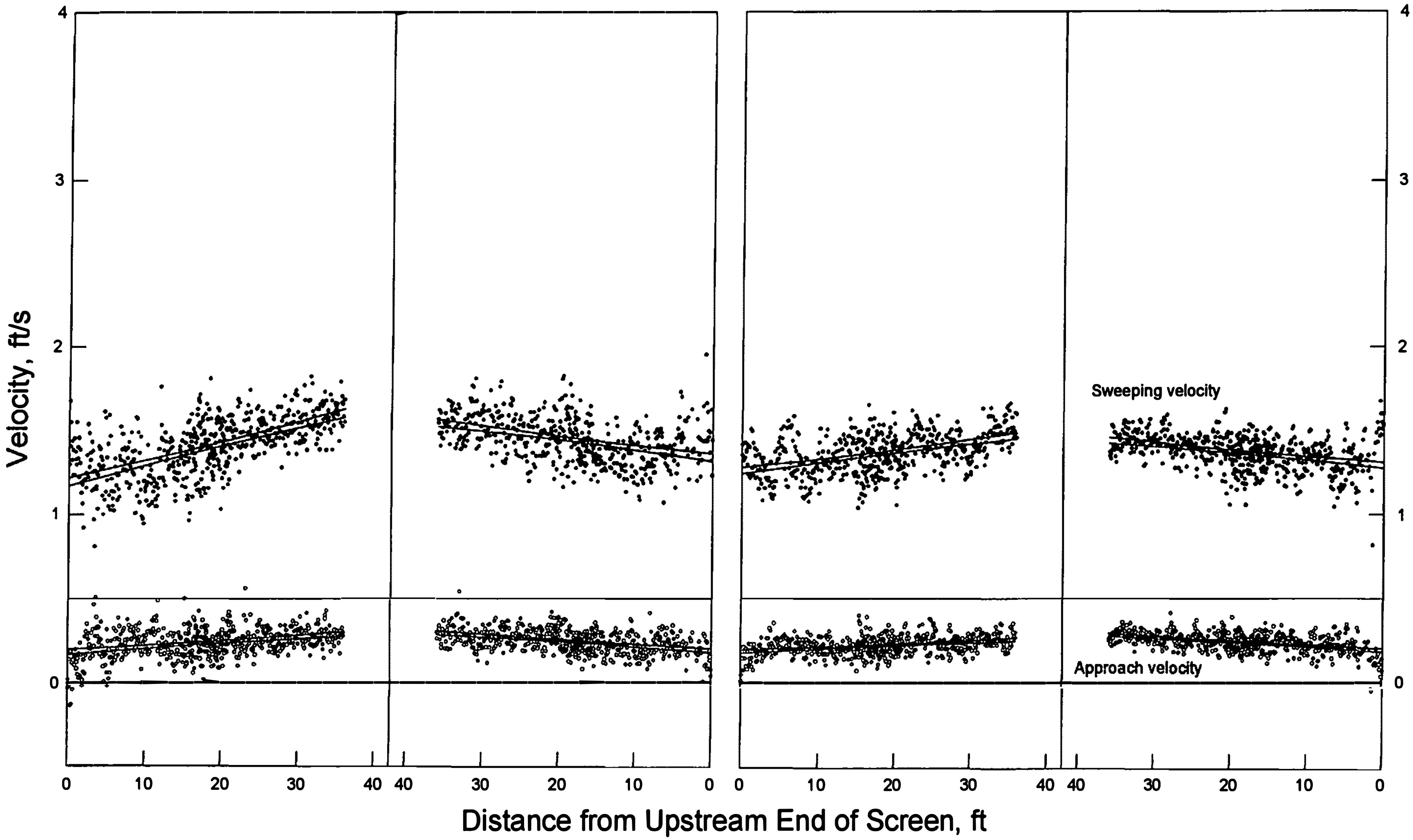

Test D01 - Approach and Sweeping Velocities at Elevation 6434.0

1996 ft³/s river flow, 668 ft³/s pumped flow (maximum pumping)

Single vane in forebay of left screen structure

56% blockage with baffle downstream of left screen structure

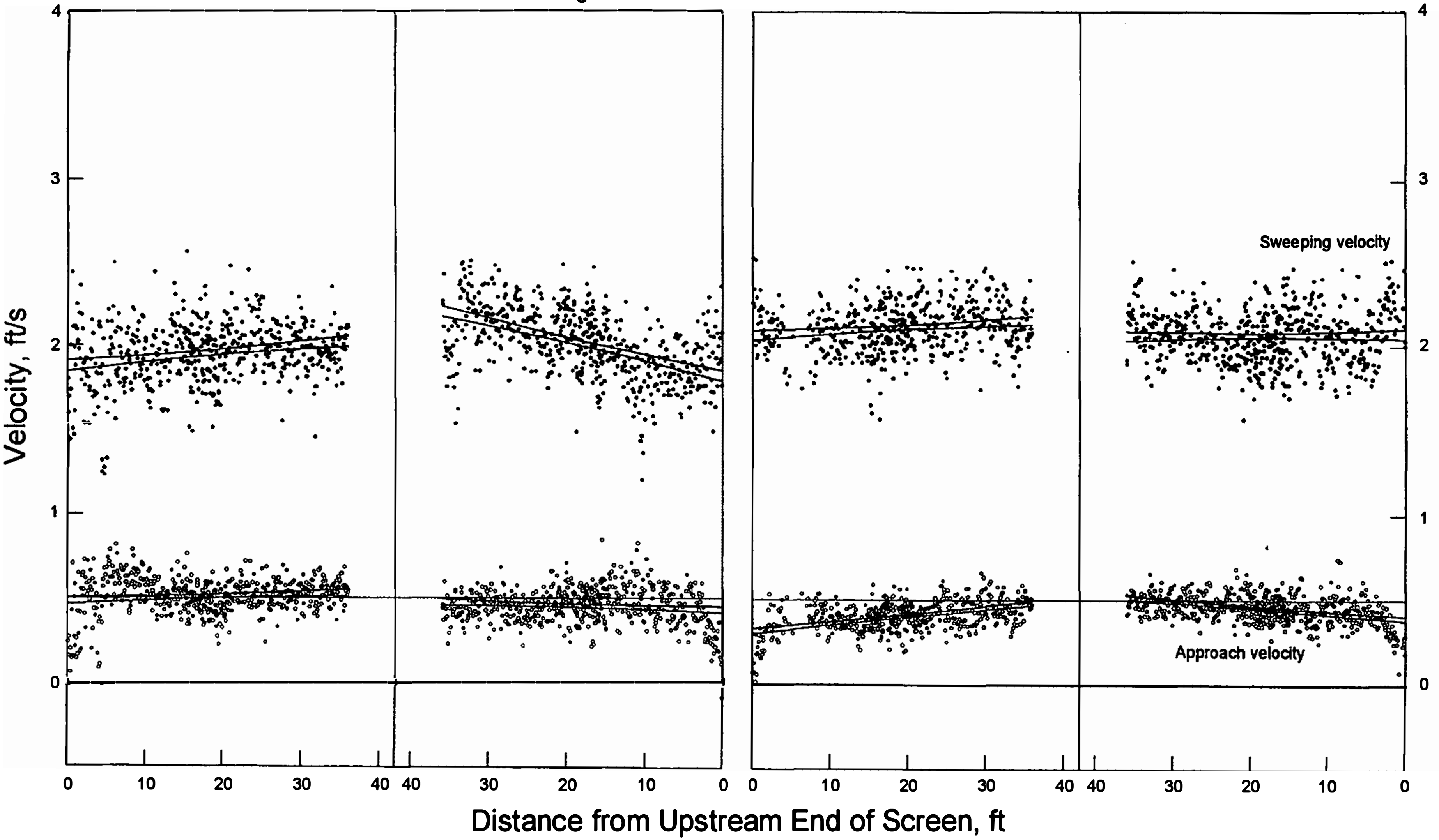

Test D06 - Approach and Sweeping Velocities at Elevation 6434.0
1798 ft^3/s river flow, 442 ft^3/s pumped flow (median pumping)

Single vane in forebay of left screen structure

56% blockage with baffle downstream of left screen structure

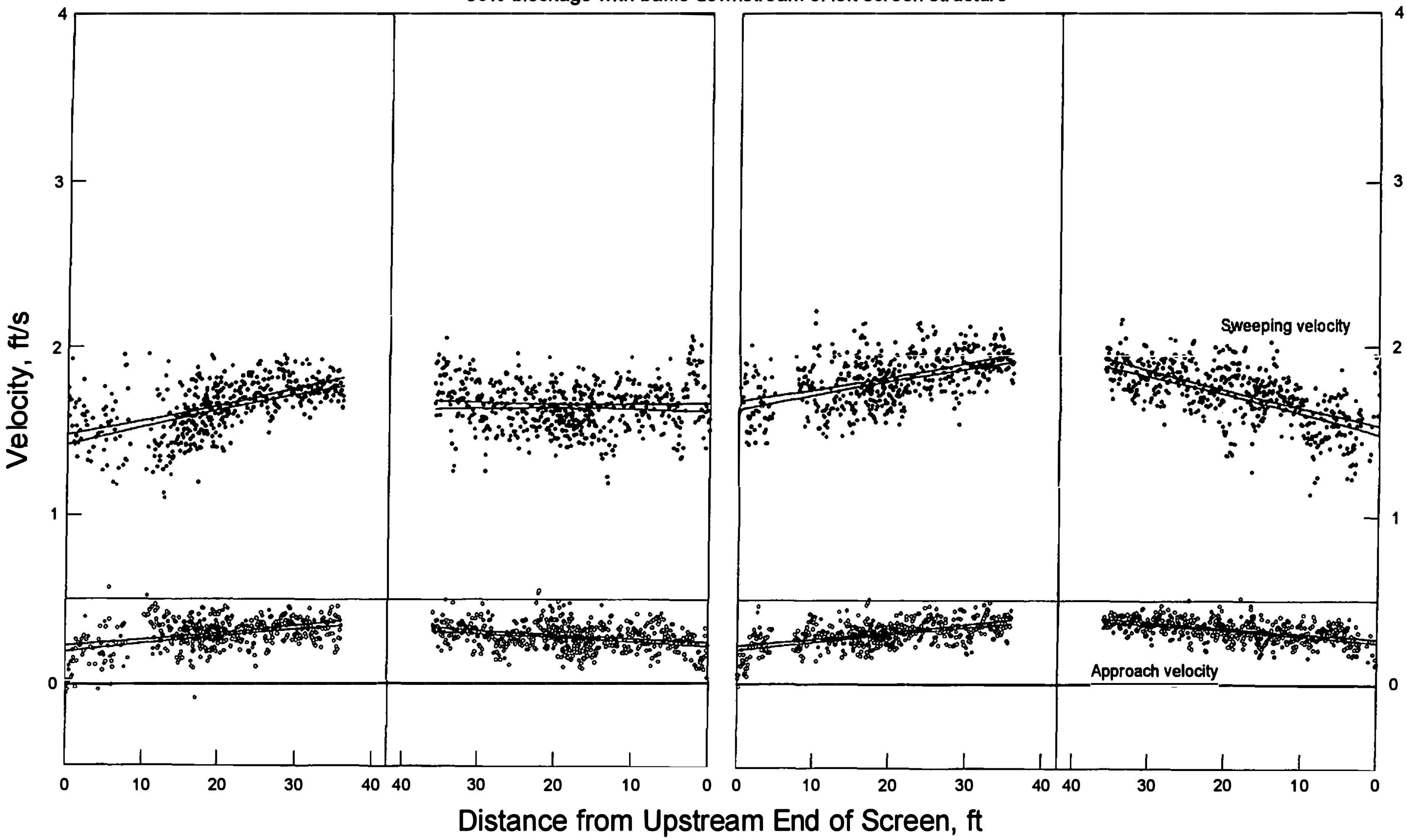

Test D08 - Approach and Sweeping Velocities at Elevation 6434.0
500 ft^3/s river flow, 334 ft^3/s pumped flow (maximum pumping)
Single vane in forebay of left screen structure
33% blockage with baffle downstream of left screen structure

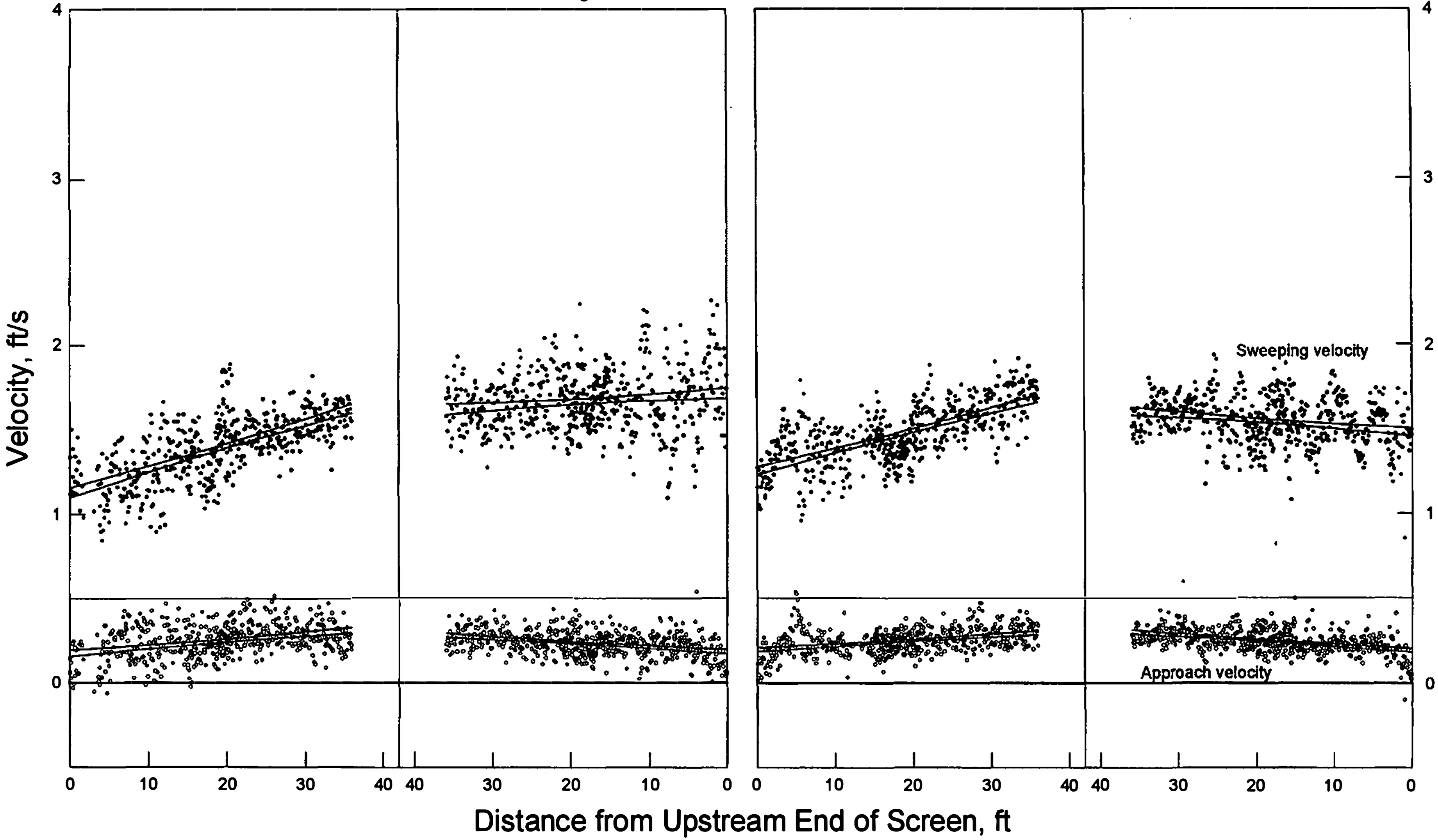

Test D12 - Approach and Sweeping Velocities at Elevation 6434.0
1996 ft³/s river flow, 669 ft³/s pumped flow (maximum pumping)

Single vane in forebay of left screen structure

33% blockage with baffle downstream of left screen structure

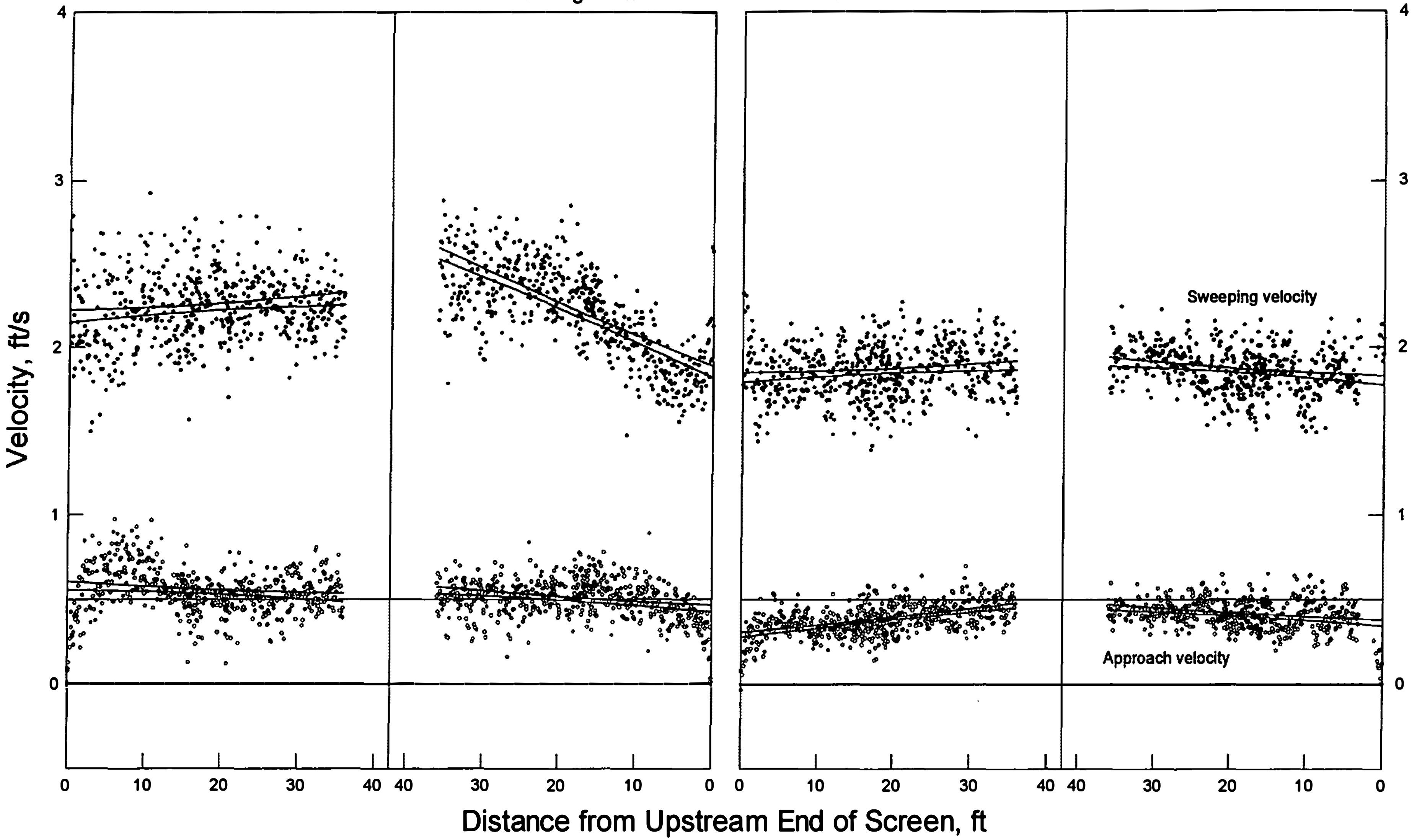

Test D80 - Approach and Sweeping Velocities at Elevation 6434.0
3995 ft^3/s river flow, 690 ft^3/s pumped flow (maximum pumping + 20 ft^3/s)

Single vane in forebay of left screen structure

56% blockage with baffle downstream of left screen structure

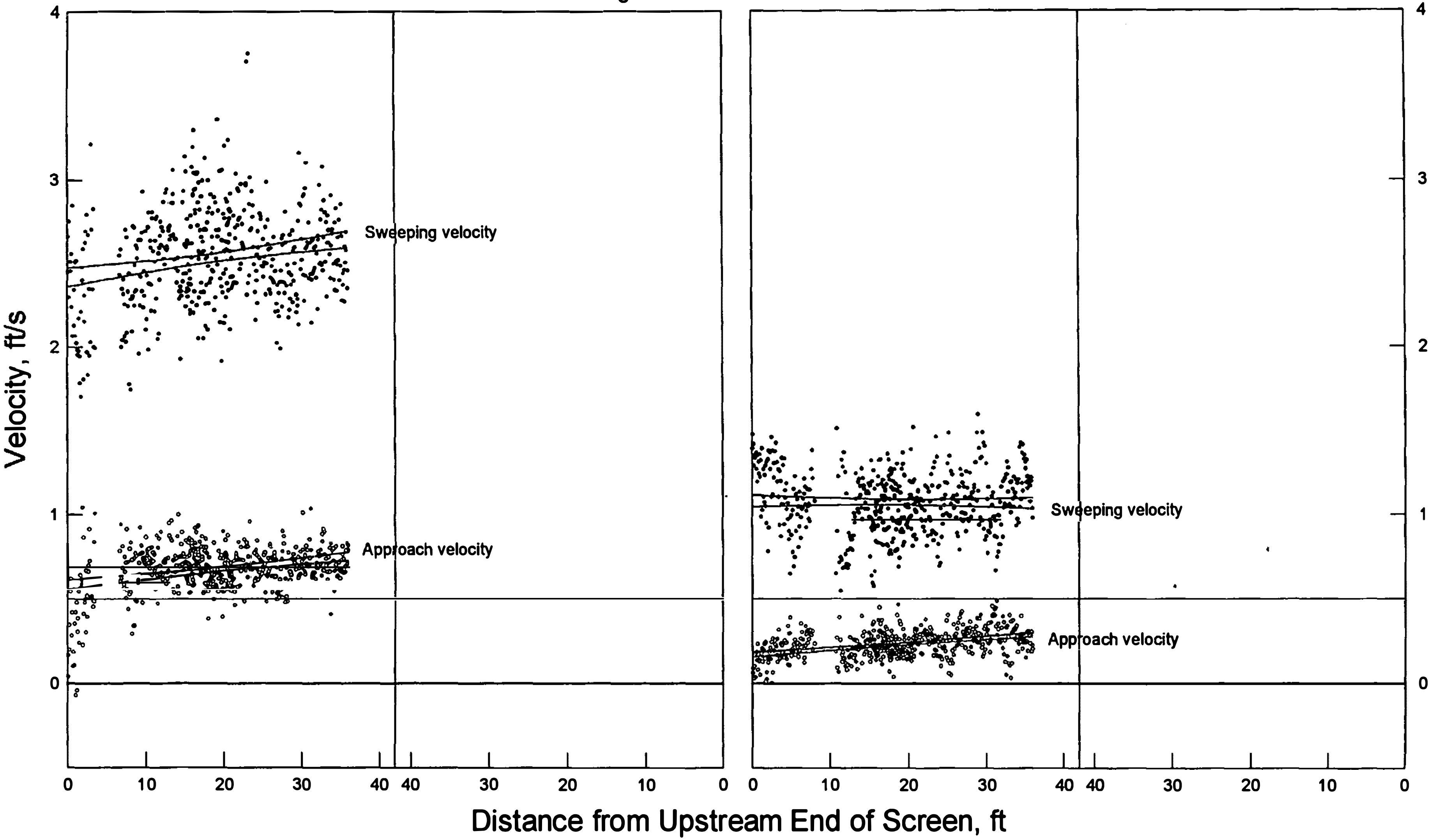

Test D81 - Approach and Sweeping Velocities at Elevation 6434.0
3995 ft^3/s river flow, 500 ft^3/s pumped flow (median pumping)

Single vane in forebay of left screen structure

56% blockage with baffle downstream of left screen structure

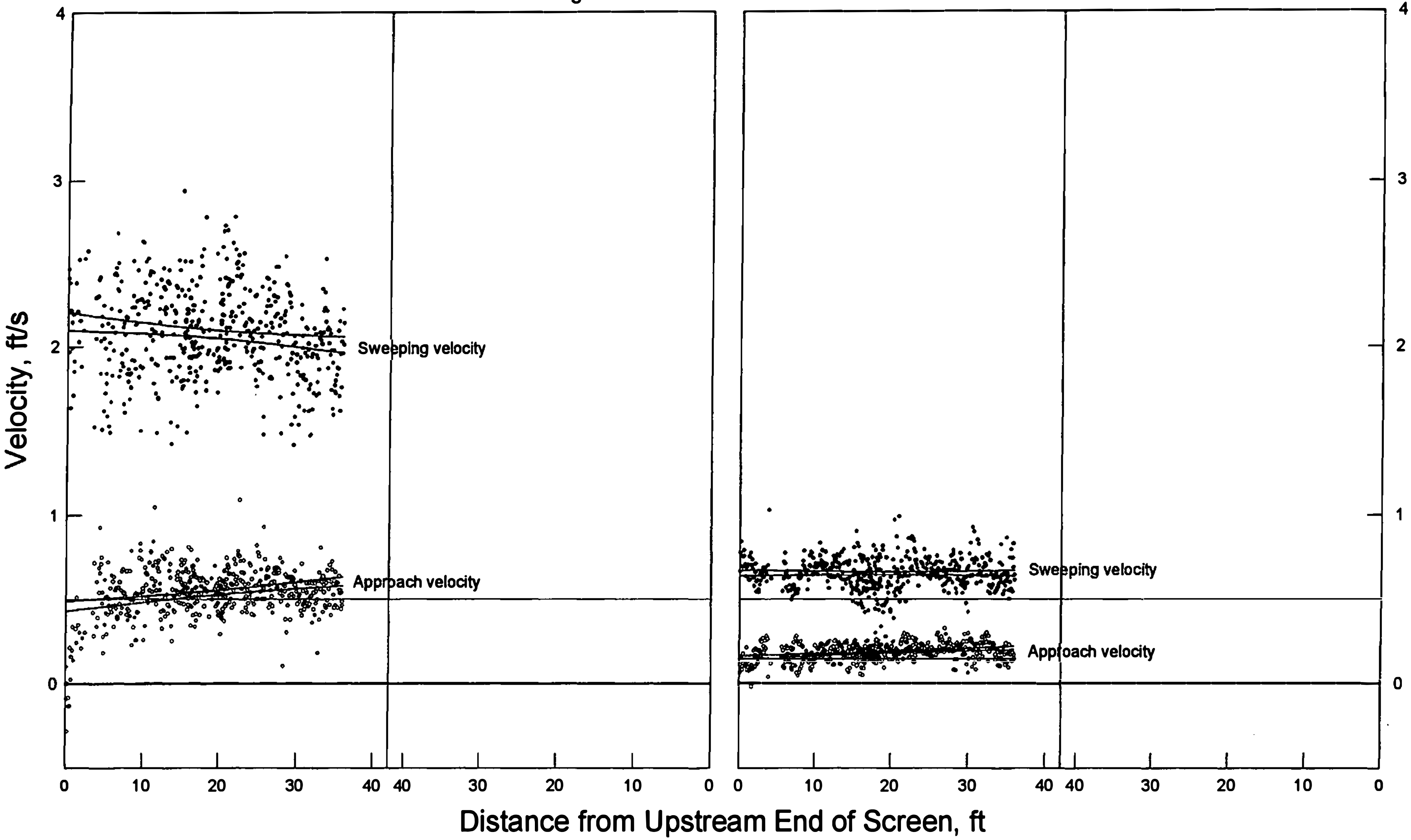

Test E42 - Approach and Sweeping Velocities at Elevation 6434.0
3995 ft^3/s river flow, 500 ft^3/s pumped flow (median pumping)
Single vane in forebay of left screen structure
Intake gates raised to equalize flow between left and right screen structures

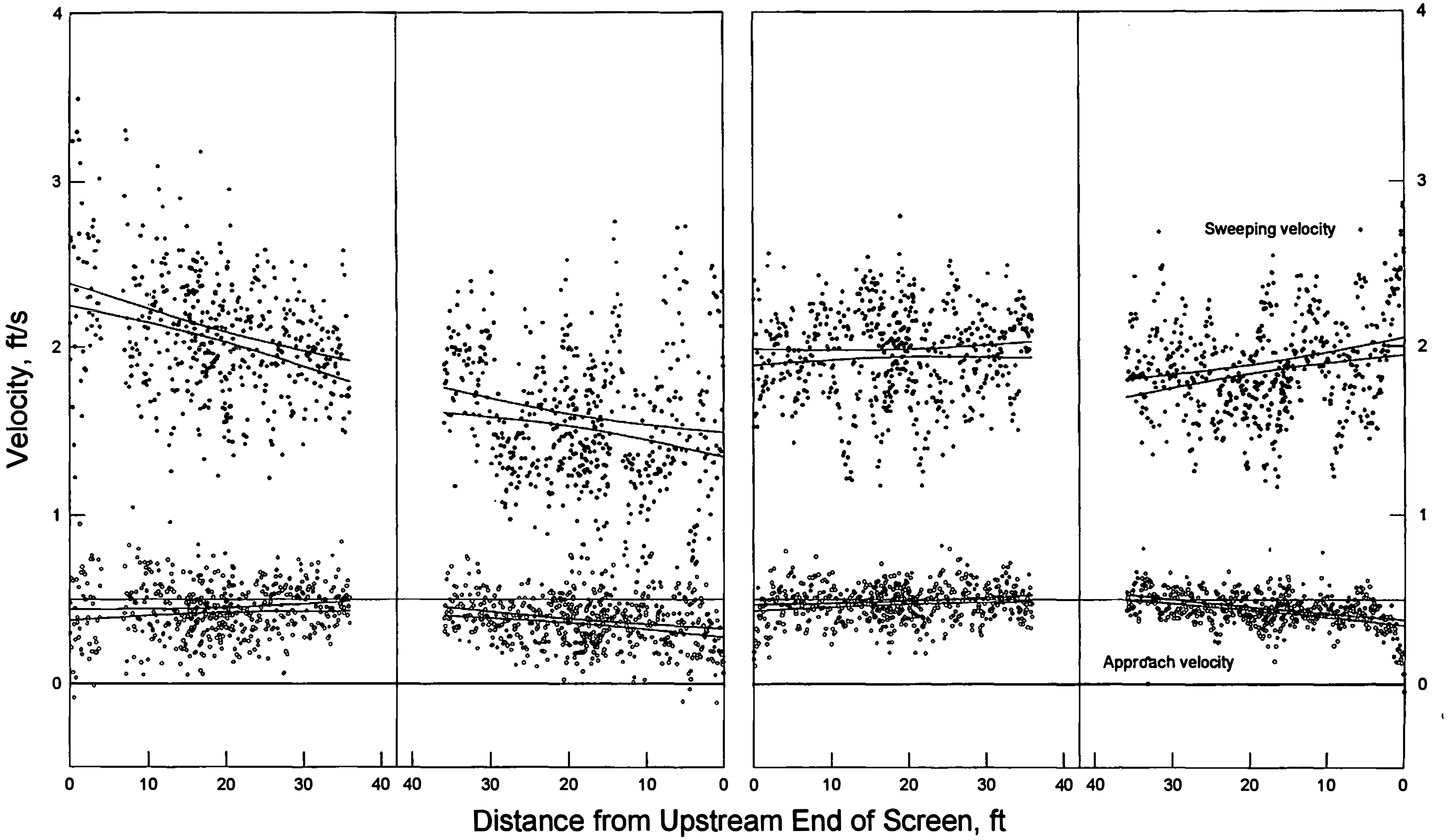

Test E4x - Approach and Sweeping Velocities at Elevation 6434.0
3995 ft^3/s river flow, 661 ft^3/s pumped flow (maximum pumping)

Single vane in forebay of left screen structure

Intake gates raised to equalize flow between left and right screen structures

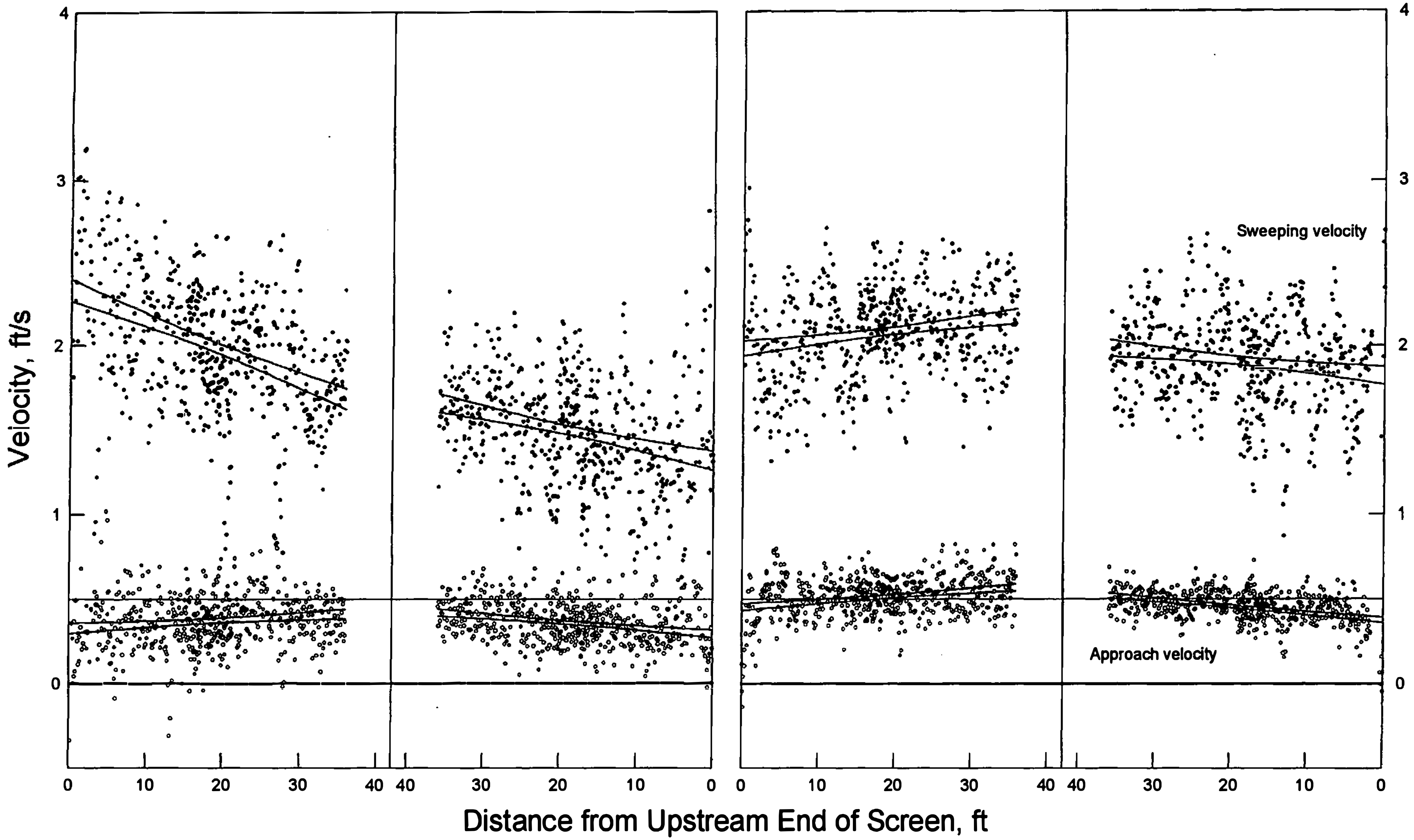

APPENDIX B - INTAKE STRUCTURE VELOCITY FIGURES

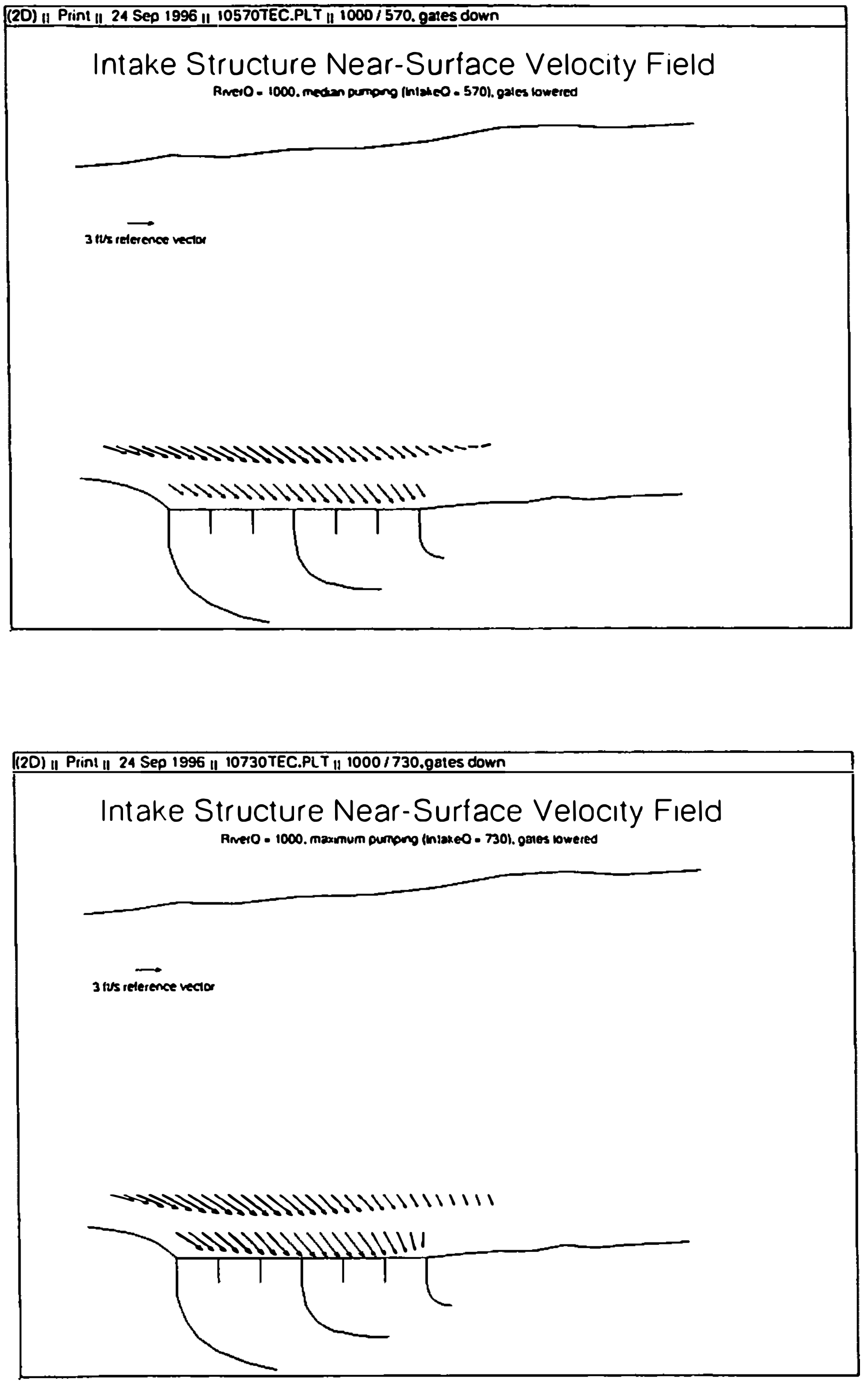

Figure B-1. — Velocity fields approaching intake structure for 1000 ft³/s river flow, at median (top) and maximum pumping rates.

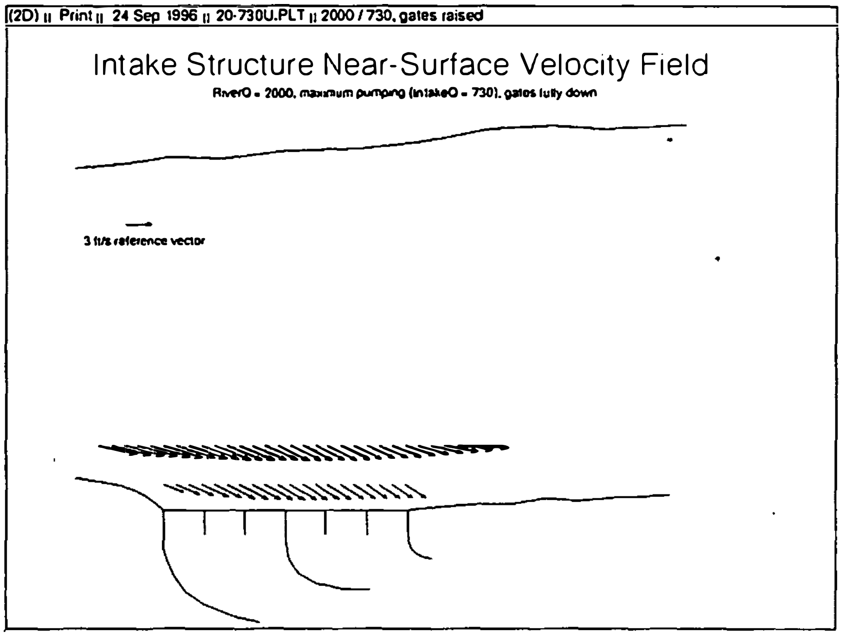

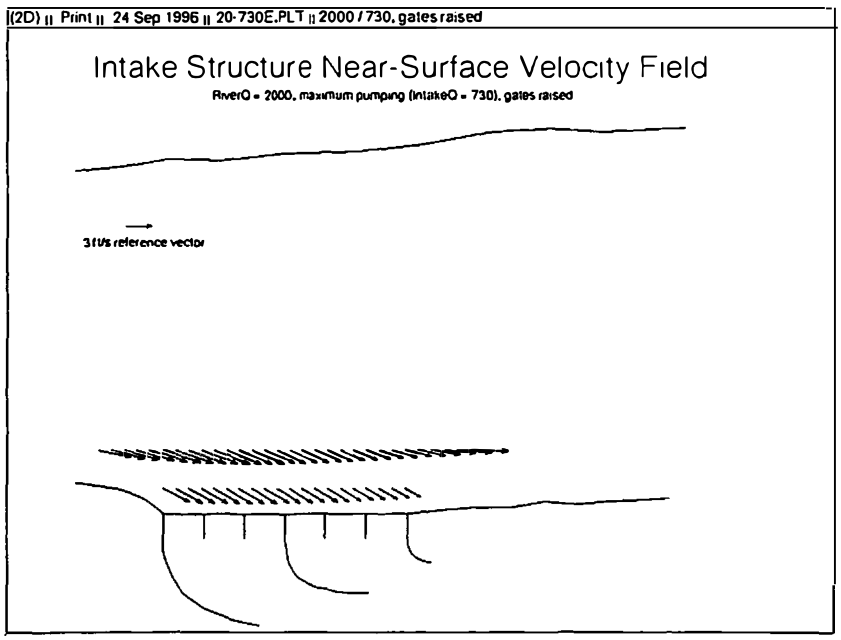

Figure B-2. — Velocity fields approaching intake structure for 2000 ft^3/s river flow, with intake weir gates fully lowered (top) and raised to equalize flows among intake bays (bottom).

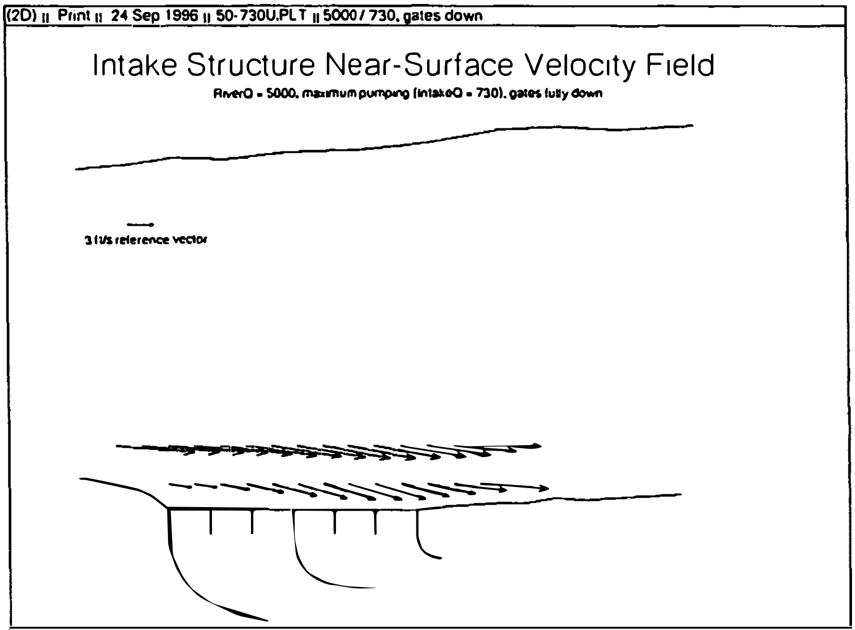

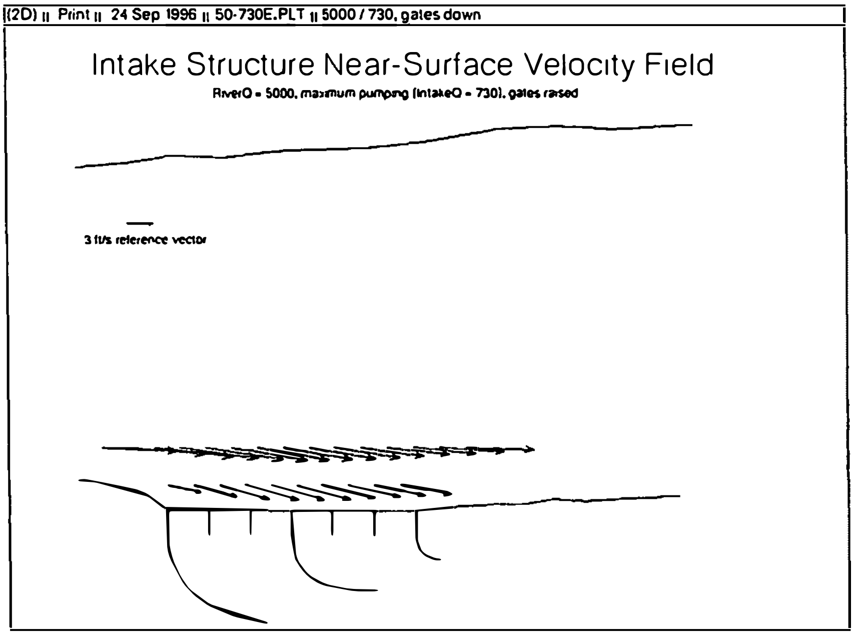

Figure B-3. — Velocity fields approaching intake structure for 5000 ft^3/s river flow, with intake weir gates fully lowered (top) and raised to equalize flows among intake bays (bottom).

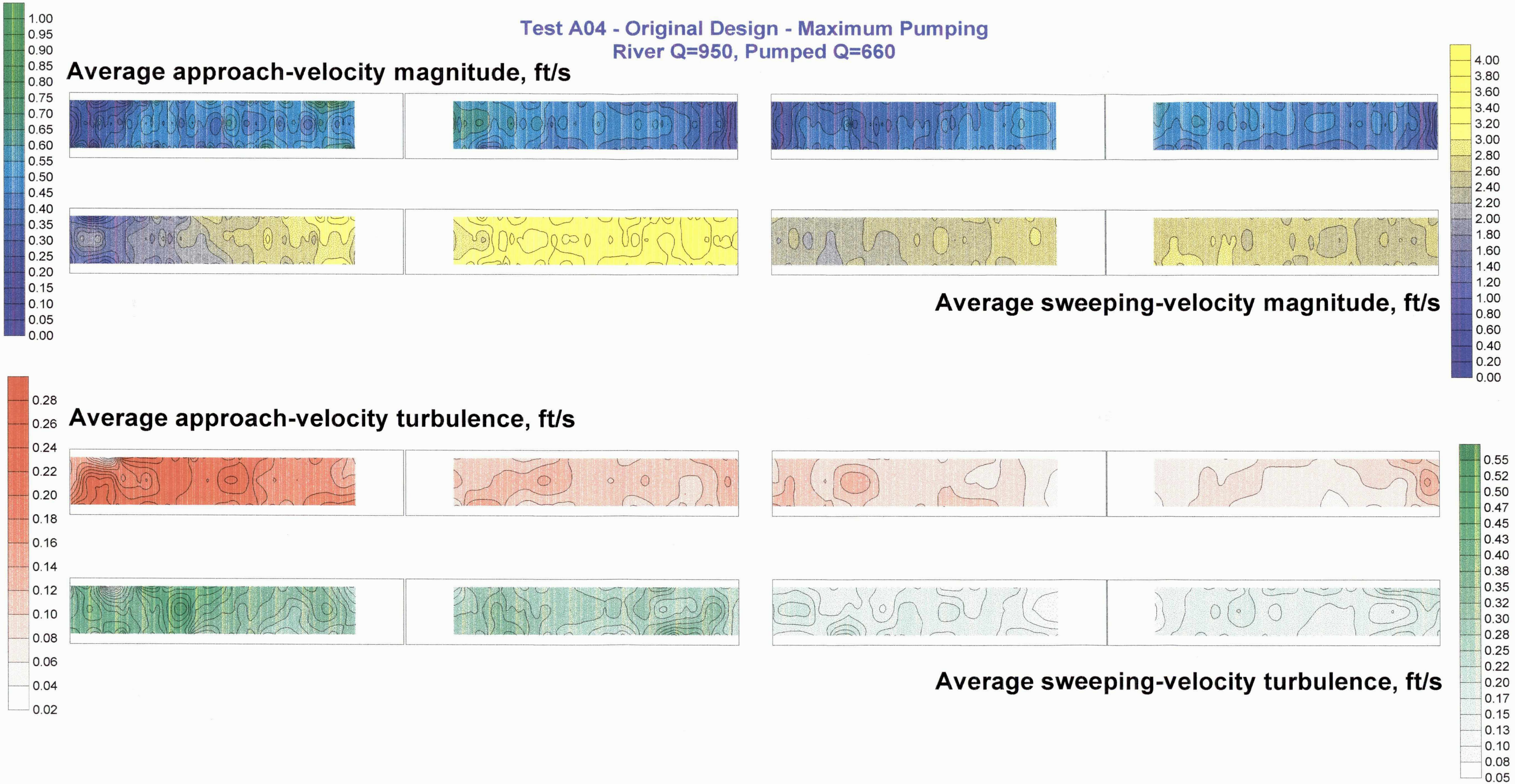
Test A04 - Original Design - Maximum Pumping
River Q=950, Pumped Q=660
Average approach-velocity magnitude, ft/s
1.00 0.95 0.90 0.85 0.80 0.75 0.70 0.65 0.60 0.55 0.50 0.45 0.40 0.35 0.30 0.25 0.20 0.15 0.10 0.05 0.00
Average sweeping-velocity magnitude, ft/s
4.00 3.80 3.60 3.40 3.20 3.00 2.80 2.60 2.40 2.20 2.00 1.80 1.60 1.40 1.20 1.00 0.80 0.60 0.40 0.20 0.00
Average approach-velocity turbulence, ft/s
0.28 0.26 0.24 0.22 0.20 0.18 0.16 0.14 0.12 0.10 0.08 0.06 0.04 0.02
Average sweeping-velocity turbulence, ft/s
0.55 0.52 0.50 0.47 0.45 0.43 0.40 0.38 0.35 0.32 0.30 0.28 0.25 0.22 0.20 0.17 0.15 0.13 0.10 0.08 0.05

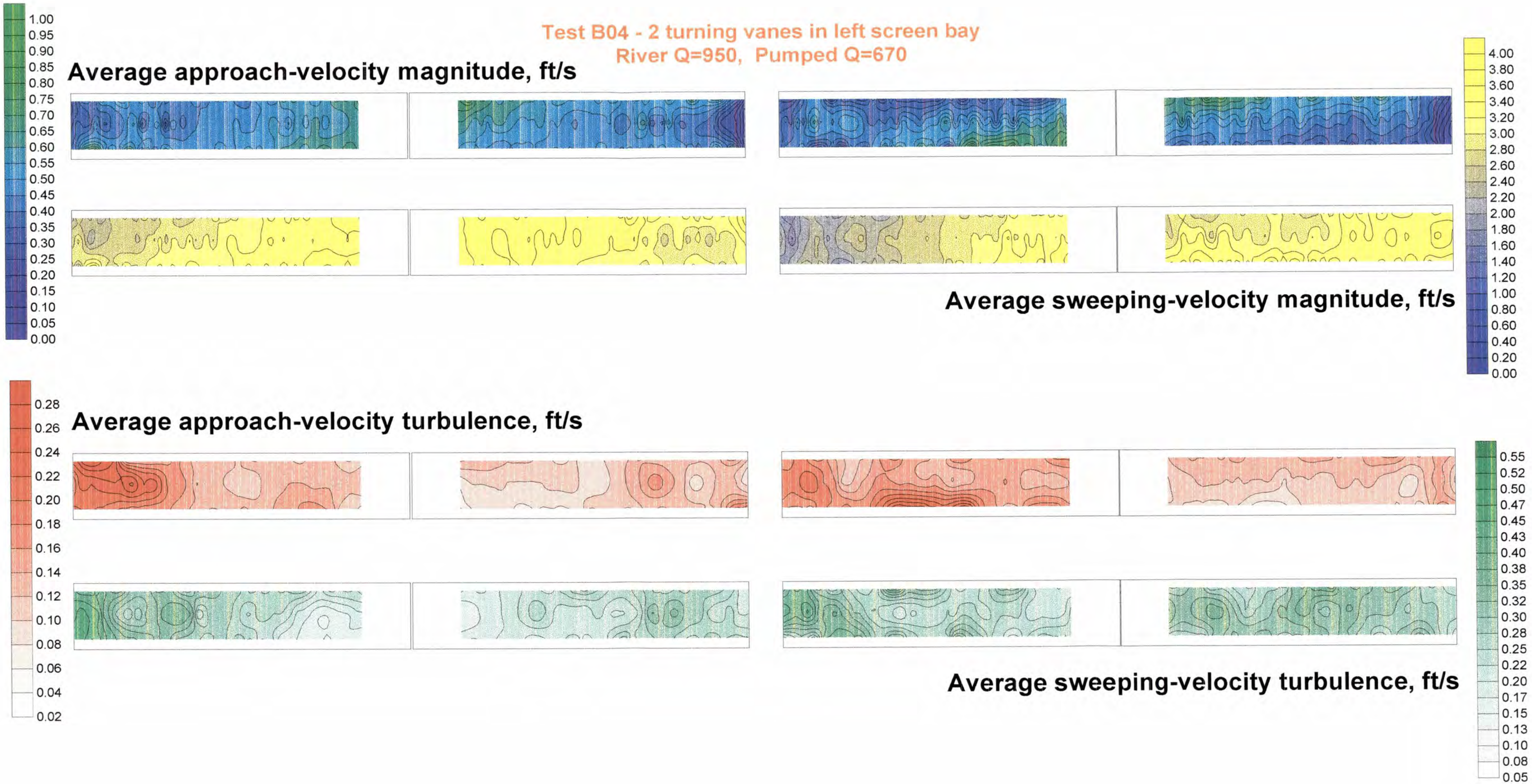
Test B04 - 2 turning vanes in left screen bay
River Q=950, Pumped Q=670
Average approach-velocity magnitude, ft/s
Average sweeping-velocity magnitude, ft/s
Average approach-velocity turbulence, ft/s
Average sweeping-velocity turbulence, ft/s
1.00 0.95 0.90 0.85 0.80 0.75 0.70 0.65 0.60 0.55 0.50 0.45 0.40 0.35 0.30 0.25 0.20 0.15 0.10 0.05 0.00
4.00 3.80 3.60 3.40 3.20 3.00 2.80 2.60 2.40 2.20 2.00 1.80 1.60 1.40 1.20 1.00 0.80 0.60 0.40 0.20 0.00
0.28 0.26 0.24 0.22 0.20 0.18 0.16 0.14 0.12 0.10 0.08 0.06 0.04 0.02
0.55 0.52 0.50 0.47 0.45 0.43 0.40 0.38 0.35 0.32 0.30 0.28 0.25 0.22 0.20 0.17 0.15 0.13 0.10 0.08 0.05

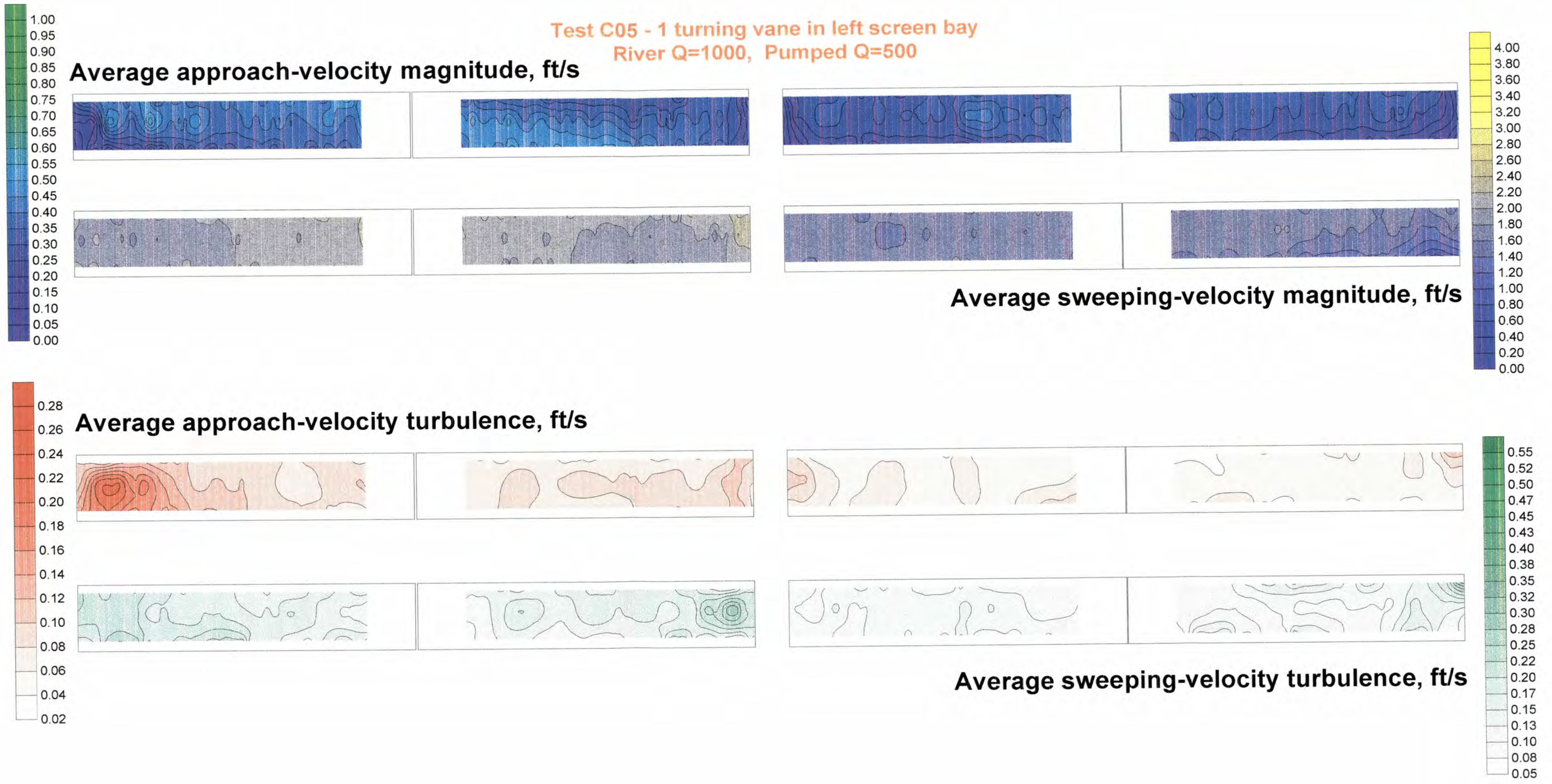

Test C05 - 1 turning vane in left screen bay
River Q=1000, Pumped Q=500
Average approach-velocity magnitude, ft/s
1.00 0.95 0.90 0.85 0.80 0.75 0.70 0.65 0.60 0.55 0.50 0.45 0.40 0.35 0.30 0.25 0.20 0.15 0.10 0.05 0.00
Average sweeping-velocity magnitude, ft/s
4.00 3.80 3.60 3.40 3.20 3.00 2.80 2.60 2.40 2.20 2.00 1.80 1.60 1.40 1.20 1.00 0.80 0.60 0.40 0.20 0.00
Average approach-velocity turbulence, ft/s
0.28 0.26 0.24 0.22 0.20 0.18 0.16 0.14 0.12 0.10 0.08 0.06 0.04 0.02
Average sweeping-velocity turbulence, ft/s
0.55 0.52 0.50 0.47 0.45 0.43 0.40 0.38 0.35 0.32 0.30 0.28 0.25 0.22 0.20 0.17 0.15 0.13 0.10 0.08 0.05